VOL. 11 NO. 2 FEBRUARY 1966
PUBLISHED MONTHLY

Journal of

ELECTROANALYTICAL CHEMISTRY

International Journal Dealing with all Aspects of Electroanalytical Chemistry, Including Fundamental Electrochemistry

ELSEVIER

GENERAL INFORMATION

See also Suggestions and Instructions to Authors which will be sent free, on request to the Publishers.

Types of contributions

(a) Original research work not previously published in other periodicals.
(b) Reviews on recent developments in various fields.
(c) Short communications.
(d) Bibliographical notes and book reviews.

Languages

Papers will be published in English, French or German.

Submission of papers

Papers should be sent to one of the following Editors:

Professor J. O'M. Bockris, John Harrison Laboratory of Chemistry, University of Pennsylvania, Philadelphia 4, Pa., U.S.A.
Dr. R. Parsons, Department of Chemistry, The University, Bristol 8, England.
Professor C. N. Reilley, Department of Chemistry, University of North Carolina, Chapel Hill, N.C., U.S.A.

Authors should preferably submit two copies in double-spaced typing on pages of uniform size. Legends for figures should be typed on a separate page. The figures should be in a form suitable for reproduction, drawn in Indian ink on drawing paper or tracing paper, with lettering etc. in thin pencil. The sheets of drawing or tracing paper should preferably be of the same dimensions as those on which the article is typed. Photographs should be submitted as clear black and white prints on glossy paper.
All references should be given at the end of the paper. They should be numbered and the numbers should appear in the text at the appropriate places.
A summary of 50 to 200 words should be included.

Reprints

Twenty-five reprints will be supplied free of charge. Additional reprints can be ordered at quoted prices. They must be ordered on order forms which are sent together with the proofs.

Publication

The *Journal of Electroanalytical Chemistry* appears monthly and has six issues per volume and two volumes per year, each of approx. 500 pages.

Subscription price (post free): £ 12.12.0 or $ 35.00 or Dfl. 126.00 per year; £ 6.6.0 or $ 17.50 or Dfl. 63.00 per volume.
Additional cost for copies by air mail available on request.
For advertising rates apply to the publishers.

Subscriptions

Subscriptions should be sent to:

ELSEVIER PUBLISHING COMPANY, P.O. Box 211, Amsterdam, The Netherlands.

A STUDY OF THE PLATING AND STRIPPING OF SILVER ON PLATINUM ELECTRODES IN HALIDE MELTS

T. B. REDDY
Bell Telephone Laboratories, Incorporated, Murray Hill, New Jersey (U.S.A.)
(Received May 1st, 1965)

Many polarographic studies of metal deposition on solid microelectrodes from molten salts have been reported in recent years[1-4]. Since the exchange currents for electrode reactions in melts are high, charge-transfer processes are controlled by diffusion in the steady-state and polarographic techniques provide much valuable information. One significant anomaly has developed in the literature. European workers have observed sigmoid current–voltage curves for the deposition of metals from dilute solutions and report that these curves fit the Heyrovsky–Ilkovic equation,

$$E = E_{\frac{1}{2}} + \frac{RT}{nF} \ln \left(\frac{i_d - i}{i} \right) \quad (1)$$

This equation was derived with the assumptions that (i) the electrode potential is determined by the activity of oxidized and reduced species at the electrode surface and (ii) diffusion controls the rate of arrival of ions at the surface and the rate of removal of deposited metal into the substrate (usually mercury). In contrast, American investigators have observed current–voltage curves with definite deposition potentials and found that these fitted the Kolthoff–Lingane equation:

$$E = E_{\frac{1}{2}} + \frac{RT}{nF} \ln (i_d - i) \quad (2)$$

This equation was derived with the assumptions that (i) the potential of the electrode is determined by the activity of the metal ion at the electrode–solution interface (ii) the deposited metal is at unit activity and (iii) mass transport is controlled by semi-infinite diffusion. For deposition on a solid substrate, the Kolthoff–Lingane equation would normally be expected to hold since the ion should be discharged to give metal atoms on the electrode surface. Once monolayer coverage is achieved, the depositing metal should be at unit activity. DELIMARSKII AND PANCHENKO[5] first advanced the hypothesis that inter-metallic diffusion occurs at molten salt temperatures giving sigmoid current–voltage curves. Later HILLS AND OXLEY[6] have advanced two other reasons for this effect: first, corrosion reactions between the deposited metal and the melt and second, the direct solubility of the metal in the melt.

One fact has frequently been cited as proving that deposited metal does not interact with a precious-metal substrate. If the direction of polarization is reversed during deposition, the current becomes zero at the equilibrium potential and then anodic without any discontinuity in the current–voltage curve. This experiment is

not meaningful because the electrode is covered by thousands of layers of deposited metal and possesses the properties of an electrode of the deposited metal. Dissolution will proceed when any anodic overpotential is imposed. Interactions between the deposit and the substrate would be evident on dissolution only if the electrode were covered by a small number of monolayers. In this case, the deposition and dissolution reactions would be essentially the reverse of one another and any deposit–substrate interaction would be evident.

Recently GAUR AND BEHL[7] have studied the polarographic reduction of a number of metal ions in a $MgCl_2$–NaCl–KCl eutectic mixture at 475°. They found that the current–voltage curves for the reduction of Cd(II) and Pb(II), both metals being liquid at 475°, obeyed the Heyrovsky–Ilkovic equation. Evidence for surface alloy formation was found in the case of cadmium and lead. On the other hand, the reduction of Sn(II), also as liquid metal, gives current–voltage curves which obey the Kolthoff–Lingane equation although liquid tin is also known to interact with platinum.

LITTLEWOOD AND EDELEANU[8,9] have treated corrosion processes resulting from oxygen and oxide species in halide melts, thermodynamically. STERN and co-workers[10–12] have considered the reactions of silver with molten NaCl at 800–900°. Initially Stern held that the reaction

$$Na^+ + Ag \rightarrow Ag^+ + Na \qquad (3)$$

proceeded because sodium metal, one of the products, was volatilized from the molten NaCl and drove the reaction to the right. Later STERN found qualitative evidence for alloying of sodium with the silver. In addition, atmospheric corrosion of silver occurs:

$$2\,Ag + \tfrac{1}{2}\,O_2 \rightarrow 2\,Ag^+ + O^{2-} \qquad (4)$$

In an inert atmosphere, reaction (3) predominates. STERN AND REID[12] have found the enthalpy and entropy of activation for reaction (3), to be 45.4 Kcal/mole and −92 e.u., respectively. The authors claim these unusual values are evidence for electron transfer as the rate-controlling step in the overall reaction.

Although no data can be found on the diffusion of silver into platinum, studies of the self-diffusion of silver atoms have been carried out by HOFFMAN AND TURNBULL[13,14] using radiotracer techniques. These authors found that at 450° the diffusion coefficients of silver atoms at low-angle grain boundaries[15] is $1.4 \cdot 10^{-7}$ cm²/sec, at incoherent grain boundaries, $2.3 \cdot 10^{-8}$ cm²/sec and in the bulk $7.4 \cdot 10^{-13}$ cm²/sec. THALMAYER, BRUCKENSTEIN AND GRUEN[16] found the diffusion coefficient of silver ion in the LiCl–KCl eutectic melt at 450° to be $3.14 \cdot 10^{-5}$ cm²/sec. If solid-state diffusion is to affect the kinetics of deposition, it is necessary that the solid-state diffusion coefficient be within a few orders of magnitude of the solution-phase value. This is the case for both types of grain-boundary diffusion but not for bulk diffusion.

This paper describes experiments designed to investigate the factors responsible for the apparent variability of thermodynamic activity during fused-salt deposition. Platinum electrodes were plated with silver from the LiCl–KCl eutectic melt containing AgCl at 450° and the electrode allowed to remain in the melt for varying times before stripping the silver. Coherent deposits were obtained under the conditions of this study. Correlation of the amount of metal plated and stripped,

with the total time from the initiation of plating to the end of stripping was made. Potential–time curves during constant-current stripping of silver-plated platinum electrodes were determined to study the interaction of silver deposits with the platinum substrate at molten-salt temperatures. Ultra-pure silver samples were exposed to high-purity LiCl–KCl eutectic melts in an argon atmosphere. The potential of the silver metal was determined as a function of time and the surface of the silver metal was examined by electron-diffraction techniques after removal from the melt.

EXPERIMENTAL

Eutectic salt mixture

Highly purified[17] LiCl (59%)–KCl (41%) melts were obtained in glass ampoules containing a nitrogen atmosphere from the Anderson Physics Laboratory, Inc., Champaign, Illinois.

Silver chloride

Fisher or Mallinckrodt reagent-grade AgCl was finely ground and dried in the dark over magnesium perchlorate for several days before use.

Electrodes

Flush-ground microelectrodes were prepared from 0.020 in. diameter wire and polished as previously described[18]. Studies of the corrosion of silver in the LiCl–KCl eutectic were carried out with rods of 99.999% pure silver metal (American Smelting and Refining Co.) which were heat treated in a vacuum at 450° for several days to remove dissolved oxygen and decompose surface oxides. The sample was etched as previously described[18]. A Pt/Pt(II) reference electrode was prepared in an isolated compartment connected to the cell by a fritted-glass disk of medium porosity by anodizing a platinum metal foil at constant current to produce a known amount of Pt(II) in the reference compartment. After an experiment, the bulk metal and isolated compartments were analyzed for chloride by standard volumetric methods. Spectrographic carbon rods were used as counter electrodes in isolated compartments.

Procedure

Experiments were conducted in 15 in. × 2-1/2 in. o.d. medium-walled Pyrex test tubes flanged to fit No. 12 silicone-rubber stoppers. Other details have already been described[17,18].

Instrumentation

A Sargent Model XV Polarograph was used for voltage-scan experiments and for deposition of silver at constant potential from the melt. Because of the high conductivity of the melt and the small currents drawn when microelectrodes are employed, the applied voltage and electrode potential are identical to within a millivolt. A Leeds and Northrup K-3 potentiometer was used to measure static-electrode potentials while a Sargent Model MR recorder measured electrode potentials which varied with time. A K and E Model 4236M compensating polar planimeter was used to integrate current–time curves. Sargent Model IV and Teletronics Laboratory Model PS-110 constant current power supplies were employed.

RESULTS

Platinum microelectrodes were plated from a 5.1 mM Ag(I) solution at a constant potential of -1.51 V *vs.* a 1 M Pt/Pt(II) reference electrode, and current–time curves recorded. The electrode remained in the melt on open circuit for a period of time from 0.6–30.0 min. The electrode was then polarized at potentials of -0.91 V which is anodic to the equilibrium potential (-1.071 V in this melt[19]). The current–

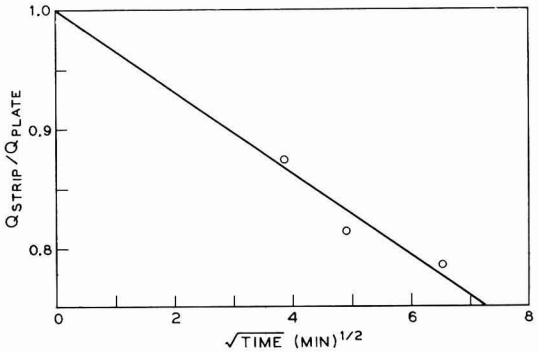

Fig. 1. The ratio of coulombs of Ag stripped to coulombs plated is plotted as a function of the square root of time in $(\text{min})^{\frac{1}{2}}$.

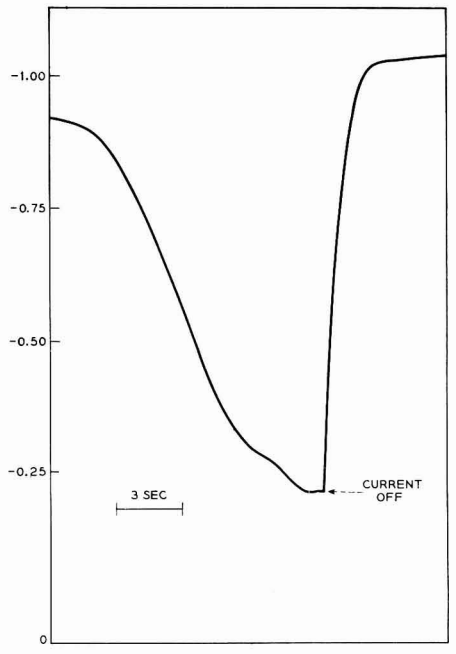

Fig. 2. The potential of a Ag-plated Pt microelectrode against a 1 M Pt/Pt(II) reference electrode is shown as a function of time at the end of a constant current stripping expt. The anodic current, 12.0 μA; 3-sec time interval.

time curve was recorded and the potential switched to −0.71 V when the current had decayed to a low value. The current–time curve was again recorded at −0.71 V. In this manner the plated silver was stripped from the surface. If the electrode were first polarized to −0.71 V, the anodic current would have become too great to record accurately with the equipment employed. Current–time curves were integrated with a planimeter and corrections for the residual-current processes applied after the manner of LORD, O'NEILL AND ROGERS[20]. The ratio of coulombs stripped to coulombs plated is shown in Fig. 1 as a function of the square root of time from the initiation of plating to the end of stripping. Similar experiments were performed by depositing the metal for 120 sec at a constant current of 12.0 μA, which was one-third of the limiting current as determined by voltage-scan experiments. The results paralleled those shown in Fig. 1 in that fewer coulombs were consumed in the stripping than in the plating cycle. Deviations from the square-root relationship shown in Fig. 1 were observed at longer times in that fewer coulombs were consumed in the stripping cycle than expected from the potentiostatic-plating experiments. The potential–time behavior during galvanostatic stripping showed an unusual effect as seen in Fig. 2. At the end of the anodization cycle, the potential of the silver-plated platinum electrode fell from the Ag/Ag(I) potential to the Pt/Pt(II) potential as the silver was removed from the surface. After the current was shut off, the potential immediately returned to the Ag/Ag(I) value which indicated that Ag° returns to the surface, although, apparently, it was completely removed by stripping. Since the concentration of Ag(I) at the electrode surface at equilibrium was much greater than that of Pt(II), the electrode then assumed the Ag/Ag(I) potential although only small amounts of silver were present on the surface. When this experiment was performed at high current densities and significant amounts of platinum substrate oxidized to Pt(II) before the current was terminated, the potential remained at the Pt/Pt(II) value. This experiment proved that the silver which returned to the surface came from the layer of platinum below the Ag/Pt interface.

Platinum electrodes were plated with silver and allowed to stand in the melt for 30 min. The electrodes were stripped and the platinum was examined by several instrumental techniques. Emission spectroscopy indicated the presence of trace quantities of silver in the platinum and X-ray milliprobe studies gave similar results.

Corrosion studies

Studies of the corrosion of silver metal in the pure LiCl–KCl melt were carried out in the absence of added AgCl. The potential of a silver rod in an isolated compartment connected to the bulk melt by a fritted disk was measured as a function of time against an isolated Pt/Pt(II) reference electrode. The quantity of impurities in the melt can be estimated from the residual current as 0.3 mM. Figure 3 shows that the Ag(I) concentration at the metal–solution interface increased as a function of time, since the potential of the silver electrode became less negative with time. The magnitude of the effect was much greater than can be attributed to impurities in the melt. The production of Ag(I) in the isolated compartment was not due to the reaction $Pt(II) + 2\,Ag \rightarrow Pt + 2\,Ag(I)$ occurring from leakage of Pt(II) out of the reference electrode, since the residual current curve of the bulk melt showed no increase due to Pt(II) reduction at the end of the experiment. Studies of the surface of silver metal exposed to the molten LiCl–KCl mixture in an argon atmosphere for long periods of

time were carried out using electron-diffraction methods. Such samples developed areas which were light purple in color. These areas were found by diffraction of a [0$\bar{1}$2] zone-axis electron beam incident on a (110) face to contain[21] the phase Li·Ag. Table 1 shows the interplanar d spacings of the indicated reflections for known Li · Ag[22] and for the phase found on the surface of silver metal exposed to the melt. The agreement between the two phases indicates that Li · Ag was formed.

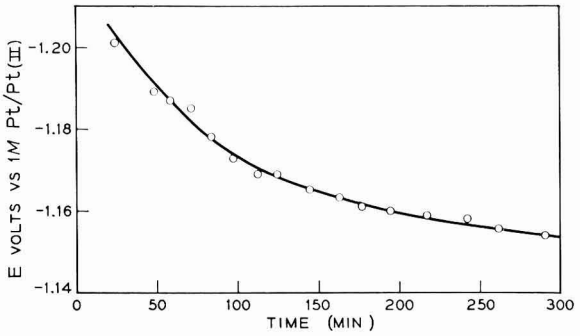

Fig. 3. The potential of a 99.999% pure Ag rod immersed in Li–KCl eutectic in an isolated compartment against a 1 M Pt/Pt(II) reference electrode is shown as a function of time in minutes.

TABLE 1

ELECTRON DIFFRACTION DATA FOR Li · Ag

Reflection (hkl)	*d(unknown) (A°)*	*d(Li · Ag) (A°)*
100	3.28	3.17
200	1.68	1.59
221	1.08	1.06
321	0.89	0.85

DISCUSSION

LAITINEN AND LIU[19] have shown that the constant-current anodization of a large number of metals, including silver, proceeds with 100% current efficiency on a macro scale in high purity LiCl–KCl melt. VAN NORMAN[23] has demonstrated that cadmium and zinc could be deposited and stripped from a molten bismuth pool electrode potentiostatically with 1% accuracy at a 10-mg level. Nickel was also deposited and stripped from platinum with the same accuracy. The prior studies have indicated that both anodic and cathodic electrode processes proceed with 100% efficiency in high-purity melts. In this study, experiments conducted on a micro level show significant differences between the amount of material plated and stripped. These effects must be due to factors other than coulometric inefficiencies in the electrode reactions.

BECKER[24], as well as NISBET AND BARD[25], have found coulometric differences between plating and stripping processes in aqueous solution on platinum electrodes which have oxide films on the surface. Since platinum oxide is soluble in the molten alkali halides, this cannot be the explanation for the results found in this study.

Figure 1 shows that the deposited metal is removed from the surface by a process which obeys a square-root-of-time relation and strongly suggests that a diffusion process is involved in the removal. The rates of self-diffusion of silver atoms at 450° show that low-angle and normal grain boundaries provide sites where appreciable loss of material may occur. Bulk diffusion is so slow as to be ruled out as a factor in the removal of silver from the surface. The recovery of the Ag/Ag(I) potential after termination of anodic current can be explained by grain-boundary diffusion of silver into the platinum substrate. Although the anodization removes all the surface silver, diffusion of silver back along the grain boundaries to the platinum surface will bring enough silver to the surface to re-establish the Ag/Ag(I) potential. If the surface of the platinum is anodized to a depth sufficient to remove all diffused silver then the Ag/Ag(I) potential is not re-established when the electrode is placed on open circuit. Thus grain-boundary diffusion is one of the factors involved in the observed coulometric inefficiencies.

The studies of the corrosion of silver in the LiCl–KCl eutectic show an increase of Ag(I) species in the melt and the appearance of a Li · Ag phase on the metal surface. Both these facts are consistent with the occurrence of[5]:

$$2\,Ag + Li^+ \rightarrow Li \cdot Ag + Ag^+ \qquad (5)$$

No explanation for the thermodynamic driving force necessary to cause this class of reaction has been presented. The present study demonstrates that corrosion reactions similar to those proposed by STERN occur at much lower temperature in a LiCl–KCl melt and that an intermetallic compound, Li · Ag, is formed. Reaction (5) will occur spontaneously only if Li · Ag has a large negative free energy of formation. Since reaction (5) is reversible, the tendency for silver to corrode in the LiCl–KCl melt will be less in the presence of added AgCl. Since STERN AND REID[12] found that silver corroded in molten NaCl at temperatures of 800–900° although as much as 8% AgCl was added, reaction (5) will probably occur in the LiCl–KCl melt at 450° with AgCl concentrations in the 1% range used in this study. Thus occurrence of this reaction is another factor in the coulometric differences found between plating and stripping cycles. While the plated silver is in the melt, corrosion occurs, forming Li · Ag and liberating Ag^+. During the stripping cycle, the amount of silver available for oxidation is less than that plated not only because Ag^+ is formed by corrosion but also because Li · Ag, being thermodynamically very stable, cannot be oxidized at the same potential as silver metal. The Li · Ag phase will be undercut by dissolving Ag and will therefore be unavailable for oxidation. Direct solubility of silver into the LiCl–KCl melt in the metallic state seems unlikely since STERN[10] found the atomic solubility of silver in NaCl at 800–900° was less than 10^{-3} mole % in silver. The solubility in the present case should be far less.

The techniques described in this paper provide a new method of studying intermetallic diffusion in a semi-empirical manner. One metal can be plated on another from a fused salt bath, the metal–metal interface heat treated directly in the melt for a known time and the deposited metal remaining on the surface stripped. The difference in coulombs plated and stripped gives the quantity of metal diffused. The method can easily be employed as a function of temperature and corrections can be applied for the corrosion reactions which occur in the melt.

This study has shown that grain-boundary diffusion of silver and its reaction

with the melt are means by which deposited metal is removed from the surface. Both these effects are factors in the apparent variability of thermodynamic activity of deposited metal during deposition from fused salts. Inter-metallic diffusion will occur more readily at higher temperatures and this may explain in part the fact that European workers have frequently observed sigmoid current–voltage curves since their experiments frequently have been carried out at high temperature. Other factors may also be involved but these two effects have been shown conclusively to occur.

ACKNOWLEDGEMENT

The author wishes to express his appreciation to Mrs. A. HUNT for the electron-diffraction studies and to H. SCHREIBER, JR. for the spectrographic and X-ray milliprobe experiments described herein.

SUMMARY

Platinum electrodes were plated with silver from LiCl–KCl eutectic melts containing AgCl at 450° and left in the melt on open circuit for varying lengths of time and then stripped. Significant differences between the amount of material plated and stripped were found in both galvanostatic and potentiostatic experiments. Samples of high purity silver in the melt were studied by potentiometric techniques and by electron-diffraction methods after removal from the salt. The reaction $2\,Ag + Li(I) \rightarrow Li \cdot Ag + Ag(I)$ occurs in the melt and both grain-boundary diffusion and corrosion are responsible for the loss of plated silver from the surface.

REFERENCES

1 T. B. REDDY, *Electrochem. Tech.*, 1 (1963) 325.
2 C. H. LIU, K. E. JOHNSON AND H. A. LAITINEN, *Molten Salt Chemistry*, edited by M. BLANDER, Interscience Publishers, New York, 1964.
3 H. A. LAITINEN AND R. A. OSTERYOUNG, *Fused Salts*, edited by B. R. SUNDHEIM, McGraw-Hill, New York, 1964.
4 H. C. GAUR AND R. S. SETHI, *J. Electroanal. Chem.*, 7 (1964) 474.
5 YU. K. DELIMARSKII AND I. D. PANCHENKO, *Dokl. Akad. Nauk* SSSR, 91 (1953) 115.
6 G. J. HILLS AND J. E. OXLEY, *Z. Anal. Chem.*, 173 (1960) 5.
7 H. C. GAUR AND W. K. BEHL, *J. Electroanal. Chem.*, 5 (1963) 261.
8 C. EDELEANU AND R. LITTLEWOOD, *Electrochim. Acta*, 3 (1960) 195.
9 R. LITTLEWOOD AND E. J. ARGENT, *Electrochim. Acta*, 4 (1961) 114.
10 K. H. STERN, *J. Phys. Chem.*, 66 (1962) 1311.
11 J. KRUGER AND K. H. STERN, *J. Electrochem. Soc.*, 109 (1962) 889.
12 K. H. STERN AND W. E. REID, JR., *J. Phys. Chem.*, 68 (1964) 3757.
13 R. E. HOFFMAN AND D. TURNBULL, *J. Appl. Phys.*, 22 (1951) 634.
14 D. TURNBULL AND R. E. HOFFMAN, *Acta Met.*, 2 (1954) 419.
15 C. KITTEL, *Introduction to Solid-State Physics*, John Wiley, New York, 2nd ed., 1960, chap. 19.
16 C. E. THALMAYER, S. BRUCKENSTEIN AND D. M. GRUEN, *J. Inorg. and Nucl. Chem.*, 26 (1964) 347.
17 H. A. LAITINEN, R. P. TISCHER AND D. K. ROE, *J. Electrochem. Soc.*, 107 (1960) 546.
18 T. B. REDDY, *J. Electrochem. Soc.*, to be published.
19 H. A. LAITINEN AND C. H. LIU, *J. Am. Chem. Soc.*, 80 (1958) 1015.
20 S. S. LORD, R. C. O'NEILL AND L. B. ROGERS, *Anal. Chem.*, 24 (1952) 209.
21 M. HANSEN, *Constitution of Binary Alloys*, McGraw-Hill, New York, 1958.
22 E. ZINTL AND G. BRAUER, *Z. Physik. Chem.*, 20B (1933) 245.
23 J. D. VAN NORMAN, *Anal. Chem.*, 34 (1962) 594.
24 J. J. BECKER, *J. Electrochem. Soc.*, 111 (1964) 480.
25 A. R. NISBET AND A. J. BARD, *J. Electroanal. Chem.*, 6 (1963) 332.

VOLTAMMETRY OF THE IODINE SYSTEM IN AQUEOUS MEDIUM AT THE PYROLYTIC GRAPHITE ELECTRODE*

F. J. MILLER AND H. E. ZITTEL
Analytical Chemistry Division, Oak Ridge National Laboratory, Oak Ridge, Tennessee (U.S.A.)
(Received May 8th, 1965)

The potentials required for the voltammetric study of the iodine system are well within the usable potential range of the pyrolytic graphite electrode (P.G.E.). An investigation was made, therefore, to determine the reactions of the I_2–I^- system that occur at anodic potentials and the probable usefulness of the P.G.E. for the estimation of I^- concentration over a fairly wide range.

The electrometric behavior of iodine in its various oxidation states has been studied frequently at other electrodes. KOLTHOFF AND LINGANE[1] discuss the anodic behavior of I^- at the D.M.E.; they state that, when the I^- concentration is greater than $5 \cdot 10^{-4}$ M, the diffusion current is poorly defined. Thus, the analytical usefulness of the D.M.E. anodic polarographic wave of I^- is restricted to very dilute solutions. Others[2–4] have studied the I_2–I^- system at the platinum electrode in order to establish electrode reactions. MUELLER[5] reports a limited study of the oxidation of I^- at the boron carbide electrode. In none of these latter studies has the quantitative usefulness of the observed electrode reactions been of primary interest.

EXPERIMENTAL

Reagents

All test compounds were reagent-grade. The I^- solutions were prepared from NaI, and the I_2 solutions from crystalline I_2. Solutions were prepared and standardized according to standard procedures when required for use; they were never stored.

Instrumentation and apparatus

Voltammeter. As described earlier[6].

Recorder. Moseley Model 2D2 X-Y, F. L. Moseley Co., Pasadena, Cal.

Cell. The cell consisted of a No. 18 weighing bottle with a 40/12 standard-taper neck. It was closed with a cap of Teflon that was drilled to permit entry of electrodes, salt bridge, and gas-inlet tube.

Electrodes. Reference, Beckman Model 39270 S.C.E.; indicator, P.G.E. (0.40- and 0.16-cm^2 area)[7]; counter, glassy carbon (G.C.E.)[8].

Salt bridge. The bridge consisted of a Vycor tube (0.328-in. diam., 5.5-in. length) with a porous tip, available from the Corning Glass Co., Corning, N.Y. The

* Research sponsored by the U. S. Atomic Energy Commission under contract with the Union Carbide Corporation.

Vycor tube was inserted vertically through the cap of Teflon and was filled with electrolyte identical with that in the cell. The reference electrode was held vertically in the tube by a short length of rubber tubing.

Cylinder argon. Used to deaerate all solutions.

General procedures

Instrumental procedure. The voltammeter was used in the three-electrode function. Because of the unique design characteristics of the voltammeter, the comparatively high resistances of the asbestos-fiber S.C.E. and of the Vycor-tube bridge have no significant effect on the peak potentials (E_p) or peak currents (i_p). The unshielded counter electrode was placed directly in the test solution. Isolation of the counter G.C.E. is unnecessary. The use of supporting electrolyte in the bridge eliminated unnecessary liquid junction potentials. To minimize the possibility of air oxidation of the iodide solutions, all dilutions were made with supporting electrolyte that had previously been deaerated with argon. The test sample was also purged and was kept under a blanket of argon during voltammetry. The voltammetric scan was carried out at the indicated rates from a potential where no electrode reaction occurred. The scan was toward more anodic potentials except in a few specified cases.

Analysis of the wave. Figure 1 shows a typical voltammogram for the oxidation of I^-. All potentials given are peak potentials (E_p) *vs.* S.C.E., and all currents are

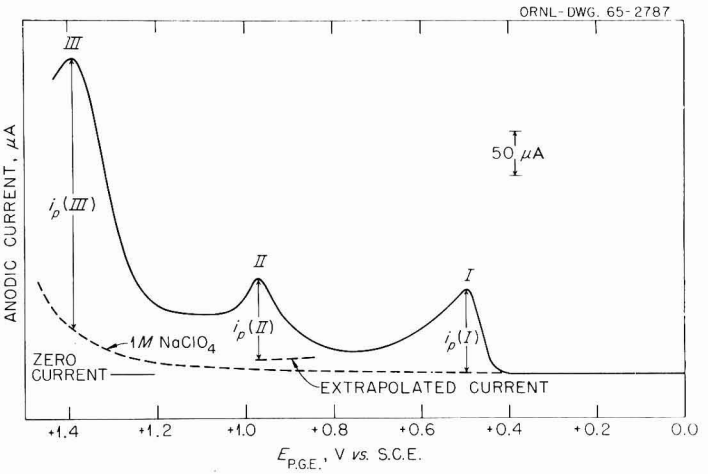

Fig. 1. Typical voltammogram of I^-. Test ion, $2 \cdot 10^{-3}$ *M* I^-; supporting electrolyte, 1 *M* $NaClO_4$; scan rate, 0.5 V/min; area of P.G.E., 0.4 cm^2.

peak currents (i_p). The anodic waves are numbered consecutively in the direction of more positive potential. The E_p values given subsequently in the discussion and tables were measured directly from the voltammograms. No corrections were made for shifts caused by the effects of waves that precede or follow the wave measured. The current produced by the supporting electrolyte was measured for each sample. The i_p values were obtained in the following ways.

The i_p value for E_p(I) was measured as the difference at E_p between the voltammogram for the supporting electrolyte and that of the I^- solution.

The i_p value for E_p(II) was obtained by extrapolation of Wave I. In order to make this extrapolation, it was necessary to assume that the electrode process is sufficiently diffusion-controlled so that the relationship[9]

$$k = it^{1/2} \quad (1)$$

holds even at a constantly varying potential. In this expression, k is a constant, i the measured current in microamperes, and t the time in seconds at which i was measured. A point on Wave I at 0.01 V more positive than the E_p was selected as the zero time point, and the value for k was calculated from several points just beyond this zero point. By use of the calculated k, the value for (I) was estimated at the E_p of the second wave. The value for i_p(II) was then obtained by measuring from that point to the peak of the wave. The validity of the above assumption was checked by scanning a solution of I^- of such concentration that Wave II was essentially absent. The extrapolation procedure was carried out, and the extrapolation point found to agree with the actual current to within ~3%. Other methods of extrapolation by mechanical means were difficult and not precise.

The i_p(III) values were obtained by direct measurement of the peak height from the background current. Because values extrapolated from Wave II fall below background values, a correction was then made for the i_p(II) of the extrapolated Wave II at that point.

Except for the i_p(I) values, the current values that are given are relative, since i_p values for Wave II are influenced by both Waves I and III, whereas i_p(III) is influenced by both Wave II and the water-decomposition wave that follows. Computer techniques for resolving the various waves were considered but were not used because of the many unknown parameters. As yet, computer techniques have been applied only when the wave is known to be caused by a very nearly ideal, reversible electrode reaction.

RESULTS AND DISCUSSION

Possible electrode reactions

Of the many possible reactions to which the three anodic waves that occur at about +0.5, +0.9, and +1.2 V *vs.* S.C.E., could be assigned, the most probable are those listed below, which were selected from the C.I.T.C.E. compilation[10].

Equation	*E (V vs. N.H.E.)*	
Wave I		
$2\,I^- \rightarrow I_2 + 2\,e$	+ 0.53	(2)
$3\,I^- \rightarrow I_3^- + 2\,e$	+ 0.54	(3)
$2\,I_3^- \rightarrow 3\,I_2 + 2\,e$	+ 0.53	(4)
Wave II		
$I_2 + 2\,H_2O \rightarrow 2\,HOI + 2\,H^+ + 2\,e$	+ 1.45–0.059 pH	(5)
$I^- + H_2O \rightarrow HOI + H^+ + 2\,e$	+ 0.99–0.029 pH	(6)
$I_3^- + 3\,H_2O \rightarrow 3\,HOI + 3\,H^+ + 4\,e$	+ 1.22–0.044 pH	(7)
Wave III		
$HOI + 2\,H_2O \rightarrow IO_3^- + 5\,H^+ + 4e$	+ 1.14–0.074 pH	(8)
$I_2 + 6\,H_2O \rightarrow 2\,IO_3^- + 12\,H^+ + 10\,e$	+ 1.19–0.071 pH	(9)
$I_3^- + 9\,H_2O \rightarrow 3\,IO_3^- + 18\,H^+ + 16\,e$	+ 1.16–0.067 pH	(10)

Since the observation of Wave II in voltammetry with electrodes other than the P.G.E. has not been reported previously, no reaction listed under Wave II has appeared as one of the anodic reactions of the $I_2 \rightarrow I^-$ system at solid electrodes.

Diffusion control

The anodic reactions of I^- at the P.G.E. were tested for ideality by examining the parameters of the equation

$$i_p = kn^{\frac{3}{2}} V^{\frac{1}{2}} D^{\frac{1}{2}} AC \qquad (11)$$

where

i_p = peak current (A);
k = constant;
n = electron change;
V = voltage scan rate (V/sec);
D = diffusion coefficient of test ion (cm^2/sec);
A = electrode area (cm^2);
C = concentration of test ion (moles/cm^3).

Equation (11) was derived[11] to describe the events that occur at a planar electrode under conditions of linear variation of potential and mass transport of the electro-

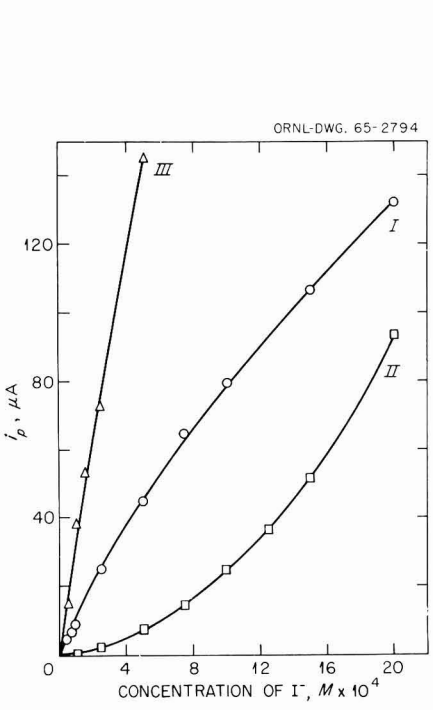

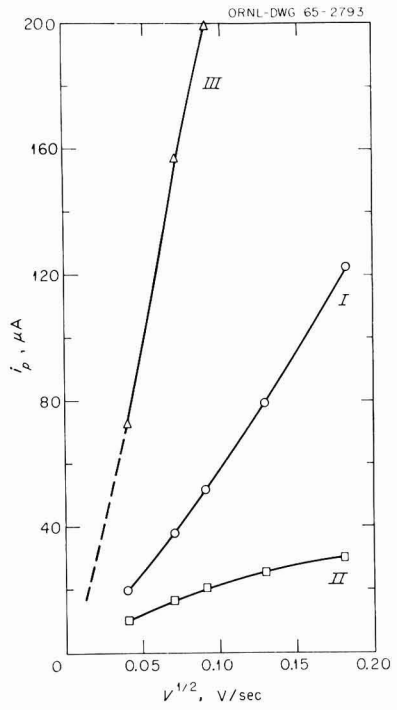

Fig. 2. i_p *vs.* I^- concn. Supporting electrolyte, 1 *M* $NaClO_4$; scan rate, 1.0 V/min; area of P.G.E., 0.4 cm^2.

Fig. 3. i_p *vs.* $V^{\frac{1}{2}}$ (voltage scan rate). I^- concn., $1 \cdot 10^{-3}$ *M*; supporting electrolyte, 1 *M* $NaClO_4$; area of P.G.E., 0.4 cm^2.

active species by diffusion only. The degree to which the anodic reactions of I^- at the P.G.E. fit eqn. (11) was tested by observing the effect of changing the concentration of I^- and the voltage scan rate. The i_p should change linearly with change in concentration of I^-. Figure 2 shows the relationship between the concentration of I^- and i_p; the i_p values for all three waves are given. The i_p is not a linear function of I^- concentration for any of the three electrode reactions, although the i_p(III) *vs.* I^- concentration relationship is more nearly linear for i_p(III) than for either i_p(I) or i_p(II). The plots for i_p(I) and i_p(II) *vs.* concentration of I^- deviate markedly from linearity and in opposite directions; i_p(II) tends to approach zero at low concentrations, and i_p(I) begins to approach a constant value at higher concentrations.

As a further test of the conformity of the iodine system to eqn. (11), the linear voltage scan rate was varied. Values for i_p were measured for each of the three waves at different scan rates. The i_p should vary with the square root of the scan rate, but, as can be seen from the data in Fig. 3, it does not for any of the three waves.

The data indicate that eqn. (11) does not properly describe the electrode processes of the iodine system at the P.G.E.

Effect of pH on E_p

The effect of pH on E_p can be used as an aid in the assignment of the reaction that occurs at each wave. From pH 1–10, the form of the waves does not change significantly. Above pH 10, the first two waves tend to coalesce into one broad wave. Figure 4 presents waves obtained at different pH values. Below pH 10, E_p(I) does not change, whereas E_p(II) shifts to a more positive value with decrease in pH. There is some indication that E_p(III) also shifts in the same direction. However, because of the influence of the water-decomposition wave that follows Wave III, this observation is largely qualitative. Figure 5 shows more exactly the influence of pH on E_p(II). The effect of pH on E_p(II) when the apparent initial electroactive species is I_2 is also shown in Fig. 5. In the latter case, the test solutions were made up to contain I_2 only, although other species may be present as a result of dissociation and electrode

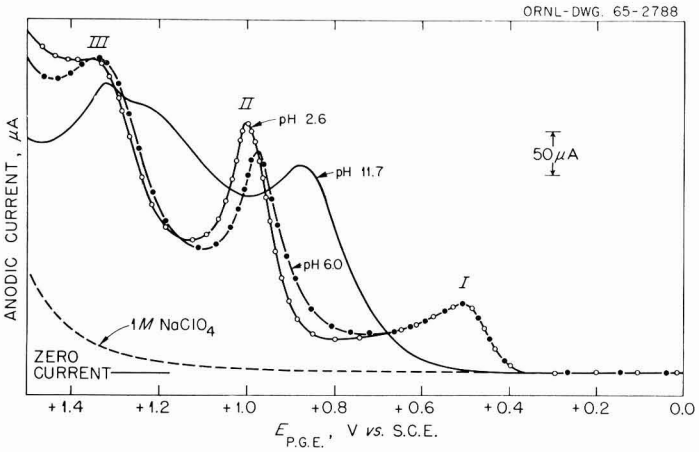

Fig. 4. *I vs. E* wave form as function of pH. I^- concn., 3.7×10^{-3} *M*; supporting electrolyte, 1 *M* $NaClO_4$; scan rate, 0.5 V/min; area of P.G.E., 0.16 cm^2.

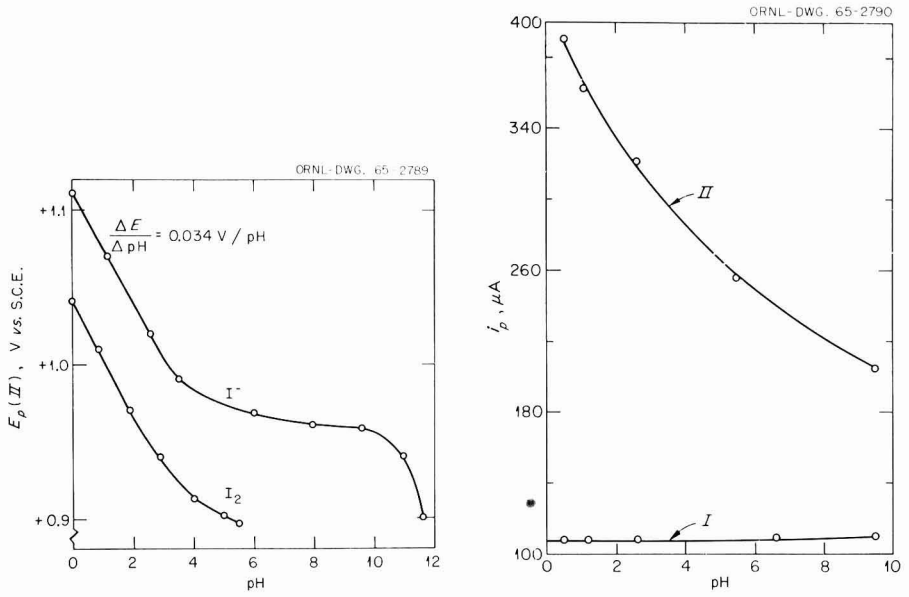

Fig. 5. E_p(II) *vs.* pH. I_2 concn., $5 \cdot 10^{-4}$ *M*; I^- concn., $1 \cdot 10^{-3}$ *M*; scan rate, 1.0 V/min; area of P.G.E., 0.4 cm².

Fig. 6. i_p(I) and i_p(II) *vs.* pH. I^- concn., $1.5 \cdot 10^{-3}$ *M*; supporting electrolyte, 1 *M* $NaClO_4$; scan rate, 1.0 V/min; area of P.G.E., 0.4 cm².

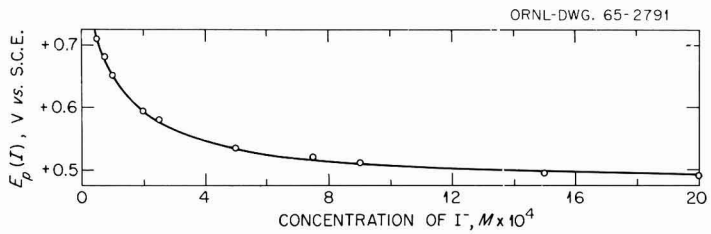

Fig. 7. E_p *vs.* I^- concn. Supporting electrolyte, 1 *M* $NaClO_4$; scan rate, 1.0 V/min; area of P.G.E., 0.4 cm².

reaction. To minimize the accumulation of other species as a result of the electrode reaction, the voltage scan in this series was made in the positive direction from a starting potential of +0.6 V *vs.* S.C.E., that is, in a potential region in which little or no I^- could be produced electrolytically. For the I_2 solution, two anodic waves that correspond to the waves developed at E_p(II) and E_p(III) are observed.

The effect of change in pH on Waves II and III is the same regardless of whether the test solution is made up to contain only I^- or only I_2, although the E_p value for the I_2 solution is displaced 0.05 V in the positive direction. No hard-and-fast explanation is offered for this shift. Possibly, it is due to the effect of Wave I, which appears in voltammograms of solutions that contain I^- and not of solutions that contain I_2 as the initial electroactive species. The $\Delta E/\Delta$pH value for each curve

shown in Fig. 5 is 0.034 V/pH unit. This quantity is within the range of values shown in eqns. (5), (6), and (7) and seems to best fit eqn. (6) or (7). Study of additional data indicates that eqn. (5) is the more probable equation.

Effect of pH on i_p

The effect of pH on i_p was studied as a corollary of the investigation of the effect of pH on E_p. The results are shown in Fig. 6. Again, only the effects on i_p(I) and i_p(II) are given because of the difficulty of measuring i_p(III) at low pH values. With change in pH from $<$1–9.5, i_p(I) does not change significantly, whereas i_p(II) is markedly affected. It is known that HOI—the postulated product of the electrode reaction of Wave II—disproportionates. The following reaction is also probable

$$HOI + H^+ + I^- \rightarrow I_2 + H_2O \qquad (12)$$

The occurrence of reaction (12) would increase the I_2 available at the electrode as the pH decreases, thus causing the observed increase in i_p(II).

Effect of I^- concentration on E_p

Figure 7 shows the effect of the change in concentration of I^- on E_p(I); the values for E_p(II) and E_p(III) are not affected. The shift in E_p(I) is characteristic of that caused by change in concentration of the electroactive species when the electrode reaction is not reversible.

Effect of I_2 concentration on i_p(I) and i_p(II)

In a further attempt to determine the electrode reactions that occur at E_p(I) and E_p(II), two series of test solutions in which the I_2 content was varied were determined. One series contained only I_2 in various concentrations as the electroactive species; the other contained I^- in fixed concentration and various concentrations of I_2. The results are recorded in Fig. 8. In those solutions that contained only I_2, the potential scan was made from +0.6 V *vs.* S.C.E. towards a more positive potential. In those solutions that contained both species, the scan was from an initial

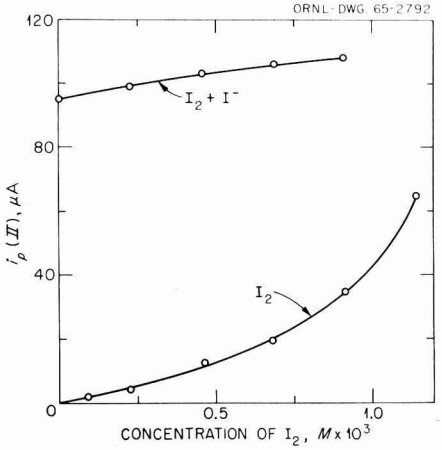

Fig. 8. i_p(II) *vs.* I_2 concn. Curve A, I_2 concn. as shown; curve B, I_2 concn. as shown, I^- concn., $2 \cdot 10^{-3}$ *M*; supporting electrolyte, 1 *M* $NaClO_4$; scan rate, 1.0 V/min; area of P.G.E., 0.4 cm^2.

potential of 0.0 V *vs.* S.C.E. towards a more positive potential. The presence of I_2 had very little effect on Wave I except for a slight rounding of the peak and a decrease in i_p(I) of about 5% that appears at the lowest I_2 concentration; the i_p(I) is then not influenced further by an increase in I_2 concentration.

The effect of change in concentration of I_2 on Wave II is very different. When only I_2 is present, the i_p(II) *vs.* I_2 concentration curve has essentially the same form and values as when only I^- is present (Figs. 2 and 8). However, when both I_2 and I^- are present and the predominant species formed is I_3^- in accordance with eqn. (13)[12]

$$I_2(aq.) + I^- \rightarrow I_3^- \qquad (K = 710) \tag{13}$$

the added increment of I_2 does not affect the i_p(II) *vs.* concentration curve to the extent anticipated. Therefore, it is evident that I_2 itself must be the dominant electroactive species for Wave II.

Proposed electrode reactions

The experimental results presented above indicate that eqn. (5)

$$I_2 + 2\ H_2O \rightarrow 2\ HOI + 2\ H^+ + 2\ e \tag{5}$$

is the optimum choice for the reaction that occurs at E_p(II). From the effect of pH on E_p(II) (Fig. 5), it seems probable that several reactions occur simultaneously and that eqn. (5) predominates. In addition, these data support the proposition that I^- is the species dominant in the production of Wave I. Otherwise, the formation of I_3^- by the addition of I_2 to the I^- solution should have greater effect on i_p(I). It is therefore probable that eqns. (2) and (4) illustrate the electrode reaction that occurs at E_p(I).

$$2\ I^- \rightarrow I_2 + 2\ e \tag{2}$$

$$2\ I_3^- \rightarrow 3\ I_2 + 2\ e \tag{4}$$

If the above propositions are sustained, then it follows that eqn. (8)

$$HOI + 2\ H_2O \rightarrow IO_3^- + 5\ H^+ + 4\ e \tag{8}$$

defines the electrode reaction that occurs at Wave III.

Facile acceptance of the proposed mechanisms is opposed by the fact that the i_p *vs.* I^- concentration relationship for Waves I and II approximates the form of the curve that is obtained when the concentration of I_3^- is plotted against the bulk concentration of I^-. The I_3^- concentration is calculated from eqn. (13) on the assumption that the I_2 concentration at the electrode interface is the same as the concentration of I^- in the solution. To clarify: the i_p(II) *vs.* I^- concentration relationship varies directly as would the calculated increase of concentration of I_3^-, whereas the i_p(I) *vs.* I^- concentration dependency tends to the other direction (Fig. 2). If I_3^- were the dominant species at E_p(I) and E_p(II), such would be the anticipated result. However, the total evidence gathered in this study indicates that the mechanisms proposed in the preceding paragraph are more probable.

Precision of i_p(I)

For the quantitative estimation of I^-, Wave I is the most useful. Although the i_p *vs.* I^- concentration relationship is not linear (Fig. 2), the reaction of Wave I is usable if a calibration curve is established. The prime requisite for a satisfactory calibration curve is precision in replicate determinations. The attainable precision was

TABLE 1

PRECISION OF DETERMINATION OF I^-

Supporting electrolyte, 1 *M* $HClO_4$; scan rate, 1 V/min (anodic); E_p, +0.47 to +0.55 V *vs.* S.C.E.

Concn. of I^- *(mM)*	*Current range* (μA)	*No. of replicates*	*Rel. std. dev.* (%)
0.08	20	7	1.56
0.18	50	10	1.03
0.54	100	8	2.15
1.10	200	10	0.90

studied at four levels of I^- concentration; the data are given in Table 1. The precision of replicate determinations estimated by measurement of Wave I is sufficient for many analytical needs. Neither I_2 nor Cl^- interferes seriously with Wave I.

SUMMARY

The voltammetric behavior of the I_2–I^- system was studied with the P.G.E. At the P.G.E., a voltage scan of a solution of I^- in acid or neutral medium shows three voltammetric waves that correspond to three successive oxidations. The peak potentials of these waves occur at about +0.5, +0.9, and +1.2 V *vs.* S.C.E. A solution of I_2 in the same medium exhibits two anodic waves that correspond to the latter two seen when I^- is the electroactive species. The data indicate that the observed anodic waves result from the stepwise reaction

$$I^- \xrightarrow{+0.5\ V} I_2 \xrightarrow{+0.9\ V} IO^- \xrightarrow{+1.2\ V} IO_3^-$$

The variables that affect these electrode reactions have been studied. It was established that the first anodic wave is suitable for the determination of I^-. The second anodic wave has not been reported previously; on the basis of the data obtained, an electrode reaction for this wave is proposed.

REFERENCES

1 I. M. KOLTHOFF AND J. J. LINGANE, *Polarography*, Vol. II, Interscience Publishers, Inc., New York, 2nd ed., 1952, p. 577.
2 F. C. ANSON *J. Am. Chem. Soc.*, 81 (1959) 1554.
3 J. JORDAN AND R. A. JAVICK, *J. Am. Chem. Soc.*, 80 (1958) 1264.
4 J. D. NEWSON AND A. C. RIDDIFORD, *J. Electrochem. Soc.*, 108 (1961) 699.
5 T. R. MUELLER, *Inert Electrodes in Solid Electrode Voltammetry*, Ph.D. Thesis, University of Kansas, Lawrence, Kansas, p. 105.
6 D. J. FISHER, W. L. BELEW AND M. T. KELLEY, *Anal. Chem.*, in press.
7 F. J. MILLER AND H. E. ZITTEL, *Anal. Chem.*, 35 (1963) 1866.
8 H. E. ZITTEL AND F. J. MILLER, *Anal. Chem.*, 37 (1965) 200.
9 P. DELAHAY, *New Instrumental Methods in Electrochemistry*, Interscience Publishers, Inc., New York, 1954, p. 51.
10 M. G. BROWN, *International Committee of Electrochemical Thermodynamics and Kinetics (C.I.T.C.E.), 7th Meeting*, Butterworths Scientific Publications, London, 1957, p. 244.
11 P. DELAHAY, *New Instrumental Methods in Electrochemistry*, Interscience Publishers, Inc., New York, 1954, p. 119.
12 H. A. LAITINEN, *Chemical Analysis*, McGraw-Hill, New York, 1960, p. 393.

AUTOMATIC RECORDING OF DUAL-ELECTRODE AMPEROMETRIC CURRENTS IN COULOMETRIC TITRATIONS

GARY D. CHRISTIAN

Division of Biochemistry, Walter Reed Army Institute of Research, Walter Reed Army Medical Center, Washington, D.C., 20012 (U.S.A.)

(Received May 11th, 1965)

INTRODUCTION

The automatic recording of end-point signals is a generally accepted technique for increasing the speed and efficiency of titration procedures. For example, the recording of potentiometric titration curves is widely used. Several workers have described various modifications for the automatic recording of photometric titration curves[10]. Coulometric titrations lend themselves readily to these automatic methods because of the ease with which the rate of titration can be controlled.

Dual-electrode amperometry (two polarized electrodes) is well-suited for the end-point detection of many reduction–oxidation, complexometric, and precipitimetric titrations. This is the system employed for the well-known "dead-stop" method in which the titration is continued until a sudden surge in amperometric current indicates excess titrant.

Precise coulometric procedures employing dual-electrode amperometry use manual recording of the amperometric current but many of these should be adaptable to automatic recording as any shape of titration curve can be recorded, and measurements are as accurate as those with manual recording.

Several coulometric titrations have been investigated to illustrate the reliability of automatic current recording; included are reversible–reversible and irreversible–reversible titration couples as well as reduction–oxidation and precipitimetric reactions. Typical titration curves are given and recoveries of titrated standards are reported.

EXPERIMENTAL

Reagent-grade chemicals were used throughout. A standard arsenic solution was prepared from arsenious oxide by conventional methods. The standard dichromate solution was prepared from primary-standard potassium dichromate. A standard solution of reagent-grade potassium iodide was stabilized by adding 0.1 g sodium carbonate/l. Sodium thiosulfate was standardized coulometrically at pH 4.5 as described by ROWLEY AND SWIFT[8].

All coulometric titrations were performed with a ChrisFeld Microcoulometric Quantalyzer, Model 6 (ChrisFeld Precision Instruments Corp., Beltsville, Md.). The

potentials impressed between the indicating electrodes were supplied by a Sargent Model XV Polarograph. All amperometric currents were recorded automatically on this polarograph. The titration cell was a 100-ml beaker. The indicating electrodes consisted of two platinum foils (1 cm^2). The working electrode was a 2-cm^2 platinum foil and the auxiliary electrode a 0.8-cm^2 platinum foil. This latter electrode was isolated from the test solution by placing it in a glass tube fitted with a sintered-glass frit end. For argentometric titrations, the working electrode and the indicating electrodes were plated with silver by electrolyzing in an alkaline silver cyanide bath. In all titrations, 50 ml of electrolyte were used. Solutions were stirred with a magnetic stirrer during titrations.

All pipettes were calibrated. In all titrations, a blank correction was found by titrating the reagents in the same manner as the sample.

DISCUSSION OF RESULTS

Iodide vs. generated cerium(IV)

The system described by LINGANE, LANGFORD AND ANSON[4] was used. They titrated 5–30 mg of iodide with an average error of $\pm 0.2\%$. Samples of 1.868 mg of iodide were titrated automatically at 2.985 mA. The blank correction was *ca.* 8 sec. A typical titration curve is shown in Fig. 1. There was a very large increase in current

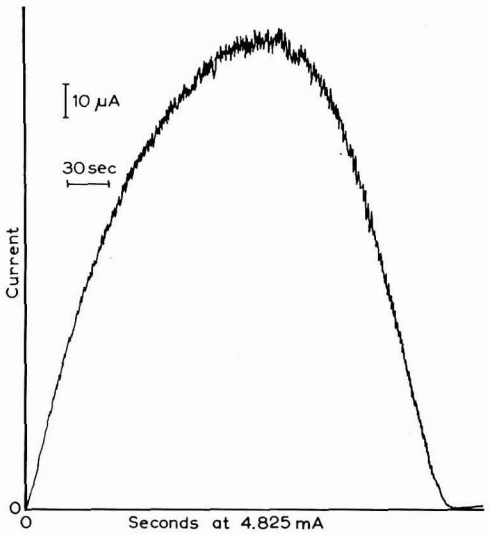

Fig. 1. Titration of 1.868 mg of iodide with generated cerium(IV).

until, approximately, the half-way point of the titration. The current change beyond the end-point was relatively small compared to that before the end-point (decrease). A curve of this type in which the current rises to a maximum at the half-way point and increases beyond the end-point is typical for systems in which both the titrant and the titrate (sample) establish reversible couples. The end-point of the titrations was determined by taking the intersection of the extrapolated straight lines before and after the end-point.

Iodide vs. generated bromine

This titration was described by WOOSTER, FARRINGTON AND SWIFT[11]. They titrated 2 mg of iodide with an average error of $\pm 0.5\%$ and 10–50 μg with an average error of $\pm 2\%$.

The shape of the titration curve in the present work depended on the amount of iodide titrated. With small amounts, the curve increased to a maximum as above and then decreased to a minimum at the end-point (see Fig. 2a). This is the type of

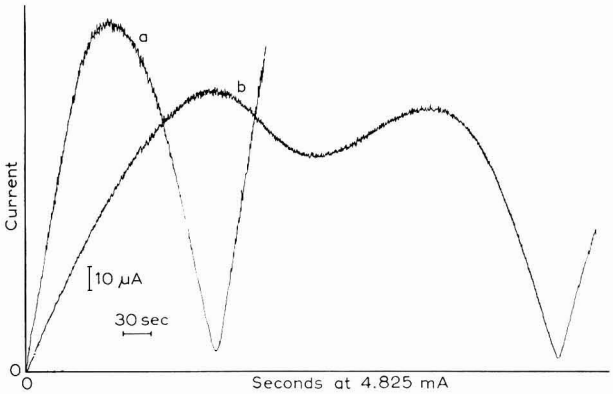

Fig. 2. Titration of iodide with generated bromine. (a), 0.6237 mg I^-; (b), 1.868 mg I^-.

curve obtained by WOOSTER, FARRINGTON AND SWIFT. LINGANE[3] concluded that since only a single maximum was obtained, the oxidation of I_2 to IBr_2^- began before the initial oxidation of I^- to I_2 was complete, *i.e.*, the I^-–I_2 and I_2–IBr_2^- couples are too close together to yield two maxima in the titration curve. In the present investigation, however, a double maximum was recorded when *ca.* 2 mg of iodide were titrated at 5 mA (Fig. 2b). Thus, the oxidation of I^- to I_2 was nearly complete before the oxidation of I_2 to IBr_2^- began.

The results of titrations of 60 μg–1.9 mg of iodide appeared to be slightly more accurate than those obtained by the manual method. The end-point in these titrations was determined by the second method described by WOOSTER, FARRINGTON AND SWIFT. Both the initial current rise and the final current rise (beyond the end-point) were extrapolated to zero current. The time equivalent of the intercept of the first was added to the latter (end-point value at zero current) to apply a correction for air oxidation of iodide. This correction was small. A blank was run and a correction was applied in a similar manner by subtracting the time-equivalent of its intercept at zero current. The initial current readings in all titrations (due to air-oxidized iodide) were less than 1 μA. The minimum at the end-point occurred at approximately 5 μA. There was no apparent effect on the titration by leaving the recording circuit closed for the entire titration.

Arsenic(III) vs. generated bromine

The system described by MEYERS AND SWIFT[6] was used. The amperometric current remained very small up to the end-point and then increased rapidly. This is

typical for systems in which the titrate establishes an irreversible couple while the titrant exhibits a reversible couple. The break was generally very sharp. A slight rounding at the end-point occurred in very dilute solutions. Sometimes a small dip (decrease) in current occurred at the end-point break. The end-point was taken as the intersection of the extrapolated base-line and final current rise. 45 μg–0.5 mg of arsenic were titrated using 1–10 mA generating current.

Arsenic(III) vs. generated chlorine

Chlorine was generated from 0.2 *M* sodium chloride in 0.5 *M* sulfuric acid[2]. The current remained small until near the end-point and increased linearly beyond the end-point. Usually, the "current-reversal" described by FARRINGTON AND SWIFT[2] occurred to a slight extent. It was not necessary to stop the titration to "allow the current to become steady". The end-point was obtained by extrapolating the final current rise to zero. The blank was determined in the same way. The blank correction was slightly greater than that obtained for titrations with bromine and iodine since chlorine is a stronger oxidizing agent.

Arsenic(III) vs. generated iodine

The system of RAMSEY, FARRINGTON AND SWIFT[7] was employed. The titrations were performed in the absence of oxygen with the pH maintained at 8.0 with a phosphate buffer, ionic strength 0.2 *M*[1]. The shape of the titration curve was essentially the same as that obtained in the titration of arsenic with bromine. The intersection of the final current rise and the base-line was taken as the end-point.

Thiosulfate vs. generated iodine

The generating solution was 0.1 *M* potassium iodide in a phosphate buffer of pH 3.0[8]. The titration curve was very sharp. At high generating currents, there was usually an appreciable residual current (a few μA) and often a slight decrease in current occurred at the end-point. When this happened, the end-point was determined by drawing a line perpendicular to the bottom of this "dip" and taking the intersection of this line with the extrapolated final current rise. Otherwise, the end-point was obtained in the same manner as described for the titration of arsenic with iodine. 2 mg of thiosulfate were titrated at 10 mA with excellent recoveries.

Dichromate vs. generated chlorocuprous ion

This is the system described by MEIER, MEYERS AND SWIFT[5]. Chlorocuprous ion was generated at a platinum cathode from a solution of 0.02 *M* cupric sulfate in 1.5 *M* hydrochloric acid. Usually, the initial amperometric current was from one to a few microamperes and it decreased gradually during the titration. A sharp decrease in the current to nearly zero occurred at the end-point. The end-point was determined in the same manner as described above for the thiosulfate titration curves which exhibited a "dip" at the end-point. The generating rate in these titrations was limited. If the current exceeded *ca.* 10 mA under the conditions described, copper was plated out on the cathode, resulting in high values.

Tetraphenyl boron vs. generated silver(I)

The generating electrolyte was the same as described by SUZUKI[9]. In the

present investigation a biamperometric end-point was employed by impressing 100 mV between two silver indicating electrodes. The current remained small up to the end-point and then increased rapidly. There was a very sharp minimum at the end-point.

The results of these titrations are summarized in Table 1. In most cases, accuracy and precision approaching or exceeding that obtained manually can be

TABLE 1

RESULTS OF COULOMETRIC TITRATIONS USING AUTOMATICALLY-RECORDED AMPEROMETRIC END-POINTS

Titrant	*Sample*	*Taken (mg)*	*Found (mg)*	*mA*	*Titrant*	*Sample*	*Taken (mg)*	*Found (mg)*	*mA*
Ce^{4+}	I^-	1.868	1.866	2.895	Cl_2	As^{3+}	0.5414	0.5413	2.895
		1.868	1.872	2.895			0.5414	0.5413	2.895
		1.868	1.864	2.895			0.5414	0.5419	2.895
Av.			1.867				0.5414	0.5414	2.895
					Av.			0.5415	
Br_2	I^-	1.868	1.864	2.895					
		1.868	1.869	2.895					
		1.868	1.865	2.895	I_2	As^{3+}	0.5414	0.5416	2.895
Av.			1.866				0.5414	0.5423	2.895
							0.5414	0.5412	2.895
		0.6237	0.6204	2.895	Av.			0.5417	
		0.6237	0.6242	2.895					
		0.6237	0.6242	2.895	I_2	$S_2O_3^{2-}$	2.354	2.359	9.65
		0.6237	0.6223	2.895			2.354	2.358	9.65
Av.			0.6228				2.354	2.351	9.65
		0.0624	0.0623	0.965	Av.			2.356	
		0.0624	0.0634	0.965					
		0.0624	0.0622	0.965	$CuCl_3^{2-}$	$Cr_2O_7^{2-}$	0.5696	0.5697	2.895
		0.0624	0.0632	0.965			0.5696	0.5696	2.895
		0.0624	0.0641	0.965	Av.			0.5696	
Av.			0.0630						
							0.1902	0.1903	2.895
Br_2	As^{3+}	0.5414	0.5417	9.65			0.1902	0.1894	2.895
		0.5414	0.5414	9.65			0.1902	0.1902	2.895
		0.5414	0.5406	2.895	Av.			0.1900	
Av.			0.5412						
					Ag^+	$(C_6H_5)_4B^-$	0.7680	0.7682	2.895
		0.0448	0.0447	0.965			0.7680	0.7667	2.895
		0.0448	0.0447	0.965			0.7680	0.7676	2.895
Av.			0.0447		Av.			0.7675	

achieved. The stirring rate and solution volume should be approximately the same for sample and blank (*e.g.* 10%). The indicating electrodes should be placed outside the field of the generating electrodes, *i.e.*, should not be placed between the electrodes. The two requisites for automatic recording of amperometric currents are that the chemical reaction between the titrant and sample be sufficiently rapid, and the reactions occurring at the indicating electrodes be rapid. Although this latter requirement is often a problem with potentiometric titrations (potential readings become "sluggish" near the end-point), it usually presents no problem in the case of dual-electrode amperometric titrations.

ACKNOWLEDGEMENT

The technical assistance of RICHARD E. WOLF is gratefully acknowledged.

REFERENCES

1 G. D. CHRISTIAN AND W. C. PURDY, *J. Electroanal. Chem.*, 3 (1962) 363.
2 P. S. FARRINGTON AND E. H. SWIFT, *Anal. Chem.*, 22 (1950) 889.
3 J. J. LINGANE, *Electroanalytical Chemistry*, Interscience Publishers, Inc., New York, 2nd ed., 1958, p. 538.
4 J. J. LINGANE, C. H. LANGFORD AND F. C. ANSON, *Anal. Chim. Acta*, 16 (1957) 165.
5 D. J. MEIER, R. J. MEYERS AND E. H. SWIFT, *J. Am. Chem. Soc.*, 71 (1949) 2340.
6 R. J. MEYERS AND E. H. SWIFT, *J. Am. Chem. Soc.*, 70 (1948) 1047.
7 W. J. RAMSEY, P. S. FARRINGTON AND E. H. SWIFT, *Anal. Chem.*, 22 (1950) 332.
8 K. ROWLEY AND E. H. SWIFT, *Anal. Chem.*, 26 (1954) 373.
9 S. SUZUKI, *Bunseki Kagaku*, 10 (1961) 837.
10 A. L. UNDERWOOD AND T. M. ROBERTSON, *Anal. Chem.*, 35 (1963) 1761.
11 W. S. WOOSTER, P. S. FARRINGTON AND E. H. SWIFT, *Anal. Chem.*, 21 (1949) 1457.

THE ADSORPTION OF IODIDE ION FROM AQUEOUS KI + KF OF CONSTANT IONIC STRENGTH

EDWARD DUTKIEWICZ* AND ROGER PARSONS
Department of Physical Chemistry, University of Bristol (England)
(Received May 15th, 1965)

INTRODUCTION

Recent theoretical discussions of the interaction between ions adsorbed in the inner part of the electrode double layer have (following ESIN AND SHIKOV[1] and ERSHLER[2]) considered the modification of the field as a result of the presence of the diffuse layer by the method of images. Although BARLOW AND MACDONALD[3] have considered the limiting cases of complete imaging in the diffuse plane and the absence of imaging, it is not clear from previous experimental work which limit is the closer to reality. In the present work we have studied the adsorption of iodide ions at constant ionic strength, and hence constant Debye thickness, in the hope that comparison with GRAHAME's measurements[4] at varying ionic strength in pure aqueous KI solutions will reveal an effect due to the change in imaging conditions in the diffuse layer. Clearly such experiments are unlikely to provide information about imaging in the dielectric step (or slope) near the inner Helmholtz plane, since this will be relatively unaffected by changes in the diffuse layer thickness.

Experimental

Double-layer capacities were measured using the bridge described by HILLS AND PAYNE[5]. Frequency-independent capacities were measured at 1 Kc/sec, otherwise a series of measurements at different frequencies was made so that extrapolation to zero frequency was possible. The potential of the dropping-mercury electrode was measured with respect to a normal KCl–calomel electrode, a junction being made directly between the normal KCl solution and the working solution. B.D.H. potassium fluoride was recrystallized from water using platinum vessels, and dried over P_2O_5 for more than two weeks. Solutions of the product in water had a pH of 7. AnalaR potassium iodide was dissolved in water at 60°, filtered and the solution cooled in ice. The product was dried in a vacuum desiccator. Laboratory-distilled water was redistilled from alkaline $KMnO_4$. Mercury was redistilled from a Hulett still.

Results

The measured capacities at 25° are shown in Fig. 1. A dependence on frequency was observed only in solutions more dilute than 1 mM in KI and then only at potentials more positive than −0.7 V. The results shown in this region in Fig. 1 are extrapolated to zero frequency by plotting measurements between 500 c/sec and 2 Kc/sec

* Now at the Department of Physical Chemistry, University of Poznan.

against square root of frequency which result in linear graphs. No part of the discussion of this paper depends on results in the frequency-dependent region.

The charge and interfacial tension were determined by back integration from a charge of $-21\ \mu C\ cm^{-2}$ at which the adsorption of iodide is negligible even in the

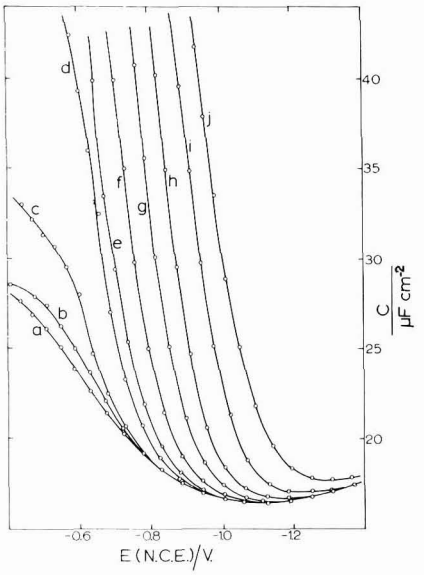

Fig. 1. Capacity/unit area of a mercury electrode in contact with aq. soln. of $x\,M$ KI + $(1-x)$ M KF at 25° as a function of the potential against a normal calomel electrode. The points correspond to integral values of the charge, the most negative point being at $-17\ \mu C\ cm^{-2}$. Values of x: (a), 0; (b), $5 \cdot 10^{-5}$; (c), 10^{-4}; (d), $5 \cdot 10^{-4}$; (e), 0.001; (f), 0.003; (g), 0.01; (h), 0.03; (i), 0.1; (j), 0.3.

highest concentrations of KI used. The potential and interfacial tension at this charge in the base solution were found from capacity measurements combined with electrocapillary and streaming-electrode measurements. The integrations were carried out with the aid of a digital computer, as described previously[6].

*Thermodynamic analysis**

The electrocapillary equation for a pure mercury electrode in contact with an aqueous solution containing KI and KF at constant temperature and pressure may be written

$$-d\gamma = \Gamma_{K^+} d\bar{\mu}_{K^+} + \Gamma_{I^-} d\bar{\mu}_{I^-} + \Gamma_{F^-} d\bar{\mu}_{F^-} \qquad (1)$$

where γ is the interfacial tension, $\bar{\mu}_i$ the electrochemical potential of species i and Γ_i the surface excess of species i relative to the water. If we introduce the salt chemical potentials and eliminate the electrochemical potentials of the anions we may write eqn. (1) again in the form

* Since this paper was submitted, we have seen in proof the essentially similar, though more general, analysis given by H. D. HURWITZ (*J. Electroanal. Chem.*, 10 (1965) 35).

$$-\mathrm{d}\gamma = q\mathrm{d}E^{+} + \Gamma_{\mathrm{I}^-}\mathrm{d}\mu_{\mathrm{KI}} + \Gamma_{\mathrm{F}^-}\mathrm{d}\mu_{\mathrm{KF}} \tag{2}$$

where q is the charge per unit area on the mercury surface, E^{+} is the potential of the mercury electrode with respect to a reference electrode reversible to the potassium ion in the working solution and μ_j is the chemical potential of the salt j.

In a mixed-salt solution of constant ionic strength the activity coefficients of both salts will be nearly constant provided that the ionic strength is sufficiently low that the cross terms in the ionic strength of the individual salts are small. This is likely to be a good approximation in KI + KF mixtures because the activity coefficients of the individual salts are closely similar.

Thus we may write

$$\mathrm{d}\mu_{\mathrm{KI}} = RT\ \mathrm{d}\ln m_{\mathrm{KI}} = RT\ \mathrm{d}\ln x \tag{3}$$

where m_{KI} is the molal concentration of KI, $x = m_{\mathrm{KI}}/(m_{\mathrm{KI}} + m_{\mathrm{KF}})$ and $m_{\mathrm{KI}} + m_{\mathrm{KF}}$ is constant. Similarly

$$\mathrm{d}\mu_{\mathrm{KF}} = RT\mathrm{d}\ln m_{\mathrm{KF}} = RT\ \mathrm{d}\ln(1-x) = -RT\{x/(1-x)\}\mathrm{d}\ln x \tag{4}$$

Substituting eqns. (3) and (4) in eqn. (2) we obtain

$$-\mathrm{d}\gamma = q\mathrm{d}E^{+} + [\Gamma_{\mathrm{I}^-} - \{x/(1-x)\}\Gamma_{\mathrm{F}^-}]RT\ \mathrm{d}\ln x \tag{5}$$

Now the total surface excess of iodide ion can be divided into that present in the inner layer, $\Gamma_{\mathrm{I}}{}^{-1}$, and that present in the diffuse layer, $\Gamma_{\mathrm{I}}{}^{2-s}$. If it is assumed that the fluoride ion is present in the diffuse layer only (a very good approximation at the strong negative charges discussed here) then it follows that

$$\frac{\Gamma_{\mathrm{I}}{}^{2-s}}{\Gamma_{\mathrm{F}^-}} = \frac{x}{1-x} \tag{6}$$

because the concentration in the diffuse layer of ions of the same charge is directly proportional to their bulk concentration. Thus it may be seen from eqn. (6) that the second term in the coefficient of d ln$x$ in eqn. (5) is simply the concentration of iodide in the diffuse layer and eqn. (5) reduces to

$$-\mathrm{d}\gamma = q\mathrm{d}E^{+} + \Gamma_{\mathrm{I}}{}^{-1}\ RT\ \mathrm{d}\ln x \tag{7}$$

Finally, since the concentration of K^{+} is constant and the activity coefficients are constant to a good approximation

$$\mathrm{d}E^{+} = \mathrm{d}E_{\mathrm{N.C.E.}} \tag{8}$$

where $E_{\mathrm{N.C.E.}}$ is the potential of the mercury electrode with respect to the normal calomel electrode. Thus the coefficients

$$(\partial\gamma/RT\partial\ln x)_{E_{\mathrm{N.C.E.}}} = -\Gamma_{\mathrm{I}}{}^{-1} \tag{9}$$

$$(\partial\xi_{\mathrm{N.C.E.}}/RT\partial\ln x)_{q} = -\Gamma_{\mathrm{I}}{}^{-1} \tag{10}$$

give directly the surface excess of iodide ion present in the inner layer, if

$$\xi_{\mathrm{N.C.E.}} = \gamma + qE_{\mathrm{N.C.E.}} \tag{11}$$

This type of system thus provides a particularly direct route to the specifically adsorbed concentration.

Calculation of the specific adsorption of iodide

Although eqns. (9) or (10) could be used to calculate the specific adsorption of

iodide in these mixtures, they are not particularly sensitive to very low concentrations of adsorbed species and we have found it more satisfactory to use the potential shift due to adsorption. If eqn. (7) is rewritten in the form

$$-\mathrm{d}\xi_{\mathrm{N.C.E.}} = -E_{\mathrm{N.C.E.}}\,\mathrm{d}q + \Gamma_{\mathrm{I}}^{-1} RT\,\mathrm{d}\ln x \tag{12}$$

with the aid of eqn. (11), and we subtract from this the equation corresponding to the absence of KI (*cf.* ref. 7), we obtain

$$\mathrm{d}\Phi = \mathrm{d}(\xi_{\mathrm{N.C.E.}}{}^{b} - \xi) = (E_{\mathrm{N.C.E.}}{}^{b} - E_{\mathrm{N.C.E.}})\mathrm{d}q\Gamma_{\mathrm{I}}^{-1} RT\,\mathrm{d}\ln x \tag{13}$$

where Φ is the surface pressure of the specifically adsorbed I^- and the superscript b indicates quantities measured in the base solution in the absence of KI. From eqn. (13) it follows that

$$\left[\frac{\partial\,(E_{\mathrm{N.C.E.}}{}^{b} - E_{\mathrm{N.C.E.}})}{RT\,\partial\ln x}\right]_q = \left(\frac{\partial\Gamma_{\mathrm{I}}^{-1}}{\partial q}\right)_x \tag{14}$$

If the adsorption isotherm for iodide is of the form $\Gamma_{\mathrm{I}}^{-1} = \Gamma_{\mathrm{I}}^{-1}(\beta x)$, *i.e.*, if it is congruent (the shape is independent of the charge) then as has already been shown[8], eqn. (14) can be integrated to obtain

$$\Delta E = (E_{\mathrm{N.C.E.}}{}^{b} - E_{\mathrm{N.C.E.}})_q = RT\,\frac{\partial\ln\beta}{\partial q}\,\Gamma_{\mathrm{I}}^{-1} \tag{15}$$

where $RT\ln\beta$ is the standard free energy of adsorption of iodide at a given charge on the electrode. From eqn. (15) it follows that the shift of the potential as the iodide ion concentration in the bulk is increased at constant charge on the electrode surface is directly proportional to the amount of iodide specifically adsorbed. In other words, the plot of ΔE against the logarithm of the bulk activity is the adsorption isotherm with the Γ_{I}^{-1} scale multiplied by the (at present unknown) factor $(\partial\ln\beta/\partial q)$. In the simplest case which is represented by the present system, $(\partial\ln\beta/\partial q)$ is a constant to a good approximation. This might be expected from the results obtained previously

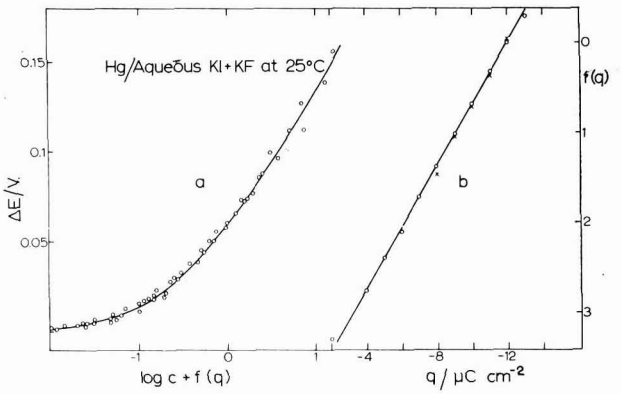

Fig. 2. (a) The shift of the electrode potential at const. charge plotted *vs.* log concn. of KI. The curves at different values of charge are superimposed by shifting parallel to the log c axis by an amount $f(q)$.

(b) $f(q)$ as a function of (q) : (o), obtained from the results of Fig. 2a; (x), obtained from the results of Fig. 3.

for iodide adsorption from pure KI solutions[8]. If $(\partial \ln \beta/\partial q)$ is constant, the plots of ΔE against log C can be superimposed by shifts parallel to the log C axis. This is demonstrated in Fig. 2a. The amount by which each curve must be shifted, is the change in log β, and this is plotted against q in Fig. 2b. The linear relation found here confirms the fact that $(\partial \ln \beta/\partial q)$ is constant within this range for this system.

Further confirmation is obtained directly from the dependence of the capacity on iodide concentration. If eqn. (15) is differentiated with respect to q we obtain

$$\Delta\left(\frac{1}{C}\right) = \frac{1}{C^b} - \frac{1}{C} = RT\left\{\left(\frac{\partial^2 \ln \beta}{\partial q^2}\right) \Gamma_I^{-1} + \left(\frac{\partial \ln \beta}{\partial q}\right)^2 \left(\frac{\partial \Gamma_I^{-1}}{\partial \ln \beta}\right)\right\} \tag{16}$$

If $\ln \beta$ is a linear function of q, the first term in the curly bracket vanishes, and if the adsorbed layer is so dilute that it obeys Henry's law

$$\Gamma_I^{-1} = \beta c \tag{17}$$

then

$$\frac{\partial \Gamma_I^{-1}}{\partial \ln \beta} = \Gamma_I^{-1} \tag{18}$$

and eqn. (16) becomes

$$\Delta\left(\frac{1}{C}\right) = RT\left(\frac{\partial \ln \beta}{\partial q}\right)^2 \cdot \beta c \tag{19}$$

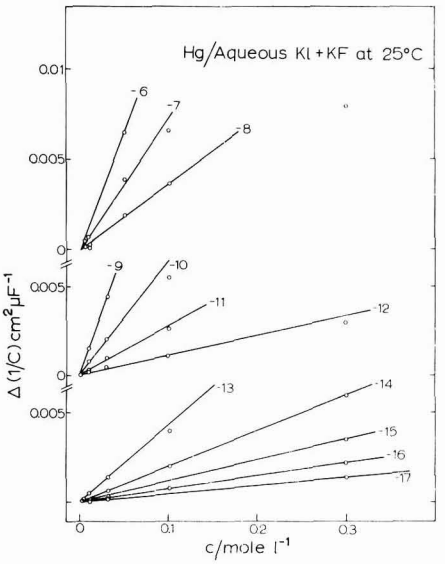

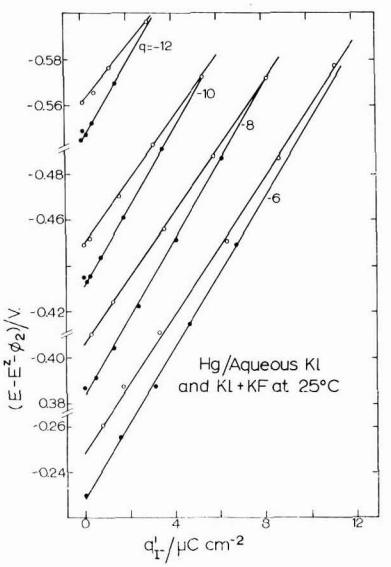

Fig. 3. Change of reciprocal capacity due to I^- adsorption plotted as a function of KI concn. at const. charge. For the middle set of curves the concn. scale must be divided by 10, and for the upper set by 100.

Fig. 4. Potential across the inner region as a function of charge due to specifically adsorbed iodide; (○), GRAHAME's results in pure KI soln.; (●), present results in KI + KF.

and a plot of $\Delta(1/C)$ against bulk concentration should be linear. This plot is shown in Fig. 3, where it can be seen that a linear dependence is found provided $\Delta(1/C)$ is less than about $5 \cdot 10^{-4}$ cm^2 F^{-1}; this corresponds to a maximum change in the measured capacity of about 1 μF cm^{-2}. If $(\partial \ln \beta/\partial q)$ is constant, the slope of these plots is directly proportional to β. The log of this slope is plotted against q in Fig. 2b for comparison with the values obtained previously and the satisfactory agreement confirms that $(\partial \ln \beta/\partial q)$ is constant. The coefficient $(\partial \ln \beta/\partial q)$ obtained can then be used to calculate the amount of specifically adsorbed iodide using eqn. (15). The value of this coefficient found was 0.793 cm^2 μC^{-1}; this is about 4% higher than the value found previously[8] using GRAHAME's measurements[4] in pure KI solutions. Besides the good agreement, we must note at this point that the assumption is made here that the isotherm should be plotted against log c while in the pure KI solution the variable log $a_{\pm}^2$ was used. We shall return to this point later.

The potential difference across the inner layer

Once the amount of specifically adsorbed iodide ion is known, standard relations[9] can be used to calculate the charge on the diffuse layer and hence the potential drop (ϕ_2) across the diffuse layer. By subtracting this and the potential of the point of zero charge (E^z) in the absence of adsorption from the measured potential against the same reference electrode, we obtain an approximation to the part of the potential drop across the inner layer due to the presence of free charges (ϕ^{M-2}). This is plotted in Fig. 4 against the amount of iodide specifically adsorbed. In the same diagram we show also GRAHAME's earlier results[4] for adsorption from pure KI solutions. Both systems give linear plots but they appear to differ significantly both in the intercept on the potential axis and in the slope; the two lines should intersect at the point corresponding to 1 M KI, the value of which is taken from GRAHAME's data and deviations from this are probably due to experimental error.

The difference in the slope of the lines in Fig. 4 is probably the most significant feature. We note in particular that the lines for the KI + KF system are almost exactly parallel; the capacity ${}_{q'}K$ being 59.5 ± 1.0 μF cm^{-2}. Over the same range of charges in the pure KI system, this capacity drops from 83 to 67 μF cm^{-2}. This leads to a value of $(x_2 - x_1)/x_2 (= {}_qK/{}_{q'}K)$ which is lower for KI than for KI + KF (in both systems, this quantity varies with charge because ${}_qK$, the integral capacity at zero specific adsorption, varies with charge). It is possible to explain this difference in the following way. The distance, (x_1), of the charge on the specifically adsorbed layer from the metal is probably determined by the size of the iodide ion and will be the same in both systems. However, the effective distance (x_2) of the outer Helmholtz plane will be determined in part by the efficiency of the imaging in the diffuse layer. If the imaging is perfect, x_2 will be equal to the thickness of the inner layer but imperfect imaging will lead to an apparent increase in the value of x_2. Since imaging will be better in the KI + KF system than in the pure KI system at the lower concentration, x_2 will be larger in the latter and this results in a smaller value of $(x_2 - x_1)/x_2$. As the effect on $(x_2 - x_1)$ is greater than the effect on x_2, so we find that the observed effect is greater on ${}_{q'}K$ than it is on ${}_qK$. The fact that ${}_{q'}K$ is independent of the charge is thus due to the constant imaging conditions in the KI + KF system. We may conclude that imaging in the diffuse double layer must be taken into account and that it is imperfect at least in the solutions of lower ionic strength.

Adsorption from mixed solutions and the chemical potential

There has been some discussion[10] about whether adsorption in ionic systems should be considered as a function of the activity of the adsorbing ion only or as a function of the better-defined salt activity. The present experiments may be used to provide a more definite experimental answer to this problem: in the mixed solution the activity of the potassium ion remains approximately constant so that the variation of the activity of the iodide ion parallels the variation of the salt activity. On the other hand, in the pure KI solution, the iodide ion activity varies approximately as the square-root of the salt activity. The results described in the last section are independent of this choice of the bulk activity factor and show that the structure of the double layer is affected, but only to a minor extent, by the addition of KF to the

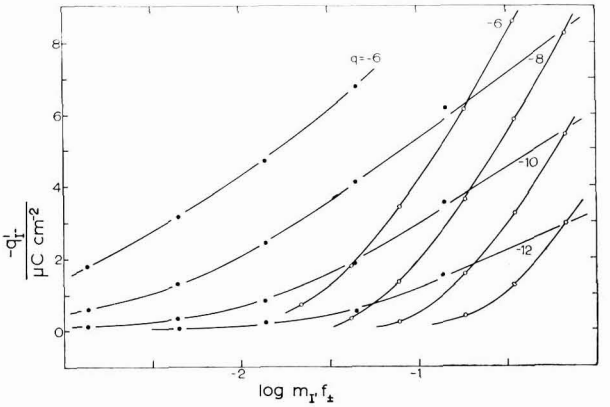

Fig. 5. Plot of charge due to specifically adsorbed iodide ion *vs.* log a_{I^-} at const. charge on the electrode. (○), GRAHAME's results in pure KI soln. (●), present results in KI + KF.

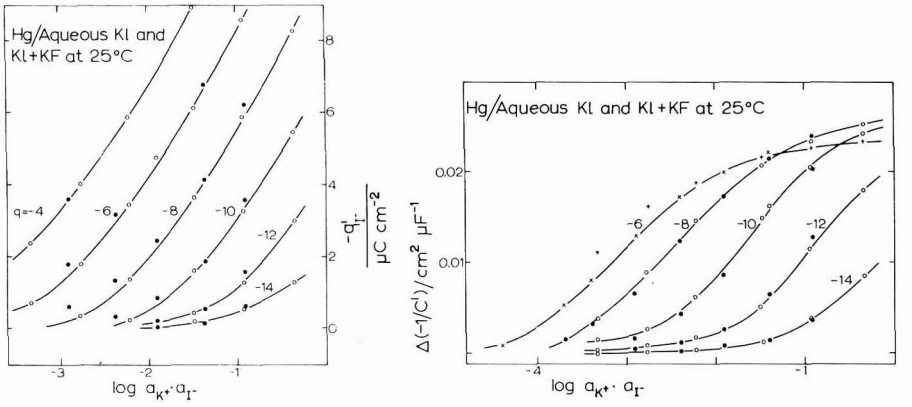

Fig. 6. Plot of charge due to specifically adsorbed iodide ion *vs.* log (a_{K^+} a_{I^-}) at const. charge on the electrode; (○), GRAHAME's results in pure KI soln.; (●), present results in KI + KF.

Fig. 7. Plot of change of reciprocal capacity *vs.* log (a_{K^+} a_{I^-}) at const. charge on the electrode; (○, +), GRAHAME's results in pure KI soln.; (●, ×), present results in KI + KF.

KI system. Hence we may conclude that isotherm plots against the correct bulk activity should give approximately coincident results while those using the incorrect activity should be widely different. The two plots are shown in Figs. 5 and 6. The iodide ion activity is assumed to be equal to the molality multiplied by the mean activity coefficient. It is clear from this comparison that the salt activity is the correct variable and that the amount of specifically adsorbed iodide ion at a given value of $a_{K^+}a_{I^-}$ and at a given value of the charge, is almost identical in the two systems. This is a particularly useful result because it means that experimental results obtained using one type of system may be used in the other type of system, for example, in the interpretation of electrode kinetic data.

Further confirmation of these conclusions is obtained by comparing the change in the reciprocal inner-layer capacities for the two systems. The plot of this quantity against log $a_{K^+}a_{I^-}$ is shown in Fig. 7. Again, good agreement is obtained although some deviation is apparent at $q = -6\ \mu C\ cm^{-2}$. This comparison is a more direct use of the experimental results and therefore depends only to a small extent (in the diffuse layer correction) on the analysis presented above.

The potential distribution in the inner layer

The thickness ratio, $(x_2 - x_1)/x_2$, was first estimated by GRAHAME[4] using an adsorption isotherm of ideal (Henry's law) form modified by introducing the potential of the inner Helmholtz plane in the free energy of adsorption and assuming that the field in the inner layer was independent of distance from the metal surface. The latter assumption is probably incorrect and it was suggested[11] that the apparent thickness ratio obtained in this way is actually a measure of the ratio of the potential drop between the inner and outer Helmholtz planes to the potential drop across the whole inner layer; for this ratio, GRAHAME's nomenclature, $\gamma/(\beta+\gamma)$, was retained in contrast to $(x_2 - x_1)/x_2$ for the thickness ratio.

However, the results of the previous section are in conflict with the method used for determining $\gamma/(\beta+\gamma)$ in that the latter is based on an isotherm of the form:

$$q^{-1} = a_{\pm} \exp[-\Delta G^{\theta}/RT] , \tag{20}$$

whereas the results presented here suggest that the correct form of the Henry's law isotherm should be

$$q^{-1} = a_{\pm}^2 \exp[-\Delta G^{\theta}/RT] . \tag{21}$$

It must be noted that this isotherm, in fact, represents the adsorption of the salt as a whole since $a_{\pm}^2$ is the salt activity for a 1 : 1 salt and adsorption of the anion at constant charge on the metal implies adsorption of an equivalent amount of cation in the diffuse layer at the same time. The standard free energy of adsorption thus contains terms relating both to the anion and to the cation; the latter on the Gouy–Chapman model will depend only on the potential in the diffuse layer. The simplest way of accounting for this is by noting that in the Gouy–Chapman theory, the salt activity is constant throughout the diffuse layer. Consequently, eqn. (21) may be equally applied to the process of adsorption from the outer Helmholtz plane. In this process only the standard free energy of the anion changes and this change involves a "chemical" term, Φ, equivalent to STERN's specific adsorption potential and the electrical term due to the potential difference between the inner and outer Helmholtz

planes. Equation (21) can then be expanded as

$$q_{-}^{1} = a_{\pm}^{2} \exp[\Phi - F(\phi_1 - \phi_2)]/RT \tag{22}$$

or

$$\ln (q_{-}^{1}/a_{\pm}^{2}) = \Phi - \frac{F}{RT}\left(\frac{\gamma}{\beta+\gamma}\right)^{M-2} \tag{23}$$

so that a plot of $RT/F \ln (q_{-}^{1}/a_{\pm}^{2})$ against ϕ^{M-2} should have a slope of $\gamma/(\beta+\gamma)$. The extension to an isotherm such as Langmuir's or the Flory–Huggins, which allows for the replacement of solvent by adsorbed species, is obvious.

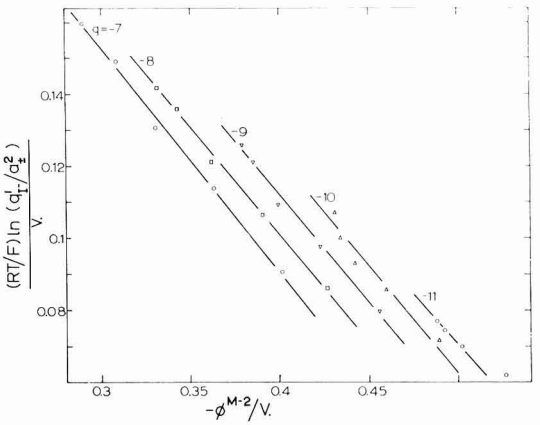

Fig. 8. Plot of eqn. (23) for aqueous KI + KF.

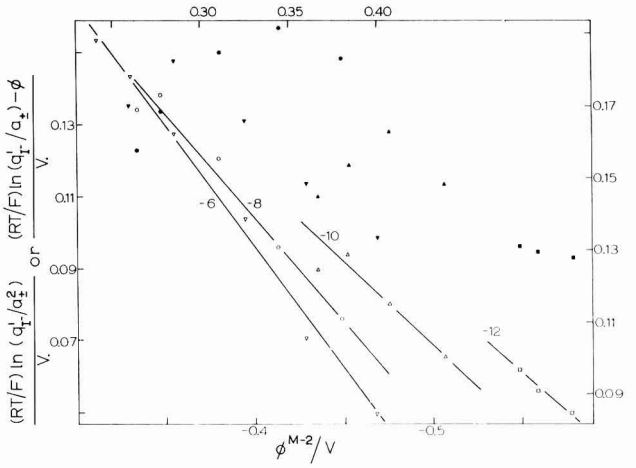

Fig. 9. (○, △, □, ▽), plot of eqn. (23) for GRAHAME's results in pure KI soln.; (●, ▲, ■, ▼), the same results plotted according to eqn. (14) of ref. 11. Upper and right-hand scales refer to the $q = -6\ \mu C\ cm^{-2}$ curves.

At the low concentration of adsorbed ions used in the present experiments, the deviations from the Henry's law form will be very small. Figure 8 shows the results for the KI + KF plotted according to eqn. (23); the slopes give the values of $\gamma/(\beta+\gamma)$ shown in Table 1 which are higher than the values of $(x_2-x_1)/x_2$, showing that the constant-field approximation breaks down even at these low densities. Figure 9 shows

TABLE 1

	$q/\mu C\,cm^{-2}$			
	-12	-10	-8	-6
Pure KI				
$_q'K/\mu F\,cm^{-2}$	82.6	71.4	68	67.3
$_qK/\mu F\,cm^{-2}$	21.4	22.3	23.1	24.2
$(x_2 - x_1)/x_2$	0.259	0.312	0.340	0.360
$\gamma/(\beta + \gamma)$	0.430	0.462	0.570	0.668
KI + KF				
$_q'K/\mu F\,cm^{-2}$	59.0	58.4	59.0	61
$_qK/\mu F\,cm^{-2}$	22.1	23.2	24.8	26.2
$(x_2 - x_1)/x_2$	0.375	0.398	0.420	0.430
$\gamma/(\beta + \gamma)$		0.600	0.596	

the results for the pure KI system plotted according to eqn. (23) and also according to eqn. (14) of ref. 11 which neglects the adsorption of cations; it is evident that the latter yields values of $\gamma/(\beta+\gamma)$ which are too low. It may therefore be concluded that equations based on eqn. (23) give a more accurate representation of ionic adsorption.

ACKNOWLEDGEMENTS

We express our gratitude to the British Council for a fellowship to E.D. for the year 1962–3 during which this work was carried out, and also to the D.S.I.R. for a grant for the apparatus comprising the a.c. bridge.

SUMMARY

Double-layer capacities have been measured in aqueous KI + KF solutions at constant ionic strength and 25° using a dropping-mercury electrode. The advantages of the thermodynamic analysis of such a system are presented. The results show that imaging in the diffuse layer exists but is not perfect. They also demonstrate that the salt activity and not the anion activity determines the amount of anion adsorption. The calculation of the potential distribution in the inner layer is discussed in the light of this conclusion.

REFERENCES

1 O. A. ESIN AND V. SHIKOV, *Zh. Fiz. Khim.*, 17 (1943) 236.
2 B. V. ERSHLER, *Zh. Fiz. Khim.*, 20 (1946) 679.
3 C. A. BARLOW AND J. R. MACDONALD, *J. Chem. Phys.*, 40 (1964) 1535, paper presented at the 38th National Colloid Symposium, A.C.S., Austin, Texas, 11th June, 1964.

4 D. C. GRAHAME, *J. Am. Chem. Soc.*, 80 (1958) 4201.
5 G. J. HILLS AND R. PAYNE, *Trans. Faraday Soc.*, 61 (1965) 316.
6 R. PARSONS AND F. G. R. ZOBEL, *J. Electroanal. Chem.*, 9 (1965) 333.
7 R. PARSONS, *Canad. J. Chem.*, 37 (1958) 308.
8 R. PARSONS, *Trans. Faraday Soc.*, 55 (1959) 999.
9 D. C. GRAHAME, *Chem. Rev.*, 41 (1947) 441.
10 R. PARSONS, *Proceedings 2nd International Congress of Surface Activity*, edited by J. H. SCHULMAN, Butterworths, London, Vol. III, 1957, p. 118, G. A. H. ELTON and D. P. BENTON, *ibid.*, p. 119.
11 J. M. PARRY AND R. PARSONS, *Trans. Faraday Soc.*, 59 (1963) 241.

THE EFFECT OF AMALGAM FORMATION ON THE POTENTIAL OF THE SATURATED CALOMEL ELECTRODE

A. M. SHAMS EL DIN AND L. A. KAMEL
Laboratory of Electrochemistry and Corrosion, National Research Centre, Dokki, Cairo (U.A.R.)
(Received May 20th, 1965)

INTRODUCTION

Recent publications from this laboratory have reported on the anodic behaviour of zinc[1] and cadmium[2] amalgams in alkaline solutions. These amalgams were found to behave as zinc or cadmium electrodes of metal atom activities equal to the mole fraction in mercury. The mercury of the anode, although present in amounts as high as 10^4 times those of the alloyed elements, lost its identity completely and did not show its characteristic oxidation step[3]. Similarly, the work of HICKLING *et al.*[4] on the anodic dissolution of metallic amalgams in non-complexing media revealed that dissolution took place at potentials near the standard values of the respective alloyed element. From these results, one might anticipate that calomel electrodes prepared from impure mercury would give rise to potentials other than the thermodynamically reversible mercury/mercurous chloride electrode. The object of the present investigation is to establish the extent to which amalgam formation affects the potential of the saturated calomel electrode (S.C.E.), and to determine the conditions under which such electrodes will function properly as reference electrodes. No work on the calomel electrode from this stand-point has been published hitherto[5].

EXPERIMENTAL

Saturated calomel electrodes were prepared with dilute (liquid) amalgams of zinc, cadmium, tin, lead, copper and silver in glass cups 10 cm long and 1.67 cm in inner diameter, provided with platinum contacts. The amalgams were prepared electrolytically *in situ*. The deposition bath was normally the metal sulphate dissolved in N H_2SO_4. Lead was plated from lead acetate + 0.4 N acetic acid, and silver from silver nitrate + 0.2 N nitric acid. The exact metal content of the plating baths was determined by standard analytical procedures. A known amount of the acid solution was introduced into the cup which contained 1.5 cm^3 of doubly-distilled mercury and electrolysis was carried out with a fixed current of 40 mA/electrode, with mercury acting as the cathode. A short platinum wire served as anode. Both the solution and mercury were stirred continuously with a short glass rod. The completion of metal deposition was marked by a brisk evolution of hydrogen from the surface of the cathode. Electrolysis was, however, continued for a further 15 min. Spot tests on portions of the residual acid solution confirmed the absence of the metal ions. The

amalgam was washed several times with doubly-distilled water and then dried with narrow strips of filter paper. Calomel electrodes were prepared by covering the amalgam with a paste, *ca.* 1 mm thick, of Hg_2Cl_2 followed by a saturated solution of KCl. The moment of addition of the calomel paste was considered as the zero time of preparation of the electrode. The potential of the amalgam electrode was measured as a function of time relative to a standardized S.C.E. on a Pye precision vernier potentiometer to ± 1 mV. Unless otherwise stated, the experiments were conducted at a room temperature of 24–26°. The surface area of the electrode was computed according to: area $=\pi(r^2+h^2)$, where r is the inner radius of the cup and h is the curvature of mercury.

RESULTS

Saturated calomel electrodes prepared from impure mercury give rise to initial potentials far removed from the expected zero values. The time–potential

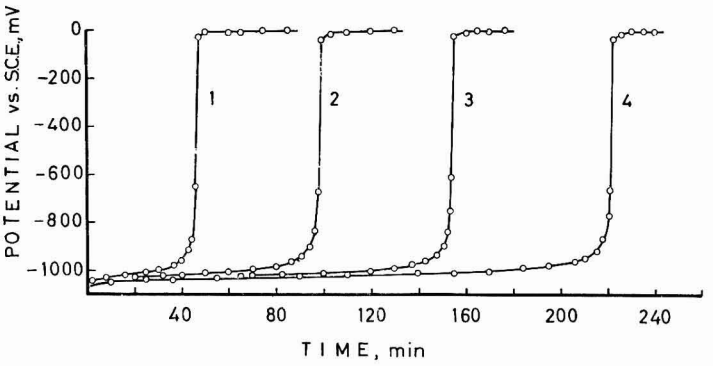

Fig. 1. Time–potential curves for S.C.E.s of Zn amalgams. (1), $3.2 \cdot 10^{-2}$; (2), $6.4 \cdot 10^{-2}$; (3), $9.6 \cdot 10^{-2}$; (4), $1.28 \cdot 10^{-1}$ wt.% Zn.

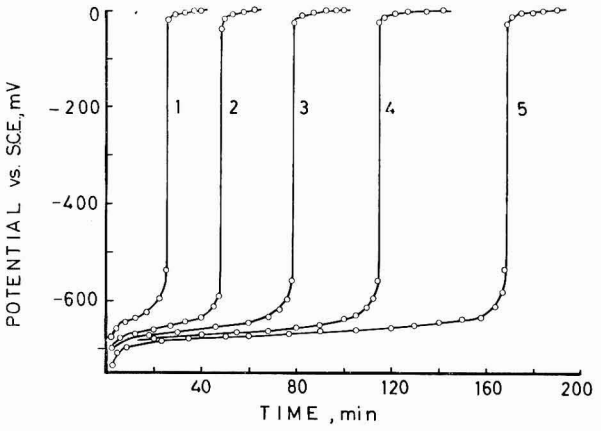

Fig. 2. Time–potential curves for S.C.E.s of Cd amalgams. (1), $1.4 \cdot 10^{-2}$; (2), $2.8 \cdot 10^{-2}$; (3), $4.2 \cdot 10^{-2}$; (4), $5.6 \cdot 10^{-2}$; (5), $8.4 \cdot 10^{-2}$ wt. % Cd.

curves of Figs. 1–3 show the effect of increasing amounts of zinc, cadmium and lead in mercury on the potentials of such electrodes. Similar curves were obtained when the mercury was contaminated with tin or copper. The magnitude of the potential difference between the pure and contaminated electrodes (*i.e.*, the effect of impurity)

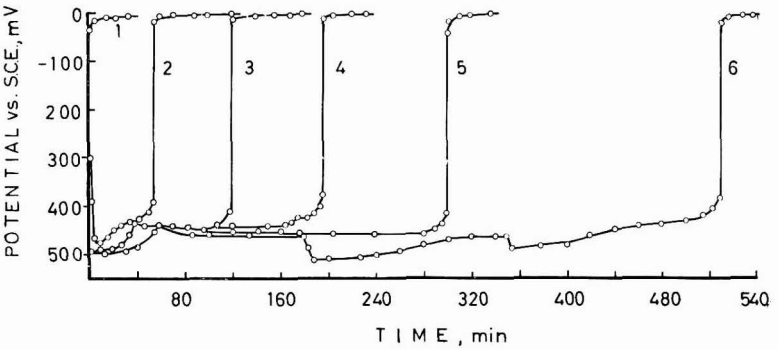

Fig. 3. Time–potential curves for S.C.E.s of Pb amalgams. (1), $3.6 \cdot 10^{-3}$; (2), $4.8 \cdot 10^{-3}$, (3), $6.0 \cdot 10^{-3}$; (4) $7.2 \cdot 10^{-3}$; (5), $8.4 \cdot 10^{-3}$; (6), $1.1 \cdot 10^{-2}$ wt. % Pb.

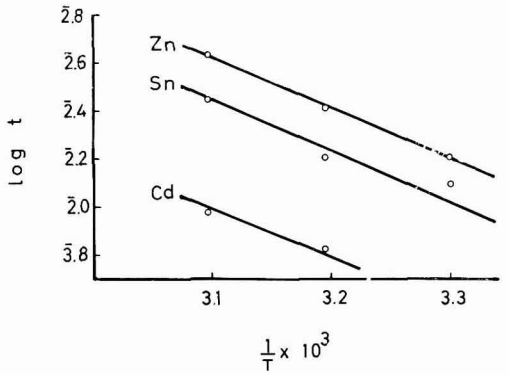

Fig. 4. Variation of $\log \tau$ with $1/T$.

depended mainly upon the type, and to a lesser extent, amount of impurity in the mercury. Average initial potentials are severally: zinc −1100, cadmium −650, tin −500, lead −450 and copper −170 mV. These potentials did not, however, persist indefinitely. After a certain time the potentials changed, rather quickly, to approach the expected value of the S.C.E. The time, τ, after which this rapid rise in potential occurred, depended again on the type of the contaminant. Within the concentration range studied, τ varied (except for lead, see later) almost linearly with the amount of impurity present in mercury.

The effect of temperature on the rate of attainment of zero potentials was studied with zinc, cadmium and tin amalgams in the range 30–50°. The increase in temperature was associated with a corresponding decrease in τ. The plot of the logarithm of τ as a function of $1/T$ for the three amalgams is shown in Fig. 4. The

lines are almost parallel and an activation energy of 9.6 kcal/g atom is calculated from their slope.

To check the effect of the electrode area, experiments were carried out with a $3.2 \cdot 10^{-2}$ wt. % zinc amalgam using electrodes of areas 2.30, 2.98 and 3.31 cm^2. Zero potentials were registered after 36, 22 and 18 min, severally.

Provided that the surface area was kept constant, the increase in the volume of the amalgam was associated with a corresponding increase in τ. Thus, for example, with 1.5, 3.0 and 4.5 ml of a $3.2 \cdot 10^{-2}$ wt. % zinc amalgam of 2.30 cm^2 surface area, zero potentials were established after 37, 66 and 107 min, respectively.

τ was also a function of the KCl concentration in the aqueous phase. Saturated-, 1 *M*- and 0.1 *M* calomel electrodes prepared of $3.2 \cdot 10^{-2}$ wt. % zinc amalgams, established zero potentials after 37, 240 and 950 min, respectively.

The behaviour of calomel electrodes in which the mercury was contaminated with more than one impurity was studied in detail with the zinc + cadmium and the zinc + tin systems. The results obtained were practically the same whether the zinc content of the amalgam was kept constant and that of cadmium (tin) varied, or when the zinc content was increased while keeping the amount of the second impurity

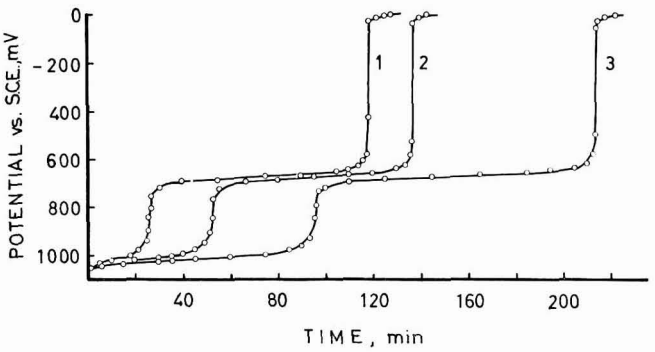

Fig. 5. Time–potential curves for S.C.E.s of Zn + Cd amalgams. (1), $3.2 \cdot 10^{-2}$ wt. % Zn + $5.6 \cdot 10^{-2}$ wt. % Cd; (2), $6.4 \cdot 10^{-2}$ wt. % Zn + $5.6 \cdot 10^{-2}$ wt. % Cd; (3) $9.6 \cdot 10^{-2}$ wt. % Zn + $5.6 \cdot 10^{-2}$ wt. % Cd.

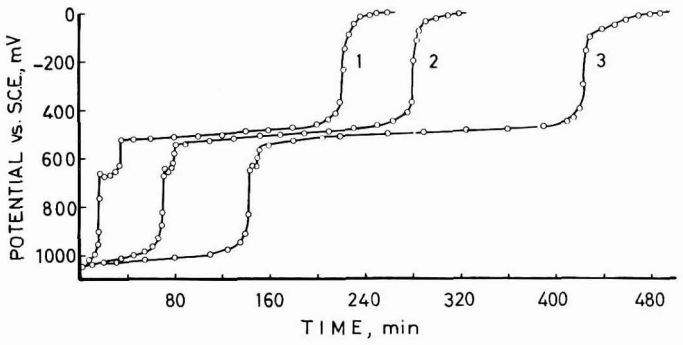

Fig. 6. Time–potential curves for S.C.E.s of Zn + Sn amalgams. (1), $3.2 \cdot 10^{-2}$ wt. % Zn + $1.16 \cdot 10^{-2}$ wt. % Sn; (2) $6.4 \cdot 10^{-2}$ wt. % Zn + $1.16 \cdot 10^{-2}$ wt. % Sn; (3), $9.6 \cdot 10^{-2}$ wt. % Zn + $1.16 \cdot 10^{-2}$ wt. % Sn.

constant. Time–potential curves for these two systems are depicted in Figs. 5 and 6. Experiments with mixed cadmium + tin amalgams were also conducted. In this case, however, the separation of the two arrests was not clear owing to the proximity of the two discharge potentials.

DISCUSSION

The bulk of the experimental results on the slow variation-with-time of the potential of S.C.E.s of impure mercury at the foot of the curves, as well as the subsequent rapid rise of the potential to zero values suggest the dissolution of the metal contaminations. The dissolution process can be formulated by the general reaction:

$$Hg_2Cl_2 = Hg_2^{2+} + 2\ Cl^-$$
$$M(Hg) + Hg_2^{2+} = M^{2+} + 2\ Hg \qquad (1)$$

These displacement reactions are favoured by a decrease in free energy which depends upon the particular impurity in mercury. A consideration of this free energy decrease[6] reveals, also, that during the discharge of lead and copper amalgams, $PbCl_2$ and Cu^+ ($CuCl_2^-$) are the most probable anodic products. The fact that the discharge potentials are very near to the standard values of the respective metal impurity under the prevailing experimental conditions, indicates that the amalgam electrodes are functioning as electrodes of the first kind rather than calomel electrodes.

There is convincing evidence to indicate that the discharge of the amalgams under consideration is governed by the rate at which the metal atoms diffuse to the amalgam/electrolyte interface.

(i) The activation energy of the discharge process, 9.6 kcal/g atom, is practically independent of the type of metal impurity present in mercury, Fig. 4. This value is, however, *ca.* 10 times larger than that associated with the anodic dissolution of similar amalgams in non-complexing media[4]. The difference appears to be related to the fact that the driving force in the discharge reactions in the S.C.E. is the result of transformations occurring at a solid interface (Hg_2Cl_2). Compared with the free dissolution under the influence of an anodic potential, such reactions appear to be intrinsically slow.

(ii) Analysis of the mercury of the electrode directly after the establishment of zero-potentials proved the alloyed element to be present. The analysis was carried out electrometrically by subjecting a portion of the amalgam to anodic oxidation in 0.1 *N* NaOH solution[1,2] in a separate polarization cell. The curves thus obtained, Fig. 7, show clear arrests corresponding to the formation of $Zn(OH)_2$ or $Cd(OH)_2$ on the surface of the electrode before the potentials for the oxidation of mercury (curve 1) or evolution of oxygen (curve 2) were established. If the dissolution arrests of Figs. 1–3 (and the like) denote the coulombic discharge of the alloyed elements, only the oxidation arrest for mercury[3] would result in the polarization experiments.

(iii) Reaction (1) occurs as a result of a constant free energy (potential) drop at the mercury/electrolyte interface which is primarily a function of the Hg_2^{2+} ion activity. This latter is fixed through the solubility product of Hg_2Cl_2 and the Cl^- ion activity in solution. Also, the exchange of mercurous ions by metal ions is not expected to affect the electrolytic conductance at the interface, since the electrolyte is extremely dilute with respect to these ions. The dissolution of the metal impurity

can, accordingly, be considered as taking place under the influence of a constant anodic current. The application of the theory of voltammetry at controlled currents[7] to the bulk of data at hand confirms this conclusion and adequately explains the experimental findings. Thus, the average current density for dissolution can be written as[7]:

$$\bar{\imath} = nFD_1\left(\frac{\partial C_1(x,\, t)}{\partial x}\right)_{x=0} \tag{2}$$

where n is the number of electrons involved in the reaction, F the Faraday of electricity, D_1 the diffusion coefficient of the metal atom in mercury, and the term in brackets, the concentration gradient at the interface. Relation (2) represents the boundary condition for the dissolution reaction. The initial conditions are:

$C_1(x, 0) = C_1^0$ and $C_2(x,0) = 0$, where C_1 and C_2 refer to the concentration of the

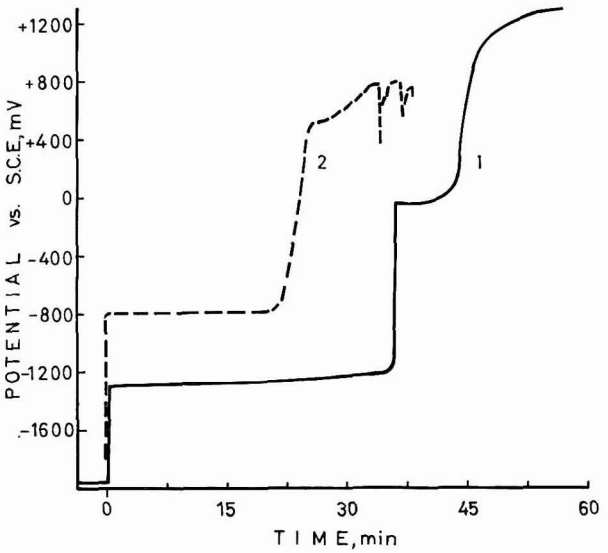

Fig. 7. Anodic behaviour of (1) Zn and (2) Cd amalgams in 0.1 N NaOH after attainment of zero-potentials (see text). Anodic currents; (1), 400; (2), 60 μA/electrode.

metal atom in mercury, and metal ion in solution, respectively. Finally, $C_1(x,t)$ and $C_2(x,t)$ tend severally to C_1^0 and 0 when x tends to infinity.

The solution of the differential equation under these conditions is given as[7]:

$$C_1(x, t) = C_1^0 - \frac{2\beta D_1^{\frac{1}{2}} t^{\frac{1}{2}}}{\pi^{\frac{1}{2}}} \exp\left(-\frac{x^2}{4D_1 t}\right) + \beta x \operatorname{erf}\left(\frac{x}{2\, D_1^{\frac{1}{2}} t^{\frac{1}{2}}}\right) \tag{3}$$

$$C_2(x, t) = \frac{2\,\beta D_1 t^{\frac{1}{2}}}{D_2^{\frac{1}{2}} \pi^{\frac{1}{2}}} \exp\left(-\frac{x^2}{4D_2 t}\right) - \frac{\beta x D_1}{D_2} \operatorname{erfc}\left(\frac{x}{2 D_2^{\frac{1}{2}} t^{\frac{1}{2}}}\right) \tag{4}$$

where $\beta = i/nFD_1$ and erfc stands for the complement of the error function: erfc

$(y) = 1 - \mathrm{erf}\,(y)$. D_1 and D_2 are, respectively, the diffusion coefficient in mercury and solution. At the electrode surface ($x = 0$), eqns. (3) and (4) reduce to:

$$C_1(0, t) = C_1^0 - \frac{2\beta D_1^{\frac{1}{2}} t^{\frac{1}{2}}}{\pi^{\frac{1}{2}}} \tag{5}$$

and

$$C_2(0, t) = \frac{2\beta D_1 t^{\frac{1}{2}}}{D_2^{\frac{1}{2}} \pi^{\frac{1}{2}}} \tag{6}$$

Substitution of these values in the Nernst equation gives:

$$E = E^0 + \frac{RT}{nF} \ln \frac{f_2 D_1^{\frac{1}{2}}}{f_1 D_2^{\frac{1}{2}}} - \frac{RT}{nF} \ln \frac{C^0 - Pt^{\frac{1}{2}}}{Pt^{\frac{1}{2}}} \tag{7}$$

where

$$P = \frac{2\beta}{\pi^{\frac{1}{2}} D_1^{-\frac{1}{2}}} = \frac{2i}{\pi^{\frac{1}{2}} nF D_1^{\frac{1}{2}}}$$

and f is the activity coefficient.

According to eqn. (7), the potential changes sharply towards more positive values when the time, t, has the value τ defined as: $\tau^{1/2} = C^0/P$. Equation (7) can accordingly be rewritten as[7]:

$$E = E^0 - \frac{RT}{nF} \ln \frac{\tau^{\frac{1}{2}} - t^{\frac{1}{2}}}{t^{\frac{1}{2}}} \tag{8}$$

Assuming that both the activity coefficients and the diffusion coefficients are independent of concentration, eqn. (8) predicts that the potential E should vary with $\log (\tau^{1/2} - t^{1/2}/t^{1/2})$, and that the slope of the line amounts to $2.303\ RT/nF$. Such plots for $6.4 \cdot 10^{-2}$ wt. % zinc, $8.4 \cdot 10^{-2}$ wt. % cadmium, $1.74 \cdot 10^{-1}$ wt. % tin and $9.3 \cdot 10^{-2}$ wt. % copper amalgams are given as examples in Fig. 8. The analysis of the

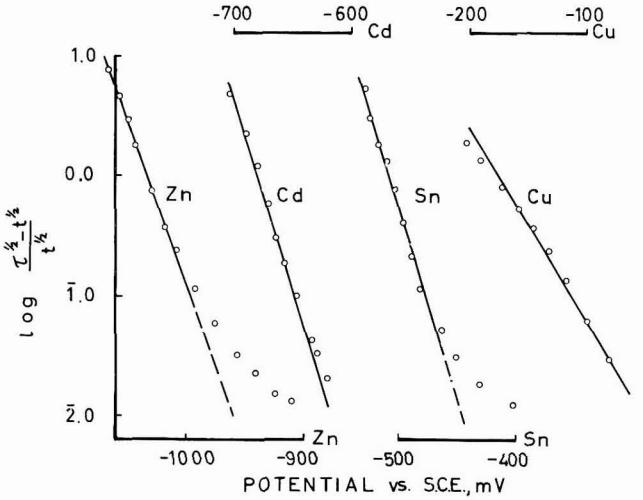

Fig. 8. Theoretical analysis of the discharge curves of amalgams of Zn, Cd, Sn and Cu.

discharge curves of amalgams of other concentrations gave similar lines ($\pm$10 mV) with practically the same slope. For cadmium, tin and zinc, the slopes of the lines are respectively 30, 30 and 36 mV, in good agreement with those expected for Cd^{2+}, Sn^{2+} and Zn^{2+} formation, although in the last case deviation from linearity sets in at advanced times. In the case of copper amalgam, the slope of the analysis line is 60 mV, supporting the conclusion that copper dissolves in the monovalent state.

According to DELAHAY[7], the $\acute{E}^\circ$ term in eqn. (8) is precisely the half-wave potential of the polarographic reduction wave of the metal ion from the same supporting electrolyte on the dropping mercury electrode. In Table 1, a comparison is made between the values of $\acute{E}^\circ$ calculated in the present study, and the available data on the half-wave potentials of the various metal ions in comparable ground electrolytes. Despite the difference in concentration and/or type of the supporting electrolyte, the figures of Table 1 show a fair agreement between the values of $\acute{E}^0$ and $E_{\frac{1}{2}}$, which supports the idea that diffusion is determining the process of amalgam discharge.

TABLE 1

COMPARISON BETWEEN THE VALUES OF $\acute{E}^0$ IN EQN. (8) AND THE POLAROGRAPHIC HALF-WAVE POTENTIALS

Ion	$\acute{E}^0$	$E_{\frac{1}{2}}$	*Supporting electrolyte*	*Ref.*
	(V vs. S.C.E.)			
Cd	−0.680	−0.642	1 *M* KCl	8,a
		−0.599	0.1 *M* KCl	8,a
Sn	−0.508	−0.470	1 *N* HCl	8,b
Cu	−0.176	−0.220	1 *N* HCl	8,c
Zn	−1.033	−0.995	0.1 *M* KCl	9
		−1.022	1 *M* KCl	8,d
Pb	(−0.450)	−0.435	1 *M* KCl	8,e
		−0.395	0.1 *M* KCl	8,e

() average discharge potential

(iv) The effect of electrode area and amalgam concentration on the time, τ, lends further support to the concept of rate-determining diffusion. Thus, for the same amalgam composition, the increase in the surface area of the electrode leads to a corresponding decrease in τ. The product $A\tau^{\frac{1}{2}}$ is practically constant. Similarly, for a constant electrode area, τ increases linearly with the concentration of the amalgam. Both effects suggest that τ is a function of (dN/dt), where N is the number of metal atoms crossing the interphase. dN/dt can be set equal to $V\ dC/dt$, where V is the volume of the amalgam, which explains also the linear variation of τ with the volume of the amalgam.

(v) The driving force causing the discharge of the impurity can be varied by changing the Cl^- concentration (activity) of the electrode. Experiment has shown that τ increases proportionally with the Hg_2^{2+} ion activity at the interphase. Complete elimination of the metal impurity can be secured in solutions of a high enough concentration of Hg_2^{2+}, *e.g.*, acidified mercurous nitrate, as is usually done in the purification of mercury. If τ were to denote the coulombic discharge of the impurity, it

would have been dificult to explain its dependence on the KCl concentration of the electrode.

The behaviour of calomel electrodes in which the mercury is contaminated by lead deserves particular mention. When the lead in mercury is present in minute amounts, the potential of the electrode approaches the zero value almost instantaneously, curve 1, Fig. 3. On increasing the lead content of the amalgam, an initial potential of *ca.* −450 mV is recorded. This value is in close proximity with that expected for the reaction:

$$Pb + 2\,Cl^- = PbCl_2 + 2\,e \qquad (9)$$

under the prevailing experimental conditions. During discharge, however, oscilla tions in potential are recorded, apparently due to the alternate formation and breakdown of a lead chloride film which isolates the electrode from the electrolyte, Fig. 3. This explains the experimental finding that the times after which zero potentials are established are not proportional to the lead content in mercury, as is the case with the other amalgams.

Of particular interest is the behaviour of calomel electrodes in which the mercury is contaminated by more than one impurity. Generally, each of the amalgamated metals discharges at its respective potential and behaves as if it alone were present in mercury. As examples for such a behaviour, the discharge curves of different zinc+cadmium and zinc+tin amalgams are depicted in Figs. 5 and 6, respectively. The first discharge step for zinc in both amalgams occurs over periods which are either equal to or slightly larger than those for single zinc amalgams of comparable composition. The second discharge arrest occurs over periods which are invariably much longer than those for similar single cadmium (tin) amalgams under the same conditions. Thus, for example, during the discharge of amalgams containing $6.4 \cdot 10^{-2}$ wt. % zinc +1.4, 2.8, 5.6 and $8.4 \cdot 10^{-2}$ wt. % cadmium, the dissolution of zinc occurs over 138, 122, 106 and 104 min, respectively, as compared to 100 min for a zinc amalgam of the same concentration. The discharge of cadmium from the abovementioned amalgams takes place over 45, 95, 167 and 425 min, severally. The corresponding figures for single cadmium amalgams are successively 25, 48, 114 and 168 min. Similar results were obtained when the cadmium content of the amalgam was kept constant and that of zinc varied, Fig. 5.

The discharge curves of amalgams containing zinc+tin present still a new feature. These curves, Fig. 6, show the development of a new step at potentials intermediate between those for zinc and tin alone. This step is more pronounced the lower the zinc/tin ratio. The time elapsed before the start of the tin step, *i.e.*, the time taken in the first two steps, is practically that associated with the discharge of single zinc amalgams of the same content as in the mixture. The new step represents, therefore, the completion of the discharge of the zinc of the amalgam. This delayed dissolution of zinc is most probably related to the formation, within the amalgam, of a zinc–tin intermetallic compound the zinc component of which, by virtue of its reduced activity, will dissolve at more positive potentials. The formation of such intermetallic compounds has been studied recently by a number of authors[10].

A common feature of the discharge curves of mixed amalgams is that the second discharge step occurs over times much longer than for single amalgams of comparable concentrations. This is most probably due to the occurrence of alter-

native displacement reactions between the noble-metal ions in solution and the less-noble metal atoms at the amalgam interface. Thus, for example, when tin enters the solution while the amalgam still contains the more-reactive zinc, the displacement reaction:

$$Zn + Sn^{2+} = Zn^{2+} + Sn \qquad (10)$$

takes place. The result of this reaction is that the surface concentration of tin in the amalgam is raised above that in the bulk, and correspondingly its discharge time increases. The step at the tin potential represents, in fact, the dissolution of both tin and zinc. Displacement reactions similar to (10) were suggested to be operative on dropping[11] as well as on stationary[4] amalgam electrodes.

Silver, being more noble than mercury, does not displace the latter from Hg_2Cl_2, and consequently does not affect the potential of the S.C.E. Similarly, iron, cobalt, nickel and chromium, which are practically insoluble in mercury, have no effect.

The results of the present investigation lead to the conclusion that unless the S.C.E. is of very pure mercury, it should be given ample time to discharge its impurity and to establish its reversible potential. The non-recognition of this fact, and the application of electrodes of impure mercury, as reference directly after their preparation, might give rise to potentials far removed from the expected values. The extent of potential shift depends on the type and concentration of the impurity in mercury. The same conclusion applies also to other mercury-based reference electrodes, *e.g.*, the Hg/Hg_2SO_4 or the Hg/HgO electrodes[12].

SUMMARY

Saturated calomel electrodes prepared from amalgams of zinc, cadmium, tin, lead and copper give rise to initial potentials very near to the standard metal/metal ion potential of the respective impurity. After a certain time, τ, the potential changes quickly to reach that of the S.C.E. τ depends on the type and concentration of the impurity in mercury, as well as on electrode area, temperature, amalgam volume and Cl^- ion concentration. The results are quantitatively explained on the basis of the diffusion of the metal impurity to the amalgam/electrolyte interface. Electrodes prepared of amalgams containing two impurities show discharge steps for each of the amalgamated metals. A S.C.E. prepared from impure mercury should be allowed sufficient time to discharge its impurities and establish its expected potential.

REFERENCES

1 S. E. KHALAFALLA, A. M. SHAMS EL DIN AND Y. A. EL TANTAWY, *J. Phys. Chem.*, 63 (1959) 1252.
2 A. M. SHAMS EL DIN, S. E. KHALAFALLA AND Y. A. EL TANTAWY, *J. Phys. Chem.*, 65 (1961) 1484.
3 A. M. SHAMS EL DIN, S. E. KHALAFALLA AND Y. A. EL TANTAWY, *J. Phys. Chem.*, 62 (1958) 1307.
4 A. HICKLING AND J. MAXWELL, *Trans. Faraday Soc.*, 51 (1955) 44.
A. HICKLING, J. MAXWELL AND J. V. SHENAN, *Anal. Chim. Acta*, 14 (1956) 287.
5 D. J. G. IVES AND G. J. JANZ, *Reference Electrodes*, Academic Press, 1961, 127.
6 W. M. LATIMER, *Oxidation Potentials*, Prentice Hall, 1953, p. 183.
7 P. DELAHAY, *New Instrumental Methods in Electrochemistry*, Interscience, New York, 1954, p. 179.

8 G. W. C. MILNER, *The Principles and Applications of Polarography*, Longmans, New York, 1957, (a) p. 204; (b) p. 263; (c) p. 214; (d) p. 283; (e) p. 228.
9 I. M. KOLTHOFF AND J. J. LINGANE, *Polarography*, Interscience, 1952, p. 503.
10 A. S. RUSSEL, P. V. F. CAZELET AND N. M. IRVIN, *J. Chem. Soc.*, (1932) 841; W. KEMULA, Z. GALUS AND Z. KUBLIK, *Nature*, 182 (1958) 1228; W. KEMULA, *Advances in Polarography*, edited by J. S. LONGMUIR, Pergamon Press, 1960, 105.
H. K. FICKER AND L. MEITES, *Anal. Chim. Acta*, 26 (1962) 172.
11 N. H. FURMAN AND W. C. COOPER, *J. Am. Chem. Soc.*, 72 (1950) 5667.
12 A. M. SHAMS EL DIN, L. A. KAMEL AND F. M. ABD EL WAHAB, in preparation.

POLAROGRAPHIC BEHAVIOUR OF HAFNIUM(IV) IN AQUEOUS–ALCOHOLIC MIXTURES

J. SANCHO, J. ALMAGRO AND A. PUJANTE

Laboratory for Physical Chemistry and Electrochemistry, Faculty of Science, University of Murcia (Spain)

(Received April 21st, 1965)

INTRODUCTION

The polarographic behaviour of hafnium has been investigated by GUTMANN AND SCHOBER[1] using $N(Et)_4NO_3$, 0.1 *M*, as supporting electrolyte; they found two waves for the reduction of this element. Later, OLVER AND ROSS[2] carried out a study of the behaviour of $HfCl_4$ (similar to that done with $ZrCl_4$ in acetonitrile) with perchlorate and tetraalkylammonium halide as supporting electrolytes. These authors found three reduction waves, at −0.60, −1.63 and −1.80 V in perchlorate medium and one wave at a potential of −2.4 V in halide medium, using a mercury pool as reference electrode.

Other authors have studied hafnium at the mercury dropping electrode with EDTA[3].

We have studied the reduction mechanism at the dropping electrode of Hf(IV) in various water–alcohol mixtures, using conventional polarographic, derivative polarography and micro-coulometry.

EXPERIMENTAL CONDITIONS

Equipment

A conventional cell shaped as a short, wide test-tube was used. The cell was tightly closed with a rubber stopper bored with holes for the capillary, the bridge of the calomel electrode, a thermometer, and an entry and an exit tube for the passage of inert gas.

TABLE 1

CAPILLARY CHARACTERISTICS FOR DIFFERENT CONDITIONS

Potential, −1.80 V

Strength of EtOH used for 0.1 M LiCl soln. (% v/v)	*Effective height Hg (cm)*	*m (mg/sec)*	*Drop-time (sec)*	$m^{2/3}t^{1/6}$
5	38.22	1.525	3.94	1.665
25	38.08	1.529	3.95	1.669
50	38.22	1.495	4.03	1.651
75	38.12	1.519	4.24	1.631

The Radiometer capillary was 15 cm long and 96 μ in diameter. The characteristics for flow, dropping time etc., for different conditions, are given in Table 1.

The recording apparatus was a direct-recording model PO4 Radiometer polarograph, using a circuit for derivative polarography in which the potential is applied to the cell by means of a drum revolving at constant speed; the bell-shaped curve is recorded directly on the recording chart. The feed current was supplied by a Philips 7776 stabiliser, achieving 0.2% stability.

A thermostat was used to keep the temperature in the cell constant to within $\pm 0.05°$.

The source of constant current for micro-coulometry was that described by MARK JR., SMITH AND REILLEY[4].

Reagents

Mercury was twice vacuum-distilled and electrolytically purified as described in previous papers from this laboratory[5].

$HfOCl_2 \cdot 8H_2O$ was prepared from 99.5% pure HfO_2 supplied by the E.H. Sargent & Co. This oxide was dissolved in concentrated sulfuric acid and $Hf(OH)_4$ which was then precipitated with ammonia, was immediately dissolved in concentrated hydrochloric acid. $HfOCl_2 \cdot 8H_2O$ crystallised in white needles which were dried before use.

Hydrochloric acid and *ammonia r.a.* were supplied by U.C.B.S.A.; *sulfuric acid* and *ethanol r.a.* by Probus; *lithium chloride r.a.* by Merck and *lithium hydroxide* by B.D.H. Ltd.

Nitrogen was taken from an industrial cylinder and the oxygen removed by passing the gas through (i) an ammonia solution with copper shavings, (ii) concentrated sulfuric acid solution, (iii) a calcium chloride drying tower and finally, (iv) a flask containing a lithium chloride solution in 5%, 25%, 50% or 75% ethanol.

Procedure

A 1 *M* solution of LiCl was prepared for diluting easily to 0.1 and 0.5 *M* when required. Similarly, a 10 *M* solution of LiCl was used for the preparation of a 1 *M* solution by dilution, and a 0.01 *M* solution of $HfOCl_2 \cdot 8H_2O$ in ethanol for dilutions to the range under investigation.

10 ml of solution was used in the cell, and nitrogen was passed over the solution for 20 min to remove oxygen. The temperature was kept constant at 25°, except in those cases when the influence of temperature on the behaviour of Hf(IV) was being studied.

The half-wave potentials were calculated by plotting E *vs.* $\log [i/(i_d - i)]$ and correcting for the potential drop within the cell. The diffusion current was measured on the polarogram by the tangent method.

The peak potentials of the polarograms obtained in derivative polarography were calculated graphically.

RESULTS

Hafnium in the range 10^{-3}–$5 \cdot 10^{-3}$ *M*, in LiCl, 0.1 *M*–5% ethanol, gives a polarographic wave increasing linearly with concentration. The i_d/C values remain

TABLE 2

POLAROGRAPHIC CHARACTERISTICS OF Hf(IV), $3 \cdot 10^{-3}$ *M*, WITH CHANGING CONCENTRATION OF THE SUPPORTING ELECTROLYTE AT DIFFERENT PROPORTIONS OF ETHANOL

% *EtOH*	*pH*	*0.1 M LiCl*		*0.5 M LiCl*		*1 M LiCl*	
		i_d	$E_{\frac{1}{2}}$	i_d	$E_{\frac{1}{2}}$	i_d	$E_{\frac{1}{2}}$
5	2.45±0.06	39.4	−1.590	34.0	−1.584	30.4	−1.584
25	2.43±0.10	32.8	−1.606	28.4	−1.571	25.2	−1.576
50	2.59±0.01	25.2	−1.575	20.4	−1.567	18.0	−1.560
75	2.81±0.11	16.4	−1.548	12.8	−1.530	9.8	−1.491

TABLE 3

POLAROGRAPHIC CHARACTERISTICS OF Hf(IV), $3 \cdot 10^{-3}$ *M*, IN LiCl, 0.1 *M*, WITH CHANGING TEMPERATURE AND EFFECTIVE HEIGHT OF THE MERCURY COLUMN, AT DIFFERENT PROPORTIONS OF ETHANOL

% *EtOH*	*pH*	*T coefficient (%/degree)*	*Slope of the graph log h_{eff}. vs. log i_d*
5	2.52	0.84	0.60
25	2.54	1.38	0.60
50	2.60	1.49	0.50
75	2.92	1.23	0.54

TABLE 4

DATA OF THE POLAROGRAPHY OF Hf(IV)

Supporting soln. % EtOH	*Concn. LiCl (M)*	*pH*	$E_{\frac{1}{2}}$ *(V vs. S.C.E.)*	*Slope E vs. log $[i/i_d - i]$*	*I*	E_p *(V vs. S.C.E.)*
5	0.1	2.52	−1.590	0.094	7.868	−1.650
5	0.5	2.42	−1.584	0.086	—	−1.630
5	1	2.40	−1.584	0.088	—	−1.635
25	0.1	2.54	−1.606	0.098	6.351	−1.630
25	0.5	2.42	−1.571	0.098	—	−1.610
25	1	2.34	−1.576	0.112	—	−1.610
50	0.1	2.60	−1.575	0.103	5.088	−1.630
50	0.5	2.60	−1.567	0.109	—	−1.615
50	1	2.58	−1.560	0.104	—	−1.600
75	0.1	2.92	−1.548	0.127	3.093	−1.600
75	0.5	2.82	−1.530	0.113	—	−1.575
75	1	2.70	−1.491	0.100	—	−1.530

TABLE 5

"*n*" VALUES (ELECTRONS TRANSFERRED) IN THE REDUCTION OF HAFNIUM(IV) IN SUPPORTING SOLN. 0.1 *M* LiCl–5% ETHANOL

Concn. Hf(IV) ($M \times 10^{-3}$)	*"n" (ref. 6)*	*"n" (ref. 4)*
1	—	1.03
1.5	0.94	—
2	1.03	0.75
2.5	—	0.84

roughly constant with changing concentration, although a slight increase has been observed. The I-value is also roughly constant. The half-wave potentials shift to more negative values with increasing concentration, and this is true for all the alcohol concentrations studied. The slope of the graph, E *vs.* log $[i/(i_d-i)]$, is very large in all cases. The effect of temperature on the $E_{\frac{1}{2}}$-values varies between 1 and 5 mV/degree.

In LiCl, 0.1 M–25% ethanol, the diffusion current is related rectilinearly with concentration. The I-values are almost constant with changing concentration, and the half-wave potentials become more negative with increasing temperature, varying between 2 and 8 mV/degree.

The behaviour of hafnium in LiCl, 0.1 M–50% ethanol, is much the same as in the preceding cases; the diffusion current is proportional to concentration, but as before, the i_d corresponding to the initial value of C, seems to be somewhat less than normal, because from this value on, the linearity is perfect. The i_d/C values are practically constant, and the values of the slope for E *vs.* log $[i/(i_d-i)]$ are between 0.098 V for 10^{-3} M and 0.117 V for $5 \cdot 10^{-3}$ M. The effect of temperature on the diffusion current is 1.49%/degree, and the half-wave potentials shift towards more positive potentials, with a variation of approximately 4 mV/degree. As the concentration of the supporting electrolyte increases, the half-wave potentials become more positive and the wave-heights decrease.

Similar behaviour was observed in LiCl, 0.1 M–75% ethanol; i_d varies linearly with increasing hafnium concentration; the effect of temperature on the $E_{\frac{1}{2}}$-values is 3 mV/degree.

Some interesting polarographic results have been recorded in Tables 2 and 3, *e.g.*, the effect of variation in the supporting electrolyte concentration and the influence of temperature and effective height of the mercury column. Other data

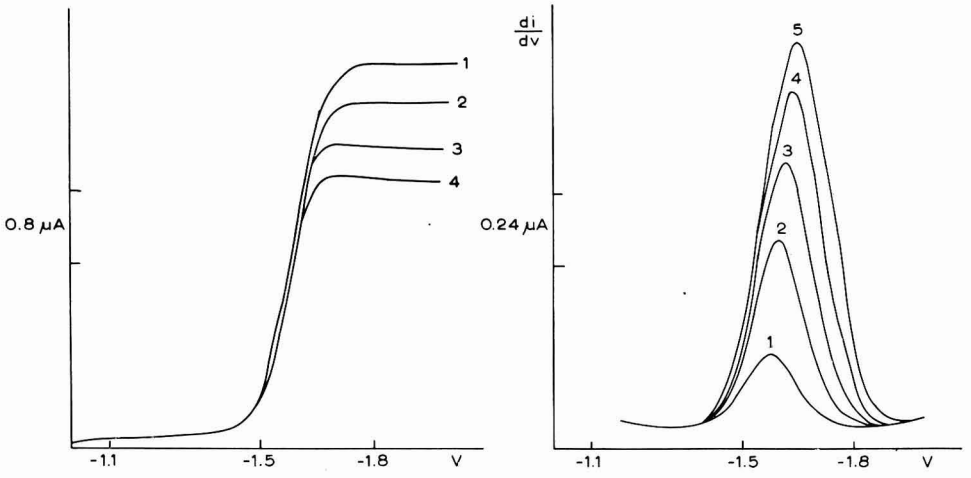

Fig. 1. Polarograms in supporting soln. 0.1 M LiCl–5% EtOH (pH = 2.52); concn. Hf(IV), $3 \cdot 10^{-3}$ M. h_{Hg}: (1), 40; (2), 35; (3), 30; (4), 25 cm.

Fig. 2. Polarograms in supporting soln. 0.1 M LiCl–50% EtOH; concn. Hf(IV): (1), 10^{-3}; (2), $2 \cdot 10^{-3}$; (3), $3 \cdot 10^{-3}$; (4), $4 \cdot 10^{-3}$; (5), $5 \cdot 10^{-3}$ M.

found in this study are given in Table 4, *i.e.*, half-wave potentials, diffusion current constant, peak potentials of the curves in derivative polarography and the slopes of E *vs.* $\log [i/(i_d - i)]$, all under different concentrations of the medium.

Figures 1 and 2 show the polarograms obtained in conventional polarography (with changing height of the mercury column), and derivative polarography (with changing hafnium concentration), respectively.

Micro-coulometric study

Two techniques have been used for this study. The first, due to GILBERT AND RIDEAL[6] which has been described in previous papers from this laboratory, follows the decrease of the wave-height with time of electrolysis, at constant potential. The second technique described by MARK JR., SMITH AND REILLEY[4], supplies a controlled current to the cell through a very large parallel capacitor, so that the current variations are corrected. This method has the advantage over methods using a constant applied potential, in that it prevents the shift of the dropping mercury electrode potential towards more negative values in the course of the electrolysis. Also, it greatly simplifies current integration

Experiments have been carried out with hafnium concentrations from 10^{-3}–$3 \cdot 10^{-3}$ M, using a micro-cell volume of 0.5 and 0.3 ml, respectively, for each method[8].

The results of both methods show that the reduction process of hafnium(IV) involves one electron (Table 5).

DISCUSSION

It has been proved that hafnium(IV) is reduced in one stage, producing one polarographic wave. The curves are well-defined, and the wave-height is proportional to concentration in every case.

The reduction process is usually diffusion-controlled, there being an approximation to the ideal diffusion state with increasing concentration of ethanol. This process has proved to be irreversible in all cases, and is very similar to that of zirconium.

The two methods used in the micro-coulometric study indicate that the process involves the participation of one electron. DESIDERI AND PANTANI[7] have suggested that the reduction is due to the hydrogen ion liberated when dissolving $HfOCl_2 \cdot 8H_2O$ in alcohol and alcohol–water,

$$Me^{4+} + 2\ EtOH \rightarrow Me(EtO)_2^{2+} + 2\ H^+$$

and not to that of hafnium. MASIK[9] and the present authors[10] have found similar phenomena with Th(IV), and HEYROVSKÝ[11] and ZUMAN[12] with Al(III).

The derivative polarographic study confirms that in the concentration range studied, there is only one reduction wave and that this wave is useful for analytical purposes.

SUMMARY

A polarographic study of hafnium has been carried out in lithium chloride (0.1, 0.5 and 1 M) in 5%, 25%, 50% and 75% (v/v) ethanol. One polarographic

wave was observed corresponding to a one-electron process agreeing with the microcoulometric study carried out at constant potential and constant current.

The observed wave is well-defined and useful analytically. The half-wave potentials have been measured against the saturated calomel electrode at different conditions of pH, temperature, and height of mercury column in the concentration range between 10^{-3} and $5 \cdot 10^{-3}$ M. The values for the diffusion current constant and the peak potentials obtained in derivative polarography, are also given.

REFERENCES

1 V. GUTMANN AND G. SCHÖBER, *Monatsh.*, 88 (1957) 206–15; *Z. Anal. Chem.*, 171 (1959) 339–43.
2 J. W. OLVER AND J. W. ROSS, JR., *J. Inorg. Nucl. Chem.*, 25 (12) (1963) 1515–19.
3 KUAN PAN, PENG-YOUNG SUN AND WEN-KUEI WONG, *J. Chinese Chem. Soc. (Taiwan)*, 8 (1961) 298–306.
4 H. B. MARK, JR., E. M. SMITH AND C. N. REILLEY, *J. Electroanal. Chem.*, 3 (1962) 98–111.
5 J. ALMAGRO, V. ALMAGRO AND J. SANCHO, *Anales Real Soc. Espan. Fis. Quim. Madrid, Sec. B*, 6 (1962) 459–68.
6 G. A. GILBERT AND E. K. RIDEAL, *Trans. Faraday Soc.*, 47 (1951) 396.
7 P. G. DESIDERI AND F. PANTANI, *Ric. Sci.*, 30 (1960) 2000–8.
8 A. PUJANTE, *Anales Univ. Murcia (Spain)*, to be published.
9 J. MASIK, *Collection Czech. Chem. Commun.*, 24 (1959) 159.
10 J. SANCHO, J. ALMAGRO AND A. PUJANTE, *Anales Real Soc. Espan. Fis. Quim. Madrid*, to be published.
11 M. HEYROVSKÝ, *Collection Czech. Chem. Commun.*, 25 (1960) 3120.
12 P. ZUMAN, *Chem. Listy*, 46 (1952) 326.

EFFECT OF HIGHLY SURFACE-ACTIVE COMPOUNDS ON POLAROGRAPHIC ELECTRODE PROCESSES

PART I. ELECTROCHEMICAL ADSORPTION AND STRUCTURE AT THE DROPPING MERCURY ELECTRODE–SOLUTION INTERFACE

R. G. BARRADAS AND F. M. KIMMERLE*

Lash Miller Chemical Laboratories, Department of Chemistry, University of Toronto, Toronto 5, Ontario (Canada)

(Received May 24th, 1965)

INTRODUCTION

Adsorption of organic compounds at electrodes has been reviewed extensively[1–3] and we are concerned with the effect of highly surface-active organic materials on the dropping-mercury electrode (D.M.E.) in polarographic processes. In an earlier communication[4] we reported very briefly on some *unusual* characteristics associated with the adsorption of surfactants that are capable of forming micelles at low bulk solution concentrations (CMC)**. Our principal aims here are (i) to elucidate the structure at the electrode–solution interface of the adsorbed film formed by these surfactants; (ii) to investigate the quantitative aspects of the effect and mechanism of maxima suppression especially from hydrodynamic considerations; and (iii) to examine the role of adsorption kinetics from current–time studies under convection- and diffusion-controlled conditions to implement the information obtained from the first two objectives.

The appearance of maxima and minima in current–voltage (i–E) curves in polarography are well known, but there remains a considerable amount of controversy regarding the theory and origin of these anomalies[5]. However, there seems to be general agreement that motion of the mercury surface and electrolyte streaming are common manifestations of maxima formation. A formidable list of neutral and ionic compounds has been cited as suitable maxima suppressors for a wide variety of polarographic analysis[6–8]. Many time-honoured prescriptions regarding the quantity of surfactant maxima suppressors to be used are often empirical and unsupported by theoretical reasons. We have chosen the first oxygen maximum for detailed quantitative study because of its common occurrence in almost every polarographic process. Since Triton X-100 is one of the most universal suppressors we have concentrated our attention on this compound, but we have also investigated related Tritons (X-45 and X-305) and other polyoxyethylenic compounds for comparative purposes. Our interest in these studies is also motivated by their relevance to an understanding of

* Holder of a National Research Council of Canada Studentship for 1964–1965.
** Critical Micelle Concentration

the adsorption behaviour of organic corrosion inhibitors[9–14]. Striking similarities have been reported between the processes involved in polarographic maxima and their suppression on one hand, and in metallic corrosion and its inhibition on the other[15].

In Part I of this study we shall confine ourselves to reporting the electrocapillary results and a discussion of the nature of adsorption of these surfactants at the D.M.E.–electrolyte interface. In Part II we shall report on the experimental aspects of the current–time studies and the discussion on maxima suppression, convection- and diffusion-controlled adsorption processes.

EXPERIMENTAL

Method, apparatus and chemicals used

The polarographic cell used, was designed on the basis of one described by GRIFFITHS AND JACKMAN[16], and all measurements were made at $25 \pm 1°$. The cell is connected by an agar–salt bridge to an external saturated calomel reference electrode. Potassium chloride of the highest analytical reagent-grade was dissolved in "equilibrium water" prepared as described previously[13,14]. Tritons X-100 and X-305 were obtained by courtesy of Rohm and Haas Co., Philadelphia, and used without further purification[17]. The solutions were de-aerated by bubbling nitrogen, which was purified by the vanadous chloride method recommended by MEITES[18], and then presaturated with "equilibrium water" prior to introduction to the cell. Ingress of oxygen or air during a run was prevented by maintaining a slightly positive pressure of nitrogen over the solution. Doubly-distilled mercury was further purified according to the procedure outlined by IVES AND JANZ[19].

Electrocapillary measurements were made by a conventional drop-time technique using a Radiometer Model PO4 Polarograph. The height of the mercury reservoir was adjusted so that the drop time, t_g, at the potential of the electrocapillary maximum (e.c.m.) or potential of zero charge (p.z.c.)[1] in a 0.1 *N* aqueous KCl solution was 4.920 sec with a corresponding drop weight of 7.94 mg. For each measurement, the D.M.E. was polarized at a fixed potential relative to the S.C.E., and at least 25 drops were counted and t_g measured by means of a precision stop-watch. Each set of measurements at a constant potential were repeated not less than three times. The electrocapillary data were obtained over a range of $+0.1$ to -1.1 V (S.C.E.), and the determination of drop times were taken at 50-mV intervals. The drop times were converted to surface tension units by calibration with published data for KCl solutions[20], and appropriate corrections were applied according to CORBUSIER AND GIERST[21]. The adsorption of pyridine in 0.1 *N* KCl solutions was determined as a test case by the drop-time method and also by means of a modern Lippmann electrocapillarometer[14]. Both sets of results agreed very favourably.

It should be pointed out that the Lippmann electrocapillarometer is unsatisfactory for examining organic materials of high adsorbability and strong wetting properties. It was previously observed that the adsorptions of acridine and N-methylacridinium chloride in aqueous KCl or HCl solutions were not easily measurable. Acridinium and N-methylacridinium ions tend to precipitate as the less soluble discharged species at high negative polarizations[22]. The difficulty encountered with neutral acridine molecules in KCl is largely attributable to its high surface activity.

The contrasting behaviour of pyridine and acridine may be compared with their relative surface adsorbabilities as indicated by their respective adsorption indices of 0.013 and 100, respectively[23]. For surfactants such as the Tritons, small amounts adsorbed on the glass capillary lower the contact angle of mercury–glass below the required value of 180°. The Tritons are strong wetting agents and at different electrode potentials varying amounts of water seep in between the mercury and glass making it impossible to determine surface tensions reproducibly at the Hg–electrolyte interface even for concentrations as low as 10^{-6} M (in Parts I and II of this work all concentration values stated in molar units are based on an average formula weight of each surfactant).

RESULTS AND DISCUSSION

(*a*) *Electrocapillary curves*

Figure 1 shows the variation of surface tension with concentration of Triton X-100 from 0.1 to −1.1 V (S.C.E.). The curves display a marked degree of asymmetry with increasing concentration of additive c_A. No breaks are observed at anodic potentials, but on the extreme cathodic side of the p.z.c. the curves break sharply from the one for the base electrolyte. The p.z.c. is progressively shifted to more positive potentials with increasing c_A. The amount of surface tension (γ) depression greatly exceeds those for the adsorption of alcohols, cyclic amines and ethers[10,14]

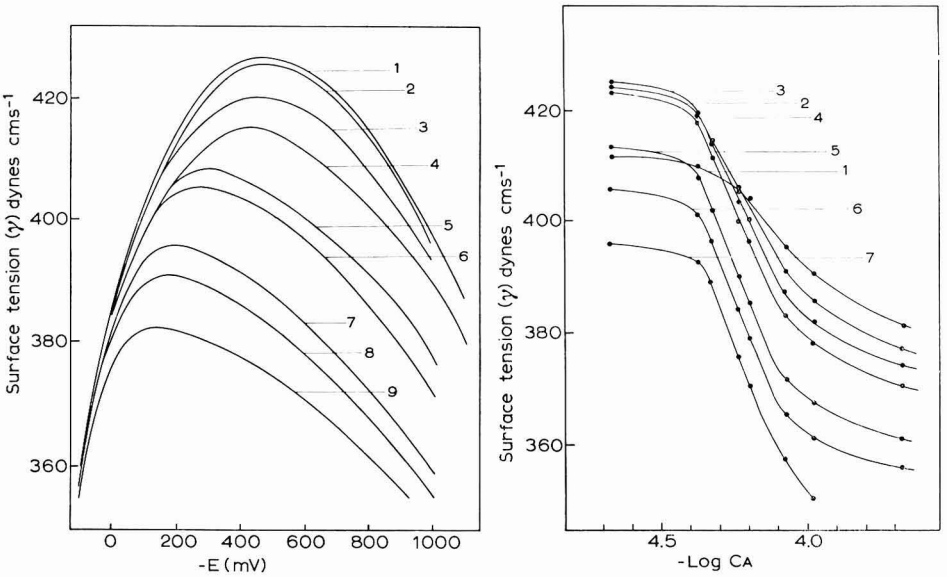

Fig. 1. Electrocapillary curves for Triton X-100 in 0.1 N aq. KCl: (1), 0.1 N KCl. (2), $3.0 \cdot 10^{-5}$; (3), $4.21 \cdot 10^{-5}$; (4), $4.68 \cdot 10^{-5}$; (5), $5.79 \cdot 10^{-5}$; (6), $6.31 \cdot 10^{-5}$; (7), $8.41 \cdot 10^{-5}$; (8), $1.01 \cdot 10^{-4}$; (9), $2.1 \cdot 10^{-4}$ M.

Fig. 2. Surface tension as a function of Triton X-100 concn. at various electrode potentials: (1), −200; (2), −400; (3), −500; (4), −600; (5), −800; (6), −900; (7), −1000 mV.

for comparable quantities of c_A. The morphology of these electrocapillary curves differs substantially from that reported for dimethyldodecylamine oxide[24,25], which should be comparable in some respects with Triton X-100 since both compounds are highly surface-active materials with strong wetting and foaming properties.

From the data in Fig. 1, we plotted γ against log c_A at several constant potentials and these are shown in Fig. 2. The form of these curves is very similar to those reported for polyoxyethylene lauryl ether (LEO)[26] and polyoxyethylene dodecyl ether (PDE)[27], which were recorded by polarographic drop times in 0.1 N aqueous KCl solutions at the p.z.c. The slope of the curves at different potentials in Fig. 2 show an initial slow change followed by a sudden sharp but relatively constant change until a critical c_A of approximately 10^{-4} M is reached, when the curves begin to show signs of flattening out. The region of high c_A values where the curves begin to flatten out has been interpreted, from determinations of γ *vs.* log c_A at the air–water interface, as the point of incipient micelle formation (refs. 28–31 and *cf.* Section (c) below).

(*b*) *Surface excess, adsorption isotherms and model of adsorbed molecules at the electrode–solution interface*

The amount of Triton X-100 adsorbed on mercury is expressed in terms of the surface excess, Γ_A, of the organic species defined and obtained from the Gibbs adsorption equation[9] as

$$-(\partial\gamma/RT\ \partial\ln a_A)_{E,\,\mu_{KCl}} = \Gamma_A \qquad (1)$$

The activities (a_A) of the organic materials are assumed to be equal to their concentrations for the purposes of calculating Γ_A according to (1), because the data shown in Fig. 1 were obtained for concentrations below the reported CMC[32]. From Fig. 2 we derived values of the surface excesses according to eqn. (1), and Γ_A is then plotted against concentration of the additive for different electrode potentials. The adsorption isotherms are shown in Fig. 3 and most of the curves tend to approach a maximum Γ_A value at a certain concentration, but the rates of reaching the maximum are dependent on potential. At very anodic potentials with respect to the p.z.c., the highest Γ_A attained is lower than $20 \cdot 10^{-10}$ moles cm^{-2}.

The maximum value of Γ_A observed at the p.z.c. is $22 \cdot 10^{-10}$ moles cm^{-2}, and will be symbolized as $(\Gamma_m)_{obs}$ in subsequent discussion. Saturation coverages at various potentials appeared to be reached at a concentration of 10^{-4} M as shown in Fig. 3, but it should be noted that the curves tend to fall below the value of $(\Gamma_m)_{obs}$ at c_A values beyond 10^{-4} M. This is not surprising because at $c_A \approx 10^{-4}$ M we are approaching the region of incipient micelle formation of the bulk solution, and the abscissa will no longer represent concentrations for singly-dispersed species.

For PDE and LEO, TAMAMUSHI and co-workers[26,27] did not derive $(\Gamma_m)_{obs}$ values at the p.z.c. from their data, but we have calculated them to be $18 \cdot 10^{-10}$ and $19 \cdot 10^{-10}$ moles cm^{-2}, respectively, and they compare favourably with $17 \cdot 10^{-10}$ moles cm^{-2} for Triton X-305 at the p.z.c. and the value of $22 \cdot 10^{-10}$ moles cm^{-2} for Triton X-100 at the same potential. $(\Gamma_m)_{obs}$ for Triton X-100 corresponds to a surface coverage* of $\theta \approx 20$, calculated from Γ_m, the theoretical surface excess for a monolayer based on a Leybold space-filling model for the planar adsorption of the molecule on mercury, or $\theta \approx 4$ if a perpendicular model is assumed with the alkyl end of the mole-

* In the present context, θ is defined as equal to $(\Gamma_{m})_{obs}/\Gamma_m$

cule in contact with the metal. However, $\theta \approx 1$, if a perpendicular model is assumed with the hydrophilic end of the molecule attached to mercury. The latter model is not likely because of steric considerations, and furthermore, plots of Γ_A against electrode potential for different concentrations (Fig. 4) show that any significant

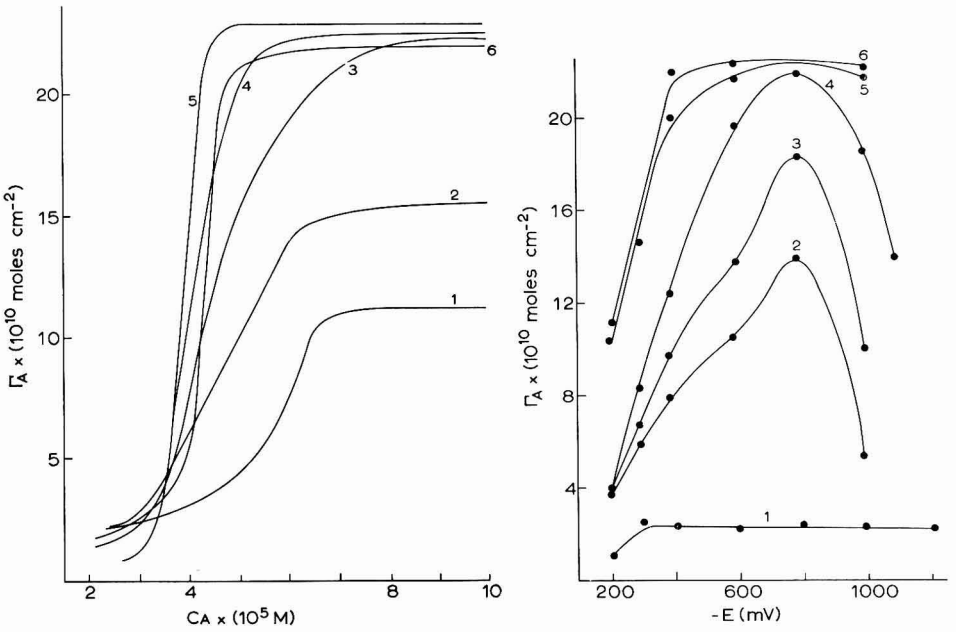

Fig. 3. Adsorption isotherms for Triton X-100 at various potentials: (1), −200; (2), −300; (3), −400; (4), −600; (5), −800; (6), −1000 mV.

Fig. 4. Variation of surface excess with electrode potential at different concns. (c) of Triton X-100: (1), 3.00; (2), 4.00; (3), 4.21; (4), 4.68; (5), 6.31; (6), 10.5 × 10^{-5} M.

shift of the potential of maximum adsorption with coverage is absent. By analogy with the adsorption behaviour of n-decylamine on solid electrodes[33], the net dipole moment of the first adsorbed layer is probably zero, hence Triton X-100 is thought to adsorb in a perpendicular configuration with the polar group towards the solution. We have suggested[4] that the best representation of multilayer adsorption may be described as a 2-dimensional micellar structure comparable to what has been called "hemimicelles"[34]. A more detailed description of our proposed model is shown in Fig. 5 where the hydrophilic portions of the molecules may contract up to about 40% in length according to X-ray evidence for comparable molecules examined by RÖSCH[35]. The first adsorbed layer of Triton X-100 extends its contracted "zig-zag" hydrophilic portions towards the solution. A second layer is then assumed to form by intermolecular hydrogen bonding between another perpendicular array of Triton X-100 molecules, and a third layer is formed by van der Waals attractive forces between similar non-polar ends of the molecules. It is also probable that each compact array of Triton X-100 molecules may hydrogen-bond with some water molecules since it is well known that micellar structures of these surfactant molecules

are usually hydrated[7]. We suggest that multilayer adsorption for Triton X-305, LEO, PDE and other comparable surfactants at the metal–solution interface could be adequately represented by the same simple model depicted in Fig. 5 for Triton X-100.

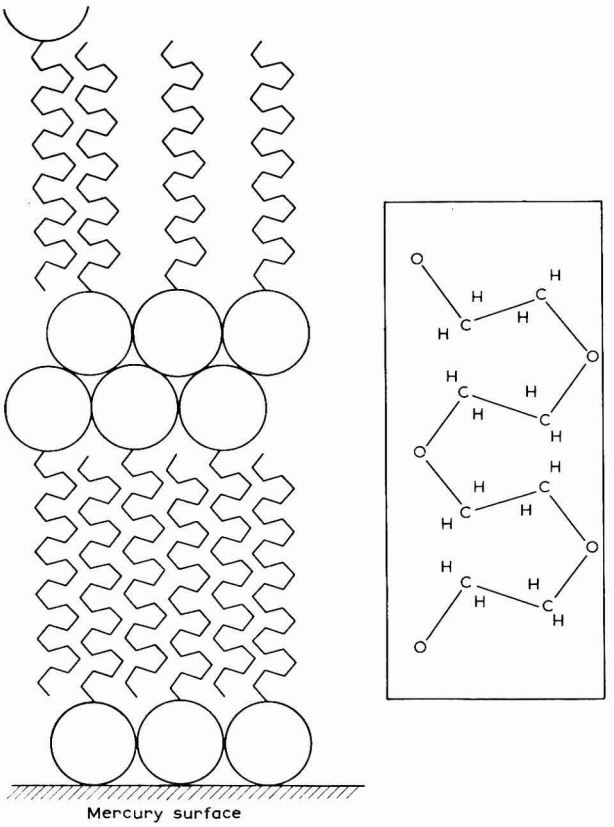

Fig. 5. Schematic model of the metal–solution interface showing multilayer adsorption of Triton X-100. The figure inset shows the atomic structure of part of the contracted polyoxyethylene chain for one adsorbed molecule.

(c) Shifts in the p.z.c. with surface coverage and with concentration of additive and their relation to critical micelle formation in the bulk phase

Figures 6 and 7 show the variation of $\Delta E_{\text{p.z.c.}}$ with log c_A and $(\Gamma_A)_{\text{p.z.c.}}$. Fig. 6 is reminiscent of the "Esin and Markov" type of behaviour reported for aliphatic alcohols, heterocyclic and aromatic compounds[41]. It is seen that $\mathrm{d}(\Delta E_{\text{p.z.c.}})/\mathrm{d}\log c_A$ changes abruptly at a certain value of $c_A \approx 1.0 \cdot 10^{-4}$ M, and this may be associated with a sudden change in orientational structure at the interface[41]. Fig. 7 shows that the change in slope is gradual for an increase in Γ_A from about 15 to $20 \cdot 10^{-10}$ moles cm^{-2}, but once the value of Γ_A reaches $21 \cdot 10^{-10}$ moles cm^{-2} (represented by the intercept of the extrapolated broken line shown in Fig. 7), $\mathrm{d}(\Delta E_{\text{p.z.c.}})/$

$d(\Gamma_A)_{p.z.c.}$ rise very steeply to a constant value. We believe that the significance of these plots confirms the suggestion made in Section (a) that incipient bulk solution micelle formation is reached when $c_A \approx 1.0 \times 10^{-4}$ M or $\Gamma_A \approx 21 \cdot 10^{-10}$ moles cm^{-2} in an aqueous base electrolyte solution of 0.1 N KCl.

The bulk solution CMC may also be estimated[36,37] from the application of the mass law to the equilibrium between singly-dispersed species and micelles in terms of their activity coefficients. Using these considerations, SHINODA[38] derived the following relation:

$$ {}_1X_2 + n({}_1f_2 \cdot {}_1X_2)^n = X_2 \qquad (2) $$

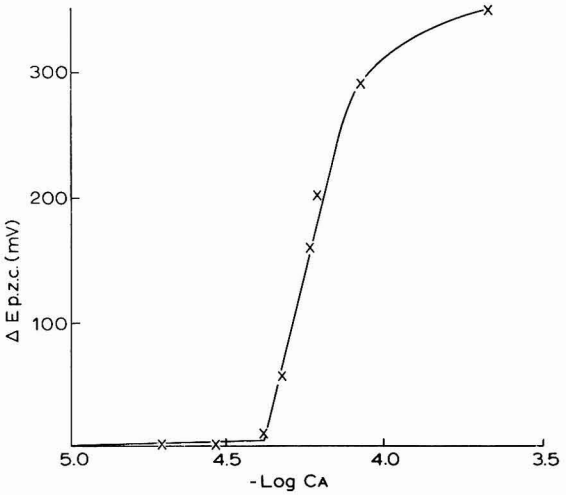

Fig. 6. Shifts of the potential of zero charge with additive concn. in 0.1 N KCl solutions of Triton X-100.

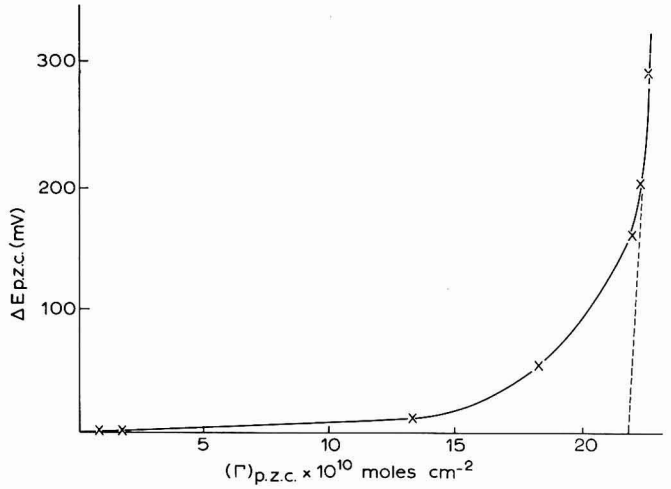

Fig. 7. Shifts of the potential of zero charge against surface excess at the p.z.c. in 0.1 N KCl solns. of Triton X-100.

where ${}_1X_2$ is the concentration of the single species, X_2 the bulk concentration, n the number of molecules comprising a micelle and ${}_1f_2$ (=1/CMC) the activity coefficient of the singly-dispersed species. From Fig. 2, the linear portions of the curves were extrapolated to obtain approximations to ${}_1X_2$ for higher concentrations in the region where the curves begin to show a flattening effect. From known values of X_2 and n[31], an approximate estimate of the bulk solution CMC was found to be $1.07 \pm 0.02 \cdot 10^{-4}$ M, which agrees favourably with $c_A \approx 1.0 \cdot 10^{-4}$ for incipient micelle formation as interpreted from Fig. 6. Both estimates of the CMC are also comparable to $2.45 \cdot 10^{-4}$ M reported by ROSS AND OLIVIER for the CMC of Triton X-100 in a pure water solution[32], which was determined by an u.v. spectrophotometric iodine solubilization method. Our indirect estimates of the CMC must of necessity be lower than that given for a pure solution[32] since it is well-known that the addition of inorganic salts to solutions of non-ionic colloidal surfactants usually decreases the CMC[39,40].

ACKNOWLEDGEMENTS

We are indebted to the Ontario Research Foundation and the University of Toronto for financial support of this work.

SUMMARY

Electrocapillary data were obtained by polarographic drop-time measurements to derive information concerning the properties of electrochemical adsorption and orientation of highly surface-active organic molecules at the electrode–solution interface. Two non-ionic iso-octylphenoxypolyethoxy ethanols (Tritons X-100 and X-305) were examined and the adsorption behaviour compared with that of other alkyl polyoxyethylenic compounds. Adsorption isotherms were determined for Triton X-100 for various electrode potentials. A model of "two-dimensional" micellar film formation was postulated for the structure of these adsorbed surfactants. Multilayer adsorption was found from solutions of concentration below that required to form micelles. The dependence of the potential of zero charge on surface coverage and on concentration of additive were determined and used to derive information relating to critical micelle concentration in the bulk solution phase.

REFERENCES

1 A. N. FRUMKIN AND B. B. DAMASKIN, Modern Aspects of Electrochemistry, No. 3, edited by J. O'M. BOCKRIS AND B. E. CONWAY, Butterworths, London, 1964, page 149.
2 C. N. REILLEY AND W. STUMM, *Progress in Polarography*, Vol. 1, edited by P. ZUMAN, Interscience Publishers, Inc., New York, 1962, page 81.
3 W. H. REINMUTH, *Advances in Analytical Chemistry and Instrumentation*, Vol 1, edited by C. N. REILLEY, Interscience Publishers, Inc., New York, 1960, page 241.
4 R. G. BARRADAS AND F. M. KIMMERLE, *J. Electroanal. Chem.*, 9 (1965) 483.
5 E. B. WERONSKI, *Trans. Faraday Soc.*, 58 (1962) 2217.
6 R. HAQUE AND W. U. MALIK, *J. Polarog. Soc.*, 8 (2), (1962) 36.
7 I. M. KOLTHOFF AND Y. OKINAKA, *J. Am. Chem. Soc.*, 81 (1959) 2298.
8 I. M. KOLTHOFF AND J. J. LINGANE, *Polarography*, Vol. 1, Interscience Publishers, Inc., New York, 2nd ed., 1952.
9 B. E. CONWAY AND R. G. BARRADAS, *Electrochim. Acta*, 5 (1961) 319.
10 R. G. BARRADAS AND B. E. CONWAY, *Electrochim. Acta*, 5 (1961) 349.
11 R. G. BARRADAS AND B. E. CONWAY, *J. Electroanal. Chem.*, 6 (1963) 314.

12 B. E. CONWAY, R. G. BARRADAS AND T. ZADWIDZKY, *J. Phys. Chem.*, 63 (1959) 1475.
13 R. G. BARRADAS AND E. M. L. VALERIOTE, *J. Electrochem. Soc.*, 112 (1965) in press.
14 R. G. BARRADAS AND P. G. HAMILTON, *Can. J. Chem.*, 43 (1965) in press.
15 H. C. GATOS, *J. Electrochem. Soc.*, 101 (1954) 433.
16 V. S. GRIFFITHS AND M. I. JACKMAN, *Talanta*, 9 (1962) 205.
17 R. W. SCHMID AND C. N. REILLEY, *J. Am. Chem. Soc.*, 80 (1958) 2087.
18 L. MEITES, *Polarographic Techniques*, Interscience Publishers, Inc., New York, 1955.
19 D. J. G. IVES AND G. J. JANZ, *Reference Electrodes*, Academic Press, New York, 1961, page 133.
20 M. A. V. DEVANATHAN AND P. PERIES, *Trans. Faraday Soc.*, 50 (1954) 1236.
21 P. CORBUSIER AND L. GIERST, *Anal. Chim. Acta*, 15 (1956) 254.
22 R. G. BARRADAS, Ph.D. THESIS, University of Ottawa, 1960.
23 H. A. LAITINEN AND B. MOSIER, *J. Am. Chem. Soc.*, 80 (1958) 2363.
24 L. M. CHAMBERS, *Anal. Chem.*, 36 (1964) 2431.
25 R. G. BARRADAS AND F. M. KIMMERLE, unpublished results.
26 B. TAMAMUSHI AND T. YAMANAKA, *Bull. Chem. Soc. Japan*, 28 (1955) 673.
27 K. SHINODA, T. NAKAGAWA, B. TAMAMUSHI AND T. ISEMURA, *Colloidal Surfactants*, Academic Press, New York, 1963, page 104.
28 J. POTNEY AND C. C. ADDISON, *Trans. Faraday Soc.*, 33 (1937) 1243.
29 C. C. ADDISON AND T. A. ELLIOT, *J. Chem. Soc.*, (1950) 3103.
30 A. S. BROWN, R. U. ROBINSON, E. H. SIROIS, H. G. THIBAULT, W. MCNEILL AND A. TOFIAS, *J. Phys. Chem.*, 56 (1952) 701.
31 L. M. KUSHNER AND W. D. HUBBARD, *J. Phys. Chem.*, 58 (1954) 1163.
32 S. ROSS AND J. P. OLIVIER, *J. Phys. Chem.*, 63 (1959) 1675.
33 J. O'M. BOCKRIS AND D. A. J. SWINKELS, *J. Electrochem. Soc.*, 111 (1964) 736.
34 P. SOMASUNDARAN, T. W. HEALY AND D. W. FUERSTENAU, *J. Phys. Chem.*, 68 (1964) 3562.
35 VON M. RÖSCH, Paper No. 27, Section A/11/1, 3rd International Congress on Surface Activity, Cologne, 1960.
36 J. GRINDLEY AND C. R. BURY, *J. Chem. Soc.*, 131 (1929) 679.
37 D. G. DAVIES AND C. R. BURY, *J. Chem. Soc.*, 132 (1930) 263.
38 Reference 27, page 28.
39 Reference 27, pages 63, 112.
40 P. H. ELSWORTHY, *J. Pharm. Pharmacol.*, 12 (1960) 293.
41 R. G. BARRADAS, P. G. HAMILTON AND B. E. CONWAY, *J. Phys. Chem.*, in press.

REVIEW

ELECTROSORPTION OF UNCHARGED MOLECULES ON SOLID ELECTRODES*

E. GILEADI
Electrochemistry Laboratory, University of Pennsylvania, Philadelphia, Pa. 19104 (U.S.A.)
(Received May 10th, 1965)

INTRODUCTION

The importance of adsorption in electrochemistry was first realized by STERN[1] in 1926. Until recently, practically all electrosorption studies have been confined to liquid mercury electrodes, where the extent of adsorption can be evaluated from the change of the interfacial tension with chemical potential of the species in the bulk of the solution (*i.e.*, from electrocapillary measurements).

The first studies of adsorption on solid electrodes were reported by FRUMKIN and co-workers[2–5], who measured the adsorption of atomic hydrogen and oxygen on noble-metal electrodes, in solutions saturated with molecular hydrogen. Until a few years ago, most of the adsorption work on solid electrodes was confined to the study of adsorption of intermediates formed in a charge-transfer process, which gives rise to an adsorption pseudocapacitance. The theory of the behavior of such intermediates has been discussed in detail in a number of recent papers by CONWAY AND GILEADI[6–8].

In this paper, the electrosorption (on solid electrodes) of organic molecules which do not themselves undergo electrochemical reaction (*e.g.*, corrosion inhibitors) or which serve as reactants in complex electrode reactions (*e.g.*, methanol or a hydrocarbon at fuel cell anodes) will be discussed.

SPECIAL ASPECTS OF ADSORPTION ON SOLID ELECTRODES

Before a detailed discussion of electrosorption on solid electrodes is undertaken, it is important to point out the fundamental differences between electrosorption, *i.e.*, adsorption on electrodes, and adsorption from the gas phase.

1. The major difference between gas-phase adsorption and electrosorption is that in the former case adsorption occurs on a bare surface, while in the latter case the substrate is solvated, *i.e.*, covered with an adsorbed layer of solvent molecules. Thus, *electrosorption is a replacement reaction*. The observed standard free energy, enthalpy and entropy of adsorption can only be related to the type of interaction between the adsorbate and the electrode if the corresponding thermodynamic quantities for the solvent are known and the number of solvent molecules replaced by each adsorbed organic molecule can be estimated.

* Paper presented at the Second Gordon Research Conference on Electrochemistry, Santa Barbara, California, 1965.

2. Since the effective standard free energy of adsorption is the difference between the corresponding quantities for solute and solvent, the solvent is expected to have a levelling effect, making the differences between different sites on the surface, and even between different metals, less pronounced. In the few instances where the rate of change of the apparent standard free energy of adsorption from solution with coverage has been measured, it was found to be much less than the corresponding value observed in gas-phase adsorption, in accord with the above argument.

3. The extent of electrosorption also depends on the solubility. Generally, the lower the solubility, the higher the adsorbability. A systematic study of the adsorption on mercury of several classes of organic compounds[9] (*e.g.*, butyl, phenyl and naphthyl derivatives) revealed a linear relationship between the standard free energy of adsorption and the free energy of solvation within each group. In a recent comparative study of the adsorption of butanol and phenol on mercury from aqueous and methanolic solutions[10], adsorption from aqueous solution was found to be much more extensive at a given bulk concentration. This is clearly due to the lower solubility of both alcohols in water, since on the basis of competition with solvent only, adsorption from methanol would be favored.

4. An important feature of electrosorption is the availability of the metal-solution potential difference as an additional degree of freedom of the system, which can be controlled and varied externally. A large part of this paper will deal with the potential dependence of adsorption. Theoretically, this is of extreme importance in evaluating the structure of the double layer at the metal–solution interface. From the practical viewpoint, the potential region over which adsorption occurs and the way in which adsorption depends on potential will influence the usefulness of a given compound as, for example, a corrosion inhibitor or a fuel in an electrochemical energy converter.

In addition, the state of the surface may be controlled and reproduced by proper control of the potential in rigorously purified solutions[11].

5. The use of solid rather than liquid electrodes gives rise to a number of new problems.

(a) Experimentally, the accurate and relatively convenient method of electrocapillary measurements cannot be applied to solids. The methods available are generally less accurate, sometimes limited in scope and in most cases very tedious.

(b) The real surface area of the electrodes is not known accurately. The methods commonly employed for roughness factor determination either measure the area of the electrode in a different state (for B.E.T. measurement the electrode must first be dried) or depend on assumptions which cannot be verified experimentally (in double-layer capacity measurements it is assumed that the value of the capacity is the same for all metals at the same rational potential). In particular, the area measured may not be the same as the area available for electrosorption of large organic molecules[7].

(c) Adsorption on different crystal faces, on grain boundaries or on dislocation sites may play an important role in determining adsorption on solid electrodes.

METHODS OF STUDYING ADSORPTION ON SOLID ELECTRODES

1. Fast potential sweep transients have been used extensively for the deter-

mination of the partial coverage, θ, of the electrode by organic compounds (*e.g.*, methanol[12], ethylene[13] or propane[13]) which may be used as fuels in electrochemical energy converters. The main assumptions made in this application are that:

(a) The rate of oxidation of the organic present on the surface at the start of the transient is fast compared to the rate of diffusion, so that no appreciable adsorption from the bulk phase occurs during the transient.

(b) The overall reaction during the transient is the same as that occurring during steady state (even though the mechanism does not necessarily have to be the same).

(c) The reactant and any intermediates formed can only be removed from the surface by complete oxidation.

(d) At the end of the transient, the electrode surface is free of organic molecules or radicals of any kind.

(e) The double-layer capacity, as well as the adsorption pseudocapacity associated with formation of an oxide layer on the electrode surface, are not affected substantially by the presence of the organic on the surface.

Of the five points mentioned above, only the first and the fourth can be tested experimentally in a satisfactory manner. Re-adsorption during the transient can be eliminated if the sweep rate is in excess of *ca.* 200 V/sec in the case of methanol[12]. Also, if the sweep is continued to high enough potentials, so that the current observed in solutions containing the organic coincides with the blank current observed in the purified solution through which only nitrogen is bubbled, one may conclude that the electrode surface is free of any organic species. The validity of the other assumptions is questionable and a substantial error of unknown magnitude may be introduced.

The fast potential sweep method may be replaced by a constant current anodic pulse of high current density[14]. The two methods are not basically different and the same limitations on the validity of results apply in both cases.

2. Cathodic charging curves have been used to determine the coverage by the organic from the change in hydrogen coverage due to the presence of organic molecules on the surface[14–16]. Several objections may be raised against this method.

(a) A fraction of the sites available for hydrogen adsorption may not be available for the adsorption of a large organic molecule[12].

(b) The effect of organic adsorption on the heat of adsorption of hydrogen (induced heterogeneity[6,17]) is neglected.

(c) Desorption of organic molecules from the surface due to replacement by adsorbed hydrogen or by strongly oriented water molecules[18] may take place during the transient.

(d) Reduction of organic molecules on the surface may occur. This will give rise to Faradaic currents in excess of the amount required to deposit hydrogen on the available free sites.

(e) Substantial amounts of hydrogen can diffuse into the metal during the transient[19,20].

It has been shown experimentally[12,14] that the two electrochemical methods described above for the determination of coverage do not necessarily yield the same results in a given system. This is not surprising since the two methods measure different properties of the adsorbed organic molecules. Thus the cathodic charging method is sensitive to the mode of adsorption on the surface and measures (at least

approximately, as discussed above) the number of sites occupied independent of the nature of the species on the surface. The anodic oxidation method, on the other hand, measures the charge required to oxidize the species on the surface. A change-over from one-site adsorption to three-site adsorption of propane will be detected only by the cathodic charging method while a partial oxidation or dehydrogenation may show up only in the anodic transients[14].

In view of the large number of unjustifiable assumptions it is doubtful whether the adsorption data obtained by either of these methods can generally be regarded as reliable. They can be used in combination with other methods (*e.g.*, the radiotracer method, see below) to detect changes in the nature of species adsorbed on the surface[21].

3. The use of ellipsometric techniques to study coverage by organics appears to be very attractive, in particular when the multiple reflection method is developed. Results obtained by this method are not available at present, however.

4. Differential capacity measurements have been used to study adsorption on solid electrodes mainly by the Russian school of electrochemists. They are all based on the fact that the capacity of the double layer is altered by any chemical or physical changes which alter the effective thickness or the permittivity in the double layer. For a rigorous determination of coverage from capacity measurements it is necessary to know the potential of zero charge (p.z.c.) and the value of the interfacial tension at this potential. Several approximate methods have been suggested for use on solid electrodes where the electrocapillary curve cannot be measured. These have been reviewed recently[22]. Only the equation suggested by FRUMKIN will be mentioned here.

The charge, q_θ, on the metal at a coverage, θ, may be written, according to FRUMKIN[22], as

$$q_\theta = q_{\theta=0}(1-\theta) + q_{\theta=1}\theta \tag{1}$$

where $q_{\theta=0}$ and $q_{\theta=1}$ are the values of the charge on the bare metal and on the completely covered metal at the same potential. Differentiating eqn. (1) with respect to potential gives

$$C_\theta = C_{\theta=0}(1-\theta) + C_{\theta=1}\theta + (q_{\theta=1} - q_{\theta=0}) \frac{\mathrm{d}\theta}{\mathrm{d}V} \tag{2}$$

where the subscripts have the same significance as in eqn. (1). In the range where the coverage varies little with potential it is possible to neglect the last term in eqn. (2) and write

$$\theta = \frac{C_\theta - C_{\theta=0}}{C_{\theta=1} - C_{\theta=0}} \tag{3}$$

Equation (3) will be applicable as a good approximation at potentials near the potential of maximum adsorption *i.e.*, from the p.z.c. a few hundred millivolts in the cathodic direction[9,18].

5. The change in concentration in solution has been used by CONWAY *et al.*[23] to measure adsorption on solids. The limitations here are that very large area electrodes have to be used and the concentration in the solution must be low, so that the change in concentration due to adsorption may be detected. The authors used u.v. spectroscopy to detect changes in concentration in the solution and were thus limited to the study of compounds which have adsorption bands in the near u.v. or visible

region. Their method could probably be extended by employing radiotracer or vapor-phase chromatographic methods to determine bulk concentrations with higher sensitivity.

6. Two radiotracer methods have been developed[24,25] and applied[26-30] to the study of organic electroadsorption.

In the foil method[24], ^{14}C-labelled organic compounds are used and the radiation through a very thin metal foil placed over the window of an end-window proportional gas counter is measured. The metal foil serves as the working electrode and its potential is set with respect to a reference electrode in the same solution. The surface concentration is proportional to the net count rate, after due allowance for counts originating from molecules in the bulk of the solution has been made. The counting efficiency is determined by counting a sample of tagged Na_2CO_3 of known activity that does not adsorb on the surface. Bulk concentrations are measured with the aid of a liquid scintillation counter. A thin gold foil ($2 \cdot 10^4$ Å) has been used[27] as the electrode. This may be coated with other metals by *e.g.* electroplating[28] or vapor deposition. In a recent modification of this method Pt was vapor-deposited on the mica window of the proportional gas counter using a graded tantalum–tantalum oxide bond[31].

The foil method is applicable to the study of adsorption of low solubility, volatile compounds. It is somewhat limited as regards the choice of electrode materials which can be used.

In the tape method the electrode is in the form of an endless tape. It is passed through two sections of a cell which is provided with narrow lips to eliminate leakage of solution and minimize diffusion of oxygen into the cell. In the first section, the electrode is chemically and/or electrochemically cleaned and activated (the exact procedure depends on the nature of the metal). The second section contains a solution of the radio-labelled organic. The electrode is kept in this part of the cell until adsorption equilibrium is reached. It is then moved in position between two proportional counters connected in parallel. The electrode emerges from the cell carrying a thin layer of solution (approximately 1 μ) and the background count from solution is small even for relatively high concentrations.

The tape method allows a larger choice of electrode materials and higher solution concentrations. It is, however, not suitable for the measurement of adsorption of volatile compounds.

Both radiotracer methods give direct unambiguous information on the extent of adsorption. They are sensitive only to the number of carbon atoms adsorbed on the surface, independent of the chemical nature of the compounds. They are thus best suited for the study of electrosorption of molecules that do not undergo chemical changes on the surface or, alternatively, form products which are quickly eliminated from the surface.

ADSORPTION AS A REPLACEMENT REACTION

The point has already been made in the introduction that the most significant feature of electrosorption as compared to adsorption from the gas phase is that the former is a replacement reaction while the latter is not. For an organic species, R, adsorbing on the surface and replacing n water molecules, the adsorption process

may, therefore, be represented as

$$R_S + n\ H_2O_A \rightleftharpoons R_A + n\ H_2O_S \tag{4}$$

where the subscripts S and A refer to the species in solution and adsorbed on the surface, respectively.

The chemical potentials of the species involved may now be written for dilute solutions as[30]

$$\mu_{R_S} = \mu_{R_S}^\circ + RT \ln X_{R_S} \doteq \mu_{R_S}^\circ + RT \ln (c_{R_S}/55.4) \tag{5}$$

$$\mu_{H_2O_A} = \mu_{H_2O_A}^\circ + RT \ln X_{H_2O_A} \tag{6}$$

$$\mu_{R_A} = \mu_{R_A}^\circ + RT \ln X_{R_A} \tag{7}$$

$$\mu_{H_2O_S} = \mu_{H_2O_S}^\circ + RT \ln X_{H_2O_S} \doteq \mu_{H_2O_S}^\circ \tag{8}$$

The condition for adsorption equilibrium is

$$\mu_{R_S} + n\mu_{H_2O_A} = \mu_{R_A} + n\mu_{H_2O_S} \tag{9}$$

The mole fractions on the surface are given by

$$X_{R_A} = \frac{\theta}{\theta + n(1-\theta)} \tag{10}$$

$$X_{H_2O_A} = \frac{n(1-\theta)}{\theta + n(1-\theta)} \tag{11}$$

which leads to the isotherm

$$\frac{\theta}{(1-\theta)^n} \frac{[\theta + n(1-\theta)]^{n-1}}{n^n} = K\, c_{R_{sat.}}/55.4 \tag{12}$$

where

$$K = \exp(-\Delta G_A^\circ/RT) \tag{13}$$

and

$$\Delta G_A^\circ = (\mu_{R_A}^\circ - \mu_{R_S}^\circ) - n(\mu_{H_2O_A} - \mu_{H_2O_S}^\circ) \tag{14}$$

The standard free energy of adsorption is thus the difference between the standard free energies of adsorption for the organic and for n water molecules. The same statement may be applied to the standard enthalpy and entropy of adsorption on electrodes.

Close examination of the energy quantities involved in adsorption from solution shows[30] that the standard free energy of adsorption may be written as

$$\Delta G_A^\circ = RT \ln (c_{R_{sat.}}/55.4) - RT \ln (P_R^\circ/P_{H_2O}^\circ) + \Delta G_V^\circ(R) - n\Delta G_V^\circ(H_2O) \tag{15}$$

where $c_{R_{sat.}}$ is the concentration of R in a saturated solution, P_R° and $P_{H_2O}^\circ$ are the vapor pressures of the pure organic and water at a temperature T and the ΔG_V° refers to adsorption from the gas phase.

The importance of the solubility and the relative vapor pressure of solvent and solute is thus brought out as factors which influence the extent of electrosorption. It may also be noted that for the comparison of adsorbabilities of different solutes or the same solute in different solvents, a concentration corresponding to saturation may best be chosen as the standard state.

POTENTIAL DEPENDENCE OF ADSORPTION

Typical plots of the variation of the extent of adsorption with coverage are shown in Figs. 1 and 2, the first of which refers to the adsorption of *n*-decylamine on Ni[30] and the second for the adsorption of ethylene on Pt[28]. Similar results were obtained for the adsorption of *n*-decylamine[30] and naphthalene[29] on a number of metals (Ni, Fe, Cu, Pt, Pb) and in the adsorption of a number of butyl derivatives on mercury[9].

The region of potential in which adsorption occurs is different for different metals. It depends mainly on the p.z.c. of the metal and to a lesser extent on the specific interaction between the adsorbed water molecules and the metal.

The "bell-shaped" form of the θ–V plot has been interpreted by BOCKRIS and co-workers[18,28–30] on the basis of the competition between organic and water

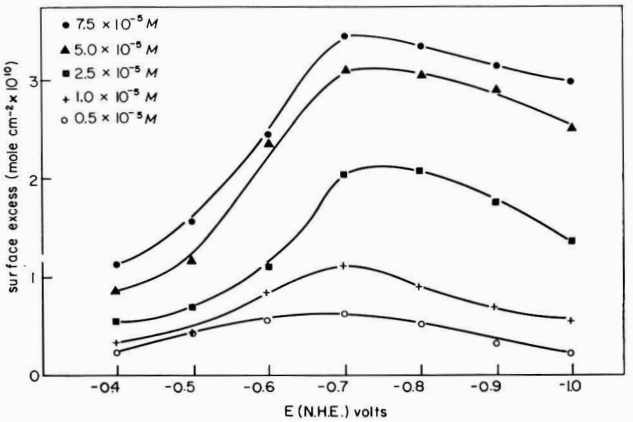

Fig. 1. The adsorption of *n*-decylamine on a nickel electrode from alkaline soln. (pH = 12).

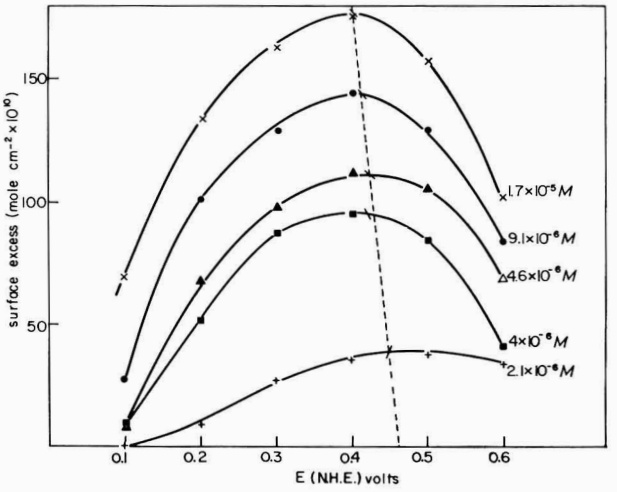

Fig. 2. The adsorption of ethylene on platinum in acid soln. (1 *N* H_2SO_4).

molecules for surface sites and the field-dependence of the standard free energy of adsorption of water.

Consider first the water molecules as symmetrical dipoles of moment, μ, in field, X, of the double layer, and assume that the free energy of adsorption of the organic is entirely independent of field. The energy of interaction of water dipoles with the field will be $\pm\mu X$ (the sign depends on orientation) and will become zero at the p.z.c. where, in the absence of a dipole potential, the field X will be zero. Since the effective free energy of adsorption depends on the difference between the values for the organic and water, maximum adsorption will occur at the p.z.c.

In practice, the potential of maximum adsorption does not coincide with the p.z.c. and a somewhat more complex model should be considered.

Let N_1 and N_2 be the number of water molecules in the two possible orientations, and let the corresponding energies be E_1 and E_2.
Then

$$E_1 = E_1^c + \mu X - RmE \tag{16}$$

and

$$E_2 = E_2^c - \mu X + RmE \tag{17}$$

where E_1^c and E_2^c are the non-field dependent interactions of water in its two positions with the metal surface, m is a co-ordination number on the surface, E is the energy of interaction between dipoles and R is given by

$$R = \frac{N_1 - N_2}{N_T} \tag{18}$$

where $N_T = N_1 + N_2$.

The average energy of a water molecule on the surface is

$$\bar{E} = \frac{N_1 E_1 + N_2 E_2}{N_T} \tag{19}$$

The potential of minimum $\bar{E}$ can be calculated from the condition

$$\left(\frac{\partial \bar{E}}{\partial X}\right)_{N_T} = 0 \tag{20}$$

Thus

$$\left(\frac{\partial \bar{E}}{\partial X}\right)_{N_T} = \frac{1}{N_T}\left[N_1\frac{\partial E_1}{\partial X} + E_1\frac{\partial N_1}{\partial X} + N_2\frac{\partial E_2}{\partial X} + E_2\frac{\partial N_2}{\partial X}\right] = 0 \tag{21}$$

Now

$$\frac{\partial E_1}{\partial X} = -\frac{\partial E_2}{\partial X} \quad \text{and} \quad \frac{\partial N_1}{\partial X} = -\frac{\partial N_2}{\partial X} \tag{22}$$

hence

$$(N_1 - N_2)\frac{\partial E_1}{\partial X} + (E_1 - E_2)\frac{\partial N_1}{\partial X} = 0 \tag{23}$$

Equation (23) has an infinite number of solutions of which only the solution $N_1 = N_2$ and $E_1 = E_2$ is physically acceptable. Thus if $\partial E_1/\partial X > 0$ (*i.e.*, the water molecules

become more weakly adsorbed with increasing field) it will be expected that $\partial N_1/\partial X < 0$. Also if $(E_1 - E_2) < 0$ then $(N_1 - N_2) > 0$. Hence the products in eqn. (20) always have the same sign and the equation can only be satisfied if each term is separately zero. The differential coefficient, $\partial N_1/\partial X$, approaches zero at very high values of the field where $\partial E_1/\partial X \neq 0$. It is, therefore, concluded that at the potential of maximum adsorption, where $\bar{E}$ is a minimum, the energy of a water molecule will be the same in either orientation and consequently there will be an equal number of molecules in the two possible orientations.

Substituting for E_1 and E_2, with $R = 0$

$$E_1^c + \mu X = E_2^c - \mu X \tag{24}$$

or

$$\Delta E^c = E_1^c - E_2^c = -2\mu X$$

The field can be related to the charge, q_m, on the metal since

$$X = 4\pi q_m/\varepsilon \tag{26}$$

and thus

$$E^c = 8\pi\mu q_m/\varepsilon \tag{27}$$

where ε is the permittivity in the inner Helmholtz layer.

For most organic molecules, the dipole moment resides at a distance from the metal surface where the field is small and is mainly due to the charge distribution in the diffuse layer and the permittivity is relatively high. Hence the effect of potential and charge on their free energy of adsorption is small, and a symmetrical θ–V curve results. The existence of π-bond interaction with the surface does not alter this situation substantially unless the energy of interaction is appreciably field-dependent.

ELECTROSORPTION OF *n*-DECYLAMINE AND NAPHTHALENE[29,30]

Very little work has been done so far on the electrosorption of neutral organic molecules on solid electrodes. Some results of this type, making use of the two radiotracer methods described above, will now be given.

The electrosorption of *n*-decylamine and naphthalene on Ni, Fe, Cu, Pt and Pb has been measured by the tape method[29,30] (*cf.* p. 141). The results are shown in Table 1 below. Several points become apparent upon examination of these results.

1. The potential of maximum adsorption, E_m, is in all cases studied here cathodic to the potential of zero charge, $E_{q=0}$. This is in accordance with the theory developed by BOCKRIS, DEVANATHAN AND MULLER[18] on the structure of the double layer and indicates stronger interaction between the metal and the water molecules when the oxygen is towards the metal.

2. The difference, $E_m - E_{q=0}$, is not the same for all metals, indicating that ΔE^c (*cf.* eqn. 22) may depend on the metal. BOCKRIS, GREEN AND SWINKELS[29] have been able to obtain reasonable values for ΔE^c, in agreement with experiment, on the basis of image force and dispersion interactions. They were unable, however, to account quantitatively for the variation of ΔE^c with metal. This may be ascribed to the uncertainty in the values of both $E_{q=0}$ and E_m on solid metals rather than to a weakness of the theory.

TABLE 1

QUANTITIES RELEVANT FOR THE ELECTROSORPTION OF *n*-DECYLAMINE AND NAPHTHALENE

Metal	*p.z.c.*	E_m $(\theta \rightarrow 0)$		ΔG_A° at E_m $(\theta \rightarrow 0)$	
	(V)	*n-Decylamine (V)*	*Naphthalene (V)*	*n-Decylamine (kcal/mole)*	*Naphthalene (kcal/mole)*
Ni	−0.47	−0.7	−0.8	−6.8	−6.0
Fe	−0.50	−0.7	−0.7	−6.6	−7.0
Cu	−0.20	−0.9	−0.9	−7.3	−7.0
Pt (pH=2)	+0.50*		+0.1		
				−7.4	−8.4
Pt (pH=12)	−0.04*	−0.4			
Pb	−0.70	−1.3		−6.2	

* The p.z.c. values for Pt reported here are from recent measurements in this laboratory[28,32].

3. Most striking perhaps, in this table, is that the standard free energy of adsorption on five metals and for two very different compounds is almost the same. It is very strongly implied that physical adsorption occurs in all these cases. The fact that naphthalene, which replaces six water molecules on the surface, has a value of ΔG_A° similar to that of *n*-decylamine (assumed here to replace only one water molecule) implies that this quantity ($-\Delta G_A^\circ = 6$–8 kcal/mole) is characteristic of the replacement on the surface, of a water molecule by one or two $-CH_2-$groups, irrespective (to a first approximation) of the overall size of the molecule.

4. The potentials of maximum adsorption given in the table were values extrapolated to zero coverage by the organic. The fundamental variable in electrosorption is the charge q_m rather than the potential[33]. Adsorption studies on mercury[9] show that while the potential of maximum adsorption may vary with coverage, the charge at which adsorption reaches a maximum is independent of it[18].

A substantial dependence of E_m on θ is indicative of a contribution of the dipole potential of the organic to the field in the compact double layer. For a molecule such as *n*-decylamine, a shift of E_m with θ, in the cathodic direction is expected if the dipolar amine group is oriented towards the metal, while practically no shift is expected if the other end of the molecule is towards the metal. The former situation is observed[30] for adsorption on iron and the latter for adsorption on the other metals tested.

ELECTROSORPTION OF ETHYLENE ON PLATINUM[28]

The coverage–potential relationship for various concentrations of ethylene at 30° is shown in Fig. 2. The symmetrical shape of the curves indicates essentially no interaction of the organic with the electric field in the double layer.

The position of the adsorption maximum E_m $(\theta \rightarrow 0) = 0.46$ V (N.H.E.) should be given some consideration. The accepted value for the p.z.c. of Pt in acid solutions is[29] near 0.3 V. This would place E_m at a potential *anodic* to the p.z.c. contrary to the data reported by BOCKRIS AND SWINKELS[29,30] for two compounds (*n*-decylamine and naphthalene) on five different metals and contrary to theoretical predictions[18]. It would seem that a re-evaluation of the value for the p.z.c. on Pt is needed. KHEIFETZ AND KRASIKOV[34] used the capacitance method to measure the p.z.c. of Pt as a func-

tion of pH over a wide range. Their values for pH 3 and 2 are 0.30 V and 0.50 V, respectively. Recent measurements in this laboratory[32] gave a value of 0.48 V at pH 3 with an average variation of 58 mV per pH unit. Extrapolation to pH 0.5 (1 N H_2SO_4) gives $E_{q=0}=0.63$ V, and thus $E_m-E_{q=0}=-0.17$ V in agreement with the position of E_m with respect to $E_{q=0}$ in previous experiments.

The adsorption isotherm obtained at 0.4 V and 30° is shown in Fig. 3. A comparison of adsorption isotherms taken at three different temperatures is shown in Fig. 4. Saturation adsorption is seen to be reached when the concentration in solution exceeds about $2 \cdot 10^{-5}$ mole/l and the extent of adsorption is essentially independent of temperature (note that the curve for 30° is *between* the curves for 50° and 70°).

The same data are represented in Fig. 5 as a plot of $c/\theta-c$. The slope of unity in this plot confirms the validity of a simple Langmuir isotherm, and the reciprocal of the intercept equals the equilibrium constant for adsorption. Further confirmation of this behavior is given in Fig. 6 in which $\theta/(1-\theta)$ is plotted *vs.* c. A linear relationship with the lines passing through the origin is found for all three temperatures, as expected.

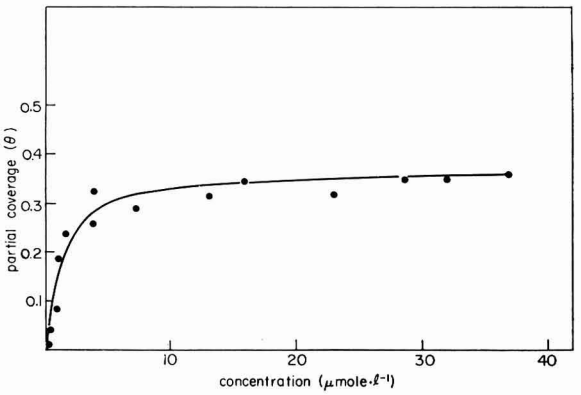

Fig. 3. Adsorption isotherm for ethylene at 0.4 V, 30° (points taken from three independent measurements).

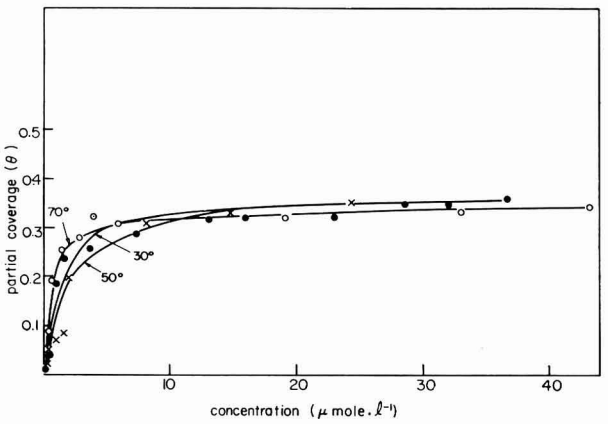

Fig. 4. Adsorption isotherms for ethylene at 0.4 V and three temperatures (30°, 50° 70°).

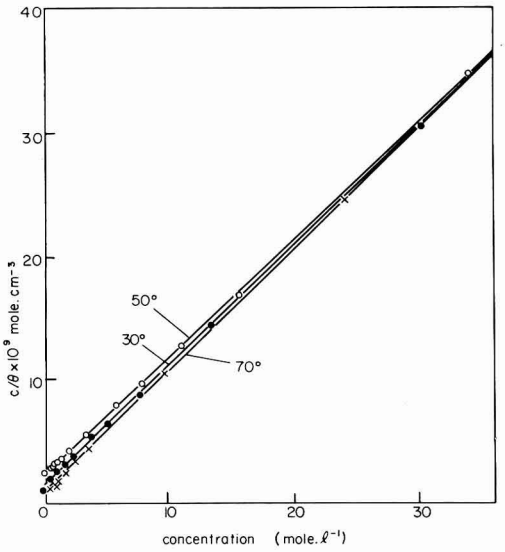

Fig. 5. A plot of C/θ *vs.* C for ethylene electrosorption on Pt.

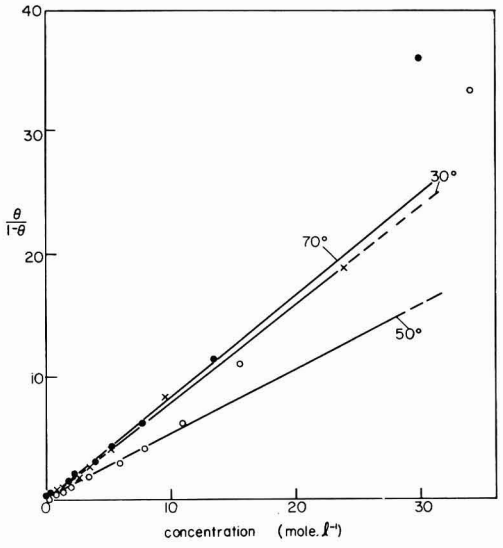

Fig. 6. A plot of $\theta/(1-\theta)$ *vs.* C for ethylene electrosorption on Pt.

The values of the equilibrium constant obtained by these two methods at three temperatures are shown in Table 2. From the average values of K at 30° and 50° one finds $\Delta H^\circ = -3.7$ kcal/mole, while from K_{30° and K_{70° a value of $\Delta H^\circ = +1.2$ kcal/mole is calculated. It is thus concluded that

$$\Delta H^\circ = 0.0 \pm 4.0 \text{ kcal/mole}$$

and

$$K = (7.5 \pm 2.5) \cdot 10^8 \text{ cm}^3\text{/mole}.$$

TABLE 2

EQUILIBRIUM CONSTANT FOR ELECTROSORPTION OF ETHYLENE

Method of evaluation *Temp. (°C)*	*c/θ vs. c* *(K cm³/mole)*	*$\theta/(1-\theta)$ vs. c* *(K cm³/mole)*	*Average* *(K cm³/mole)*
30°	$6.7 \cdot 10^8$	$8.0 \cdot 10^8$	$7.4 \cdot 10^8$
50°	$4.6 \cdot 10^8$	$5.4 \cdot 10^8$	$5.0 \cdot 10^8$
70°	$10 \cdot 10^8$	$8.3 \cdot 10^8$	$9.2 \cdot 10^8$

The heat of adsorption of ethylene on various metals (as well as that of CO_2 and H_2) from the gas phase was found to depend on the position of the metal in the periodic table. No data are available for ethylene adsorption on Pt but a value of -58 kcal/mole obtained on Ni may be taken as a good approximation[35,36]. The low value of the heat of electrosorption must be interpreted in terms of the replacement of water molecules from the surface.

The electrosorption can be represented by the following thermodynamic cycle

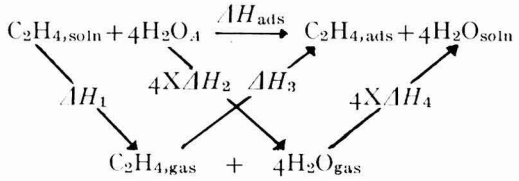

The numerical values for the ΔH terms are: $\Delta H_1 \doteqdot 4$ kcal/mole; $\Delta H_2 = 22.6$; $\Delta H_3 = -58$ kcal/mole; $\Delta H_4 = -9.6$ kcal/mole.

The value of ΔH_2 was calculated as the sum of the dispersion energy and the image force interaction[29].

Summing up one obtains

$$\Delta H_{ads} = -2.0 \text{ kcal/mole}$$

in excellent agreement with the observed value.

With the standard heat of adsorption of ethylene from solution taken as zero

$$\Delta G_{ads}^{\circ} = -T\Delta S_{ads}^{\circ} \tag{28}$$

and hence

$$\Delta S_{ads}^{\circ} = 2.3\, R \log K \tag{29}$$

It is convenient here to choose a standard state of unit activity of ethylene. This corresponds to a concentration of $4 \cdot 10^6$ moles/ml. With this standard state, the equilibrium constant becomes

$$K = (3 \pm 1) \cdot 10^3$$

and hence

$$\Delta S_{ads}^{\circ} = 16 \pm 1 \text{ e.u.}$$

It is noted that a positive entropy of adsorption is measured here, in contrast to negative values of the entropy usually observed in adsorption from the gas phase. This behavior is well understood when one remembers that electrosorption is a replacement reaction. When a molecule is adsorbed from the gas phase it loses at least

one and often three degrees of freedom of translation, in addition to loss of rotational degrees of freedom. Hence a decrease in entropy is usually observed for adsorption processes. In electrosorption of ethylene, four water molecules are desorbed per ethylene molecule adsorbed[28] and the net increase in the number of degrees of freedom of the system gives rise to a positive entropy of adsorption.

CONCLUSION

The theory of electrosorption of neutral molecules is discussed. The most significant aspect of electrosorption is that it is a replacement reaction, A bell-shaped plot of coverage *vs.* potential (*cf.* Fig. 2) can arise due to the field-dependent energy of adsorption of water molecules. A symmetrical curve is expected if the interaction of the adsorbed organic molecules with the field in the double layer is negligible.

The potential of maximum adsorption does not coincide with the p.z.c. It occurs at a negative potential on the rational scale, where the total energy of interaction of water molecules with the surface is the same in both orientations. The field, and hence the charge, corresponding to E_m, is characteristic of the metal and is related to the difference, ΔE^c, in the field-independent parts of the interaction of water molecules with the surface in the two possible orientations. On mercury, $q_m \doteqdot -2\mu C/cm^2$. Theoretical image force and dispersion interaction calculations show that q_m should be in the range -2 to $-3\mu C/cm^2$ for several metals. Experimentally, a much larger range of q_m values is found for different metals. This, however, may be due to the uncertainty in the measured values of E_{max} and the p.z.c. for solid metals. At the potential of maximum adsorption, equal numbers of water molecules are oriented in both directions and the dipole potential, $\Delta\chi$, tends to zero. Under these conditions, the field in the compact Helmholtz layer can be calculated accurately from the known value of the charge on the metal.

The apparent standard free energies of electrosorption for naphthalene and *n*-decylamine on four different metals are essentially the same. This indicates that these two compounds are physically adsorbed and the observed values of ΔG_A° (-6 to -8 kcal/mole) are characteristic of the replacement of a volume of water by an equal volume of organic groups on the surface, independent of whether these groups are connected to the same or different adsorbed molecules.

The results of electrosorption of ethylene on Pt are consistent with a four-point attachment with opening of the double bond and a heat of adsorption from the gas phase of -58 kcal/mole. The potential of maximum adsorption is $E_m = 0.46$ *V* (N.H.E.) and shifts slightly in the cathodic direction with increasing coverage. A new value for the p.z.c. of Pt in acid solutions of about 0.55–0.65 V N.H.E. is suggested.

A positive entropy of electrosorption is observed and is consistent with the view that electrosorption is a replacement reaction.

ACKNOWLEDGEMENTS

The author thanks Professor J. O'M. BOCKRIS for helpful discussion and suggestions.

Financial support for this work by U.S. Army Engineer Research and Develop-

ment Laboratory under Contract No. DA44-009-AMC-469(7) is gratefully acknowledged.

SUMMARY

The theory of electrosorption of uncharged organic molecules on solid electrodes is reviewed. The fundamental differences between electrosorption and adsorption from the gas phase are pointed out. Experimental techniques for the study of electrosorption on solid electrodes are described and the limitation of the electrochemical methods are emphasized. Some results on the adsorption of *n*-decylamine and naphthalene on several metals at room temperature and on the adsorption of ethylene on Pt over a range of temperatures are presented.

REFERENCES

1 O. STERN, *Z. Elektrochem.*, 30 (1924) 508.
2 A. N. FRUMKIN AND A. SLYGIN, *Acta Physicochim.*, 3 (1935) 791.
3 A. SLYGIN AND B. V. ERSHLER, *ibid.*, 11 (1939) 45.
4 A. N. FRUMKIN, P. DOLIN AND B. V. ERSHLER, *ibid.*, 13 (1940) 779.
5 P. DOLIN AND B. V. ERSHLER, *ibid.*, 13 (1940) 747.
6 B. E. CONWAY AND E. GILEADI, *Trans. Faraday Soc.*, 58 (1962) 2493.
7 E. GILEADI AND B. E. CONWAY, *Modern Aspects of Electrochemistry*, Vol. III, edited by J. O'M. BOCKRIS AND B. E. CONWAY, Butterworths Scientific Publications, 1964, chap. 5.
8 B. E. CONWAY, E. GILEADI AND M. DZIECIUCH, *Electrochim. Acta*, 8 (1963) 143.
9 E. BLOMGREN, J. O'M. BOCKRIS AND C. JESCH, *J. Phys. Chem.*, 65 (1961) 2000.
10 J. O'M. BOCKRIS, K. MULLER AND E. GILEADI, in preparation.
11 S. GILMAN, *J. Phys. Chem.*, 68 (1964) 2098.
12 M. W. BREITER AND S. GILMAN, *J. Electrochem., Soc.*, 109 (1962) 622.
13 R. CH. BURSHTEIN, V. S. TIURIN AND A. G. PSHENICHNIKOV, Paper presented at the C.I.T.C.E. meeting (London, 1964).
14 S. B. BRUMMER, Second Interim Technical Report, Contract No. DA44-009 AMC 410(T), Tyco Laboratories, Inc.
15 M. OIKAWA AND T. MUKAIBO, *J. Electrochem. Soc. Japan*, 20 (1952) 568.
16 T. C. FRANKLIN AND R. D. SOTHERN, *J. Phys. Chem.*, 58 (1954) 951.
17 M. BOUDART, *J. Am. Chem. Soc.*, 72 (1962) 1531; 3556.
18 J. O'M. BOCKRIS, M. A. V. DEVANATHAN AND K. MULLER, *Proc. Roy. Soc. London*, A274 (1963) 55.
19 S. SCHULDINER AND T. B. WERNER, *J. Electrochem. Soc.*, 112 (1965) 212.
20 E. GILEADI AND M. FULLENWIDER, in preparation.
21 R. J. FLANNERY, G. ARONOWITZ AND D. C. WALKER, American Oil Company Progress report No. 1, Contract No. DA-49-186-AMC-167(X), 1965.
22 A. N. FRUMKIN AND B. B. DAMASKIN, *Modern Aspects of Electrochemistry*, Vol. III, edited by J. O'M. BOCKRIS AND B. E. CONWAY, Butterworths Scientific Publication, 1964, chap. 3.
23 B. E. CONWAY, R. G. BARRADAS AND T. ZAVIDZKY, *J. Phys. Chem.*, 62 (1958) 676.
24 E. BLOMGREN AND J. O'M. BOCKRIS, *Nature*, 186 (1960) 305.
25 M. GREEN, D. A. J. SWINKELS AND J. O'M. BOCKRIS, *Rev. Sci. Instr.*, 33 (1962) 18.
26 H. DAHMS, M. GREEN AND J. WEBER, *Nature*, 196 (1962) 1310.
27 H. WROBLOWA AND M. GREEN, *Electrochim. Acta*, 8 (1963) 679.
28 E. GILEADI, B. T. RUBIN AND J. O'M. BOCKRIS, *J. Phys. Chem.*, in press.
29 J. O'M. BOCKRIS, M. GREEN AND D. A. J. SWINKELS, *J. Electrochem. Soc.*, 111 (1964) 743.
30 J. O'M. BOCKRIS AND D. A. J. SWINKELS, *J. Electrochem. Soc.*, 111 (1964) 736.
31 R. J. FLANNERY, American Oil Company, Final Report M64-341.
32 J. O'M. BOCKRIS, S. D. ARGADE AND E. GILEADI, in preparation.
33 R. PARSONS, *Trans. Faraday Soc.*, 51 (1955) 1518.
34 V. L. KHEIFETS AND B. S. KRASIKOV, *Zh. Fiz. Khim.*, 31 (1952) 1992.
35 D. O. HAYWARD AND B. M. T. TRAPNELL, *Chemisorption*, Butterworths Scientific Publication, 1962.
36 G. C. BOND, *Catalysis by Metals*, Academic Press, 1962.

SHORT COMMUNICATIONS

Electrode de référence de palladium–hydrogène, avec réserve propre de gaz

La constance et la bonne réproductibilité de la valeur du potentiel de palier aux électrodes de (Pd–H) ($\alpha+\beta$) pendant l'absorption, a déterminé divers auteurs[1-3] d'employer ces électrodes comme électrodes de référence. Les électrodes de ce type fonctionnent soit en présence de l'hydrogène barboté dans la solution, soit en son absence, la suppression du barbotage de l'hydrogène étant faite après ce que le potentiel de l'électrode ait atteint la valeur constante de palier.

Les électrodes de premier type ne présentent aucun avantage sur les électrodes normales platine–hydrogène. En ce qui concerne les électrodes de deuxième type le maintien du potentiel de palier constant après l'écartement du barbotage de l'hydrogène, impose le meilleur isolement du système pour conserver si longtemps que possible la réserve d'hydrogène dans la solution. Les implications constructives qui en résultent font ces électrodes difficilement à utiliser[3].

Les propriétés du système (Pd–H) en équilibre[4] permettent l'utilisation de celui-ci comme électrode de référence à hydrogène avec réserve propre de gaz. En ce cas, on réalise une électrode (Pd–H) en désorption. L'influence du pH sur le potentiel d'une pareille électrode est la même que sur celui d'une électrode réversible à hydrogène[4]. Dans ce travail-ci on décrit la construction et l'expérimentation d'une électrode de référence de ce type.

La description et la préparation de l'électrode

L'esquisse de l'électrode de référence est présentée dans la Fig. 1(a).

Dans la barre en Téflon (1), on introduit la pièce de palladium (2). Les dimensions de celle-ci sont portées dans la Fig. 1(b). Par l'intermédiaire du ressort (3), la tige (4) en acier inoxydable, réalise la liaison électrique du palladium avec le circuit extérieur et, en même temps, à l'aide des écrous (5) et (6), maintient la pièce de palladium en contact intime avec la pièce en Téflon; l'étanchéité est assurée par conicité. L'électrode réalisée de cette manière est prévue d'une chemise de protection de verre au capillaire, qui s'applique étanchement sur la barre en Téflon. La chemise de protection limite l'accès de l'oxygène dissous dans la solution vers la surface du palladium et, en même temps, rend difficile la diffusion de l'hydrogène désorbé de palladium, à travers la couche de liquide.

Après ce qu'on place la pièce de palladium dans la barre en Téflon, on polit la surface de l'électrode à l'aide du papier d'émeri métallographique, 700; on la nettoie soigneusement à jet d'eau, puis à solution d'acide chromique fait de substances p.a. et finalement on la rince à l'eau distillée. On palladise ensuite la surface pendant 5 min avec un courant de 0.25 mA d'intensité, dans une solution de 2% $PdCl_2$ en HCl 1 *N*. Puis, on fait le chargement cathodique de palladium à hydrogène en solution H_2SO_4 2 *N* pendant 50 h, à un courant de 0.1 mA d'intensité. Le chargement finit, la concentration de l'hydrogène en palladium s'homogénise dans 24 h environ et le potentiel arrive à la valeur du palier de désorption; on introduit alors l'électrode dans la

chemise de protection (7), on aspire de la solution par le capillaire et on écarte les bulles d'air qui peuvent se trouver entre le capillaire et la surface du palladium. Le potentiel de l'électrode préparée de cette manière, a une valeur constante, correspondante au palier de désorption, qui se maintient au moins trois semaines en solution H_2SO_4 2 N exposée à l'air. A la température de $25 \pm 0.1°$, nous avons obtenu la valeur moyenne $\varepsilon = 61.70 \pm 0.04$ mV par rapport à l'électrode normale à hydrogène.

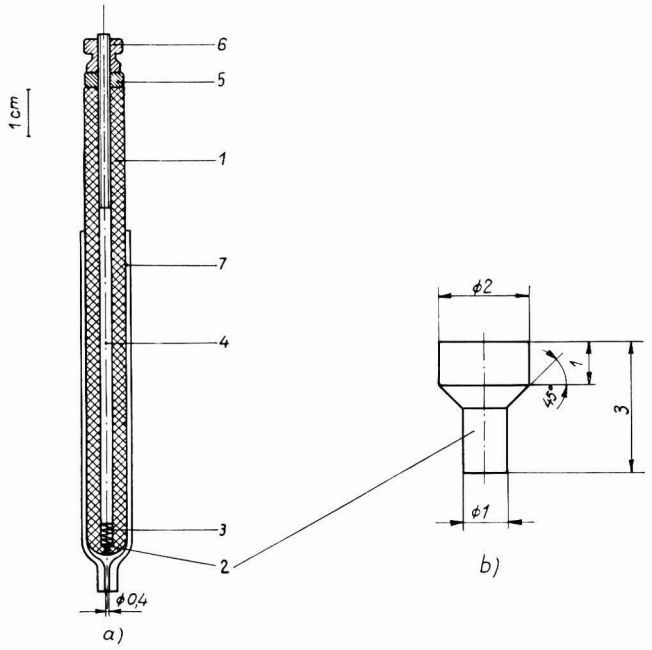

Fig. 1. Electrode de référence (Pd–H). (a), Esquisse d'ensemble; (b), la pièce de palladium.

Des expériences effectuées sur des électrodes fil de platine palladisés, ont montré que la valeur du potentiel de palier dépend non seulement de la quantité et de la manière du dépôt, mais, également, de "l'histoire" de l'électrode. L'étude de ces expériences-ci est en cours. D'après les résultats qu'on a obtenus jusqu'à présent, il résulte que la valeur de palier du potentiel de désorption de l'hydrogène de palladium doit être mésurée chaque fois qu'on fait une nouvelle électrode.

Conclusions

1. L'électrode décrite fonctionne comme une électrode réversible à hydrogène, avec propre réserve de gaz et, par conséquent, elle ne nécessité pas une installation de hydrogène purifié.

2. On peut l'employer dans toutes les circonstances dans lesquelles on emploie une électrode réversible à hydrogène. De plus, on peut l'employer également dans les cas où la présence de l'hydrogène barboté en solution pourrait produir des effets mécanique ou chimique indésirables.

3. L'électrode ne demande ni l'écartement de l'oxygène de la solution, ni l'isolement du système électrode–solution.

4. La construction de l'électrode est simple et son utilisation est commode.

5. Grâce au capillaire court, la résistance électrique de l'électrode est petite.

6. La vie de l'électrode, conservée en solution H_2SO_4 2 N exposée à l'air est relativement longue: au moins trois semaines.

7. A chaque nouvelle préparation de l'électrode, son potentiel de palier doit être mésuré par rapport à l'électrode normale à hydrogène.

Institute de Physique Atomique,
Section Cluj,
Cluj (Roumanie)

R. V. BUCUR
LIVIA STOICOVICI

1 D. J. G. IVES ET G. J. JANZ, *Reference Electrodes*, Academic Press, New York and London, 1961.
2 HAJIME SHIRATORI, *J. Electrochem. Soc. Japan*, 29 (1961) E-161.
3 J. P. HOARE, *Gen. Motors Eng. J.*, (1962) 14-16.
4 R. V. BUCUR, *Stud. Cercet. Chimie (Bucuresti)*, 12 (1964) 171.

Reçu le 21 Juin, 1965

J. Electroanal. Chem., 11 (1966) 152–154

On the mechanism of charge transfer at electrodes

Satisfactory theoretical treatments of the electron transfer process at metal electrodes have been developed by a number of authors[1–5]; these have differed considerably in their complexity, but yield identical results under equivalent approximations. Two further contributions to the subject have recently appeared in the literature[6,8], and the purpose of this communication is to describe their relationship to the uniform viewpoint derived from the work of the above-mentioned authors.

DE HEMPTINNE[6] used the theoretical approach of GURNEY[4] and GERISCHER[5], but made an extension which gives expression to the transmission coefficient for the electron through the interfacial energy barrier. There is a difference, however, in the choice of the *most likely* transition state among those which contribute to the current. DE HEMPTINNE assumes a "nearly delta like" distribution function for the solution-phase species among its possible electronic energies, centred on the energy of the equilibrium state. Thus, he envisages for the cathodic direction, reaction between an oxidised species in its equilibrium solvation configuration, and a "hot" electron.

The previous theories require a Boltzmann form for the above-mentioned distribution function, and an approximately parabolic potential energy function of the reaction co-ordinate for both the oxidised and reduced species. Then it follows that a minimum activation energy is needed for the reaction, when the electronic energy levels in the solution and the solid are equal to the Fermi level. This involves reorientation of the solvation shell of the reactant prior to electron transfer, as discussed in detail by MARCUS[1]. With these assumptions, the principal contribution to the integral over electron energy levels quoted by DE HEMPTINNE arises from the Fermi level; indeed, the integral becomes identical to one evaluated by DOGONADZE, KUZNETSOV AND CHIZMADZHEV[7]. When treated in this manner, the transfer coefficient appears directly in the equation for the rate constant and there is no need of DE

HEMPTINNE's argument concerning the loss of symmetry of the polarization field about an ion in the transition state.

BOCKRIS AND MATTHEWS[8] have suggested that the stretching of ion–solvent bonds might be the rate-determining aspect of charge transfer reactions at electrodes; in particular, they argue that this process consumes the activation energy for the hydrogen evolution reaction (h.e.r.). Hence, they conclude that the symmetry factor is independent of the charge distribution in the activated state, but is proportional to the amount of energy fed into the ion–solvent bond during activation. This, however, is an extreme point of view. Consider the two-dimensional representation of the free energy surface for the h.e.r., having as axis y, the fraction of the H_2O–M distance traversed by the proton, and as axis x, the effective charge on the H_3O^+ ion with which the orientation-polarization of the solvent would be in equilibrium.

BOCKRIS AND MATTHEWS seem to imply as reaction path, movement parallel to the y and x axes in succession, since they argue that the electronic energy levels are equalised by activation of the H^+–OH_2 bond. Although it is impossible to calculate the shape of the surface without postulating a detailed model, it would seem that this course would be rendered unlikely because of the necessity of passage through the high energy state resulting from removal of the proton from its solvation sheath in solution. In fact, the most favourable transition state probably lies near the centre of the surface, with co-ordinates which depend upon the applied overvoltage. Since the symmetry factor is related to these co-ordinates, it may be defined either in terms of the effective charge distribution or of the vibrational energy in the H^+–OH_2 bond in the transition state. Specifically, we can predict asymmetry of the charge distribution and of the position of the proton if the ratio of the concentrations of oxidised to reduced forms were far from unity because of the dissimilarity of the energy levels of initial and final states.

Hence, we conclude, in disagreement with BOCKRIS AND MATTHEWS, that (i) the activation energy for an electrode reaction is shared between several elementary processes (ii) there are several equivalent definitions of the transfer coefficient and (iii) the effective charge distribution need not be symmetrical.

Cyanamid European Research Institute,
Cologny, Geneva (Switzerland)

J. M. HALE

1 R. A. MARCUS, *Ann. Rev. Phys. Chem.*, 15 (1964) 155; *Can. J. Chem.*, 37 (1959) 155.
2 R. R. DOGONADZE AND YU. A. CHIZMADZHEV, *Proc. Acad. Sci. USSR, Phys. Chem. Sect., English Transl.*, 144 (1962) 463; 145 (1962) 563.
3 N. S. HUSH, *J. Chem. Phys.*, 28 (1958) 962; *Trans. Faraday Soc.*, 57 (1961) 557; *Z. Elektrochem.*, 61 (1957) 734.
4 R. W. GURNEY, *Proc. Roy. Soc. (London)*, A 134 (1931) 137.
5 H. GERISCHER, *Z. Physik. Chem. (Frankfurt)*, 26 (1960) 223, 325; 27 (1961) 48.
6 X. DE HEMPTINNE, *Bull. Soc. Chim. France*, (1964) 2328.
7 R. R. DOGONADZE, A. M. KUZNETSOV AND YU. A. CHIZMADZHEV, *Russ. J. Phys. Chem., English Transl.*, 38 (1964) 652.
8 J. O'M. BOCKRIS AND D. B. MATTHEWS, *J. Electroanal. Chem.*, 9 (1965) 325.

(Received July 10th, 1965)

BOOK REVIEWS

Treatise on Analytical Chemistry, Part II, Vol. 6, edited by I. M. KOLTHOFF AND PHILIP J. ELVING, Interscience Publishers, New York, London, Sydney, 1964, xxii + 627 pages, price £ 8-13-0.

This is one of a series in three parts which aims at an account of the subject under the headings: I. Theory and practice, II. Analytical chemistry of the elements, and III. Analysis of industrial products.

Part II, Vol. 6 covers the elements, Be, Pb, Nb, Ta, Tc, Ac, At, Fr, Po, Pa; these elements largely involve fields of analysis of quite recent growth which makes this a unique volume. Many types of analyses and methods of separation are included, and this is best illustrated by taking one of the chapters—*e.g.* that on technetium—and considering its main headings: introduction; properties: separation and isolation; detection and identification; toxicology and industrial hygiene; determination of technetium—gravimetric, titrimetric, polarographic, spectrophotometric; recommended laboratory procedures of analysis; references. Thus, the claim to make the series comprehensive is well substantiated, and although the style varies in the six sections by different authors or groups of authors, there is nevertheless, a high standard throughout as one might expect from such reputable editors and authors.

This is a most useful volume not only to those actually engaged in the analysis of the elements treated, but also to those who have little knowledge or experience of these new elements of the atomic age. In all this analytical development, the electrochemist has played his part.

F. H. POLLARD, University of Bristol

J. Electroanal. Chem., 11 (1966) 156

Méthodes d'Analyses, Commissariat à l'Énergie Atomique, Part 2, CETAMA, Presses Universitaires de France, 1964,

This is a technical handbook of analyses recommended for estimations used by those working in the atomic energy field, although, of course, many of the determinations will find application elsewhere. The instructions for each analysis are clearly laid out and described and although in French should present little difficulty in translation.

For the electrochemist, polarographic methods for uranium in plutonium, cobalt and nickel and a potentiometric method for iron, are given. The remainder are mainly spectrophotometric or radio-counting chemical methods.

No doubt this is a useful book for some analysts, but it cannot be widely recommended.

F. H. POLLARD, University of Bristol

J. Electroanal. Chem., 11 (1966) 156

Annual Surveys of Organometallic Chemistry

Volume 1 covering the year 1964

The upsurge of interest in organometallic chemistry which has taken place in little over a decade has found its natural outlet in an almost mushroom-like explosion of literature.
Notwithstanding the creation of periodicals devoted wholly to this field (notably **THE JOURNAL OF ORGANOMETALLIC CHEMISTRY),** an all too large proportion of papers concerned with organometallic compounds remain scattered throughout the pages of almost 100 non-specialist journals. The chemist, of course, has neither the time nor the funds to keep abreast of his subject in this manner.
In recognition of this problem, and in an attempt to alleviate the situation, **ELSEVIER PUBLISHING COMPANY** has undertaken publication of this new book series **ANNUAL SURVEYS OF ORGANOMETALLIC CHEMISTRY.**
The series will provide a comprehensive (but not necessarily exhaustive) and critical summary of organometallic chemistry on a year-to-year basis, each volume being published as soon as possible after the end of the year.
This first volume deals with 1964. For this review an organometallic compound is defined by the editors as one "which contains at least one metal-to-carbon bond and we include metal carbonyls in this definition". The organic derivatives of some elements usually considered in discussions of organometallic chemistry, e.g. boron and silicon, are included. The survey consists of two parts; one, edited by D. Seyferth presents a discussion of organic compounds of the main group (non-transition) metals and the second, by R. B. King, discusses transition metal organometallic chemistry dealing first with general developments in transition metal chemistry in 1964 followed by a discussion of advances in the chemistry of specific groups of transition metals organized according to the Periodic Table.

by

DIETMAR SEYFERTH,

Department of Chemistry, Massachusetts Institute of Technology, Cambridge, Mass., U.S.A.

and

R. BRUCE KING,

Senior Fellow, Mellon Institute, Pittsburgh, Pa., U.S.A.

6½ x 9½"
ix + 330 pages
13 illustrations
over 1400 lit. refs.
1965, £5.10.0

CONTENTS:

ELSEVIER PUBLISHING COMPANY
AMSTERDAM LONDON NEW YORK

294 E

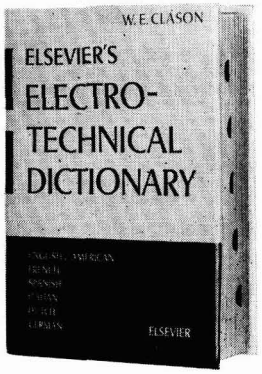

ELSEVIER'S ELECTROTECHNICAL DICTIONARY

English/American, French, Spanish, Italian, Dutch, German

Compiled and arranged on an English alphabetical base by **W. E. Clason,** formerly Head of the Translation Department, N.V. Philips' Gloeilampenfabrieken, Eindhoven, The Netherlands.

6 x 9″ viii + 731 pages 7,100 terms 1965 £ 7.0.0 $ 25.00 Dfl. 70.00

The author has selected 7,100 terms dealing with such fundamental and ancillary aspects of this science such as: fundamental electricity; electric energy generation, transmission and supply; electrical machines and transformers; electric traction applied to traffic, railways, automobiles etc.; illumination; installation of electrical equipment; measuring apparatus; electrochemistry; electrical heating; cables; electrobiology; welding; and electric lifts/elevators.

In common with all preceding volumes in the series of Elsevier Multilingual Dictionaries, this work is provided with cross-keyed alphabetical indexes for each of the languages included. This volume will again prove to be of great value in resolving all the more complicated aspects of translation.

ELSEVIER PUBLISHING COMPANY
AMSTERDAM LONDON NEW YORK

Annual Surveys of Organometallic Chemistry

The upsurge of interest in organometallic chemistry which has taken place in little over a decade has found its natural outlet in an almost mushroom-like explosion of literature.
Notwithstanding the creation of periodicals devoted wholly to this field (notably **THE JOURNAL OF ORGANOMETALLIC CHEMISTRY),** an all too large proportion of papers concerned with organometallic compounds remain scattered throughout the pages of almost 100 non-specialist journals. The chemist, of course, has neither the time nor the funds to keep abreast of his subject in this manner.
In recognition of this problem, and in an attempt to alleviate the situation, **ELSEVIER PUBLISHING COMPANY** has undertaken publication of this new book series **ANNUAL SURVEYS OF ORGANOMETALLIC CHEMISTRY.**
The series will provide a comprehensive (but not necessarily exhaustive) and critical summary of organometallic chemistry on a year-to-year basis, each volume being published as soon as possible after the end of the year.
This first volume deals with 1964. For this review an organometallic compound is defined by the editors as one "which contains at least one metal-to-carbon bond and we include metal carbonyls in this definition". The organic derivatives of some elements usually considered in discussions of organometallic chemistry, e.g. boron and silicon, are included. The survey consists of two parts; one, edited by D. Seyferth presents a discussion of organic compounds of the main group (non-transition) metals and the second, by R. B. King, discusses transition metal organometallic chemistry dealing first with general developments in transition metal chemistry in 1964 followed by a discussion of advances in the chemistry of specific groups of transition metals organized according to the Periodic Table.

Volume 1 covering the year 1964

by

DIETMAR SEYFERTH,

Department of Chemistry, Massachusetts Institute of Technology, Cambridge, Mass., U.S.A.

and

R. BRUCE KING,

Senior Fellow, Mellon Institute, Pittsburgh, Pa., U.S.A.

6½ x 9½"
ix + 330 pages
13 illustrations
over 1400 lit. refs.
1965, £5.10.0

CONTENTS:

ELSEVIER PUBLISHING COMPANY
AMSTERDAM LONDON NEW YORK

294 E

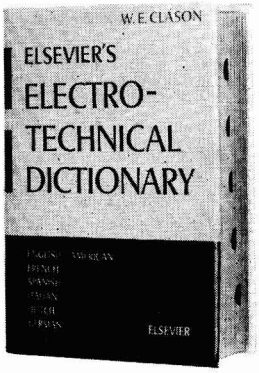

ELSEVIER'S ELECTROTECHNICAL DICTIONARY

English/American, French, Spanish, Italian, Dutch, German

Compiled and arranged on an English alphabetical base by **W. E. Clason,** formerly Head of the Translation Department, N.V. Philips' Gloeilampenfabrieken, Eindhoven, The Netherlands.

6 x 9″ viii + 731 pages 7,100 terms 1965 £ 7.0.0 $ 25.00 Dfl. 70.00

The author has selected 7,100 terms dealing with such fundamental and ancillary aspects of this science such as: fundamental electricity; electric energy generation, transmission and supply; electrical machines and transformers; electric traction applied to traffic, railways, automobiles etc.; illumination; installation of electrical equipment; measuring apparatus; electrochemistry; electrical heating; cables; electrobiology; welding; and electric lifts/elevators.

In common with all preceding volumes in the series of Elsevier Multilingual Dictionaries, this work is provided with cross-keyed alphabetical indexes for each of the languages included. This volume will again prove to be of great value in resolving all the more complicated aspects of translation.

ELSEVIER PUBLISHING COMPANY
AMSTERDAM LONDON NEW YORK

218 E

VOL. 11 NO. 2 FEBRUARY 1966

JOURNAL OF ELECTROANALYTICAL CHEMISTRY

CONTENTS

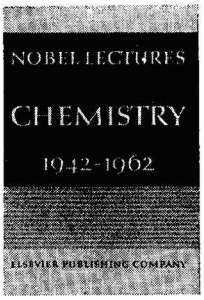

NOBEL PRIZE LECTURES

CHEMISTRY

In three volumes 1901–1921
1922–1941
1942–1962

Total price: £24.0.0 or Dfl. 240,00

In the world of science, the history of research and progress during the present century is largely a history of the accomplishments of the winners of the Nobel Prize. These achievements are placed in perspective at the Nobel Prize ceremonies held each December in Stockholm. The official Nobel Lectures, delivered by the laureates on these occasions have hitherto appeared in the Nobel Foundation's annual publication "Les Prix Nobel" in the language in which they were presented. They are now being published in the English language, arranged in chronological order and according to Prize fields. They are preceded by the presentation addresses to the prize-winners and followed by a biography. For a large circle of readers, the appearance of this series will provide the first opportunity to read the Nobel Laureates' own accounts of the long years of preparation and creative effort which led up to their celebrated achievements.

published

NOBEL LECTURES CHEMISTRY 1942–1962

Alder – Calvin – Diels – Giauque – Hahn – Hevesy – Heyrovsky – Hinshelwood – Kendrew – Libby – McMillan – Martin – Northrop – Pauling – Perutz – Robinson – Sanger – Seaborg – Semenov – Stanley – Staudinger – Sumner – Synge – Tiselius – Todd – Vigneaud – Virtanen

xiv + 712 pages, 41 tables, 228 illustrations, 481 lit. references, 1964

in preparation

NOBEL LECTURES CHEMISTRY 1922–1941

Aston – Bergius – Bosch – Butenandt – Debye – H. Fischer – Harden – Haworth – Joliot – Joliot-Curie – Karrer – Kuhn – Langmuir – Pregl – Ružicka – Soddy – Svedberg – Urey – Von Euler-Chelpin – Wieland – Windaus – Zsigmondy

xvi + 499 pages + indexes, 13 tables, 128 illus., 1965

NOBEL LECTURES CHEMISTRY 1901–1921

Arrhenius – Buchner – Marie Curie – E. Fischer – Grignard – Haber – Moissan – Nernst – Ostwald – Ramsay – Richards – Rutherford – Sabatier – Van't Hoff – Von Baeyer – Wallach – Werner – Willstätter

ELSEVIER PUBLISHING COMPANY
AMSTERDAM LONDON NEW YORK

272 Ea